

University of Warwick institutional repository: <http://go.warwick.ac.uk/wrap>

**A Thesis Submitted for the Degree of PhD at the University of Warwick**

<http://go.warwick.ac.uk/wrap/3154>

This thesis is made available online and is protected by original copyright.

Please scroll down to view the document itself.

Please refer to the repository record for this item for information to help you to cite it. Our policy information is available from the repository home page.

The Use of Recently Developed Mass  
Spectrometry Approaches for the  
Characterisation of Biological  
Mixtures

Richard J. Holland B.Sc. (Hons)

A thesis submitted for the degree of Doctor of Philosophy

University of Warwick

Department of Biological Sciences

September 2009

# Contents

<b>Contents</b>	<b>i</b>
<b>List of Figures</b>	<b>vi</b>
<b>List of Tables</b>	<b>x</b>
<b>Acknowledgements</b>	<b>xi</b>
<b>Declaration</b>	<b>xii</b>
<b>Summary</b>	<b>xiii</b>
<b>Abbreviations</b>	<b>xiv</b>
<b>Chapter 1: Introduction</b>	<b>1</b>
Analytical biochemistry .....	2
Glycosylation .....	4
Glycans in cancer .....	4
Glycosylation in pharmaceuticals .....	4
Glycan structure .....	7
GPI Anchors.....	7
N-linked glycosylation.....	7
O-linked glycosylation.....	8
Current strategies in glycan characterisation .....	9
Identifying glycoproteins .....	9
Glycan release methods.....	11
Enzymatic release.....	11
Chemical release .....	12
Compositional analysis .....	13

Sequence analysis.....	13
Introduction to mass spectrometry .....	16
Ionisation.....	16
Electrospray Ionisation (ESI).....	17
Mass analysers .....	18
Quadrupole.....	18
Time of Flight .....	20
Detectors .....	23
Data systems .....	24
Analogue to digital converter.....	24
Time to digital converter.....	25
Tandem Mass Spectrometry.....	26
Ambient mass spectrometry.....	27
ESI related ambient ionisation sources .....	30
Desorption electrospray ionisation.....	30
Extractive electrospray ionisation and neutral desorption extractive electrospray ionisation .....	31
APCI related ambient ionisation sources .....	32
Direct analysis in real time.....	33
Desorption atmospheric pressure chemical ionisation.....	33
Atmospheric solids analysis probe.....	34
Ion mobility spectrometry .....	34
DCIMS .....	34
DCIM-MS .....	37
TWIMS .....	37

TWIM-MS .....	38
Tandem MS on the Synapt HDMS .....	40
Cross section calibration .....	41
Aims and objectives .....	41
<b>Chapter 2: Ambient Ionisation of Pharmaceuticals</b>	<b>55</b>
Introduction .....	56
Aims .....	57
Materials and Methods .....	58
DART .....	59
DESI .....	59
DAPCI .....	60
Solventless DAPCI .....	61
ND-EESI .....	61
Sample Preparation .....	61
Accurate Mass Measurement on the Q-TOF I .....	61
Results and Discussion .....	62
Anadin Extra .....	62
Solpadeine Max .....	64
Metcolopramide .....	65
Erythromycin .....	68
Nicotine from Tobacco .....	69
Proctosedyl ointment .....	71
Detection of Ibuprofen Gel From Skin .....	75
Detection of ibuprofen metabolites from human urine .....	76
Conclusions .....	77
<b>Chapter 3: Shape Selective Studies of Isomeric Glucose Homopolymers</b>	<b>81</b>
Glucose Homopolymers .....	82
Dextran .....	82

Maltodextrin.....	83
Previous Studies of Poly-Glc Structures.....	83
Objectives.....	84
Materials.....	85
Experimental.....	85
Cation Attachment.....	85
TWIM-MS Analysis.....	86
Cross Section Calibration and Estimation.....	87
Results and Discussion.....	88
Product Ion Mass Spectra.....	88
Cross Section Calibration.....	89
Cation Attachment.....	92
TWIMS-MS Separation and Cross Section Estimation.....	92
Variation of Cross Section with Attached Cation.....	97
Conclusions.....	101
<b>Chapter 4: Ion Mobility of Glycans</b>	<b>106</b>
Introduction.....	107
Characterisation of Glycosylation.....	107
Ion mobility-mass spectrometry.....	108
Ion mobility based analysis of oligosaccharides.....	110
Objectives.....	111
Experimental.....	113
Ion mobility spectrometry-mass spectrometry (IMS-MS).....	113
DCIM-MS.....	113
TWIM-MS instrument.....	114
Materials.....	116
Molecular modelling.....	117
Results and Discussion.....	118

The rapid separation of chemically released N-linked glycans .....	118
Reproducibility of Ion Mobility Separations .....	118
Ion Mobility Separation of Glycans.....	120
Charge state separation of multiply charged multimers.....	122
Reproducibility of separation of common glycans from different sources	123
Separation of Isomeric Glycan Structures.....	124
Comparison of the TWIMS and DCIMS methods.....	130
Conclusions .....	135
<b>Chapter 5: Conclusions</b>	<b>144</b>
Summary of Project and Future Directions.....	145
Ambient Ionisation.....	145
Ion Mobility-Mass Spectrometry of Carbohydrates .....	146
<b>Appendix</b>	<b>148</b>

# List of Figures

Figure 1.1: The central dogma of molecular biology.....	3
Figure 1.2: Number (and percentage values) of recombinant proteins approved as biopharmaceuticals in different production systems.....	6
Figure 1.3: Accumulated number of recombinant biopharmaceuticals obtained in different production systems, in front of year of their first time approval.....	6
Figure 1.4: A) Some common monosaccharide subunits; B) Shorthand notation for glycosidic linkages and some sugar residues; C) A polypeptide chain with potential N-linked glycosylation sites and some example high mannose glycans.....	9
Figure 1.5: A schematic of an example glycan characetisation workflow .....	15
Figure 1.6: A schematic block diagram of a mass spectrometer.....	16
Figure 1.7: Electrospray ionisation process .....	18
Figure 1.8: Schematic of a quadrupole mass analyser .....	20
Figure 1.9: Representation of a reflectron-time of flight instrument.....	23
Figure 1.10: A schematic of the DESI ambient ionisation source .....	30
Figure 1.11: A schematic of the EESI and ND-EESI ambient ionisation source .....	32
Figure 1.12: A schematic of the DART source.....	33
Figure 1.13: A representation of DCIMS.....	36
Figure 1.14: Schematic of the Waters Synapt HDMS instrument .....	38
Figure 2.1: Positive mode mass spectra of Anadin Extra by A) DESI, B) DAPCI and C) DART, and D) accurate mass MSMS of protonated caffeine.....	63
Figure 2.2: Positive mode mass spectra of Solpadeine Max by A) DAPCI-MS, B) DESI-MS and C) DART-MS, and D) accurate mass MSMS of protonated codeine .....	65



Figure 2.3: DAPCI-MS spectra of metoclopramide in A) negative ion, B) positive ion. Accurate mass DAPCI-MSMS spectra of C) deprotonated, and D) protonated metoclopramide. E) Positive ion DART-MS spectrum of metoclopramide. Proposed fragmentation pathways of F) deprotonated metoclopramide in negative mode, and G) protonated metoclopramide in positive mode.....	67
Figure 2.4: Positive mode DESI-MS (A) and ND-EESI (B) spectra of erythromycin, and proposed fragmentation pathways of protonated erythromycin (C and D).....	68
Figure 2.5: Positive ion mass spectra of tobacco ionised by: A) DAPCI, B) DESI and C) DART. Positive ion accurate mass MS/MS spectrum (D) and proposed positive ion fragmentation pathway (E) of protonated nicotine. ....	70
Figure 2.6: Positive ion mass spectra of proctosedyl ointment ionised by DESI (top) DAPCI without solvent (middle) and DAPCI with solvent.....	72
Figure 2.7: A) Positive ion DART-MS spectrum, and B) positive ion DAPCI-MS spectrum of proctosedyl ointment.....	73
Figure 2.8: DAPCI-MS spectra of proctosedyl ointment in A) negative ion mode and B) positive ion mode. Accurate mass MS/MS of C) deprotonated cinchocaine hydrochloride in negative ion mode, and D) protonated cinchocaine hydrochloride in positive ion mode. E) Proposed negative ion fragmentation of $[M-H]^-$ and F) proposed positive ion fragmentation of $[M+H]^+$ of cinchocaine hydrochloride.....	74
Figure 2.9: A) Negative ion DESI-MS spectrum of ibuprofen gel desorbed from skin. B) Negative ion DAPCI accurate mass MS/MS spectrum obtained from deprotonated ibuprofen .....	75
Figure 2.10: Negative ion DAPCI-MS spectrum of a urine sample taken 60 minutes after an oral dose of 400 mg of ibuprofen (A and B). C) Negative ion DAPCI-MS/MS spectrum of $m/z$ 221 (hydroxyl-ibuprofen). ....	76
Figure 3.1: Molecular structures of A) dextran and B) maltodextrin .....	82

Figure 3.2: Tandem MS spectra of tetramers of sodiated maltodextrin (top) and dextran (bottom).....	89
Figure 3.3: A plot of corrected arrival times against corrected absolute cross sections for 14 dextran oligomers .....	90
Figure 3.4: A plot of corrected arrival times against corrected absolute cross sections for 19 tryptic peptides .....	90
Figure 3.5: A comparison of published absolute and estimated cross sections for 19 tryptic peptides estimated using a dextran based calibration.....	91
Figure 3.6: A comparison of published absolute and estimated cross sections for 19 tryptic peptides estimated using a peptide based calibration .....	91
Figure 3.7: Estimated cross sections for dextran and maltodextrin oligomers cationised with H <sup>+</sup> .....	93
Figure 3.8: Estimated cross sections for dextran and maltodextrin oligomers cationised with Li <sup>+</sup> .....	94
Figure 3.9: Estimated cross sections for dextran and maltodextrin oligomers cationised with Na <sup>+</sup> .....	94
Figure 3.10: Estimated cross sections for dextran and maltodextrin oligomers cationised with K <sup>+</sup> .....	95
Figure 3.11: Estimated cross sections for dextran and maltodextrin oligomers cationised with Rb <sup>+</sup> .....	95
Figure 3.12: Estimated cross sections for dextran and maltodextrin oligomers cationised with Cs <sup>+</sup> .....	96
Figure 3.13: Estimated cross sections for all singly cationised dextran oligomers ...	98
Figure 3.14: Estimated cross sections for all doubly cationised dextran oligomers ..	98
Figure 3.15: Estimated cross sections for all triply cationised dextran oligomers.....	99
Figure 3.16: Estimated cross sections for all singly cationised maltodextrin oligomers .....	99

Figure 3.17: Estimated cross sections for all doubly cationised maltodextrin oligomers.....	100
Figure 3.18: Estimated cross sections for all triply cationised maltodextrin oligomers .....	100
Figure 4.1: Glycans released from ribonuclease B .....	119
Figure 4.2: TWIMS ATDs for the sodiated $\text{Man}_n\text{GlcNAc}_2$ , $n=5-8$ glycan mixture from ribonuclease B. Glycan structure labels follow key shown in Figure 4.1 .....	120
Figure 4.3: TWIMS ATDs for sodiated $\text{Man}_5\text{GlcNAc}_2$ released from ribonuclease B, chicken ovalbumin, porcine thyroglobulin and desialylated thyroglobulin.....	121
Figure 4.4: Mass spectrum of the singly charged monomer of $\text{Man}_5\text{GlcNAc}_2$ obtained from the most prominent feature in the $m/z$ selected ATD .....	122
Figure 4.5: TWIMS ATDs for sodiated $\text{Man}_5\text{GlcNAc}_2$ released from ribonuclease B, chicken ovalbumin, porcine thyroglobulin and desialylated thyroglobulin.....	124
Figure 4.6: Positive ion mass spectrum, obtained on the Synapt instrument, for glycans released from chicken ovalbumin. ....	126
Figure 4.7: a) The MS/MS spectrum for species present in the equivalent negative mode, early feature of the $\text{GlcNAcMan}_3\text{GlcNAc}$ ATD. b) The MS/MS spectrum for species present in the equivalent negative mode, late feature of the $\text{GlcNAcMan}_3\text{GlcNAc}_2$ ATD from Figure 6.....	128
Figure 4. 8: Typical low-energy structures for sodiated BP-S, iso-BP-S, LNFP I, LNFP V, LNDFH I and LNDFH II determined by molecular dynamics calculations. The corresponding theoretical ( $\sigma_{\text{th}}$ ) and experimental ( $\sigma_{\text{exp}}$ ) cross sections are also given for each oligosaccharide.....	132
Figure 4.9: ATDs for $[\text{LNFP I} + \text{H}]^+$ obtained using a) DCIMS and b) TWIM-MS and the tandem mass spectra of the c) early and d) late TWIMS ATD peaks .....	134

# List of Tables

Table 1: A compilation of atmospheric pressure-surface sampling/ionisation techniques (Modified from (Van Berkel <i>et al.</i> , 2008)) .....	28
Table 2.1: Pharmaceutical formulations and their active ingredients .....	58
Table 2.2: Accurate masses of some DAPCI-MS/MS generated fragments of protonated caffeine .....	64
Table 2.3: Accurate masses of some DAPCI-MS/MS generated fragments of protonated codeine .....	64
Table 2.4: Accurate masses of some DAPCI-MS/MS generated fragments of deprotonated metoclopramide .....	67
Table 2.5: Accurate masses of some DAPCI-MS/MS generated fragments of protonated metoclopramide .....	68
Table 2.6: Accurate masses of some DAPCI-MS/MS generated fragments of protonated nicotine .....	71
Table 2.7: Accurate masses of some DAPCI-MS/MS generated fragments of deprotonated cinchocaine hydrochloride .....	74
Table 2.8: Accurate masses of some DAPCI-MS/MS generated fragments of protonated cinchocaine hydrochloride .....	74
Table 4.1. Glycans Investigated in this Study .....	112
Table 4.2. Optimised TWIMS Cell Parameters .....	116
Table 4.3. Experimental and Theoretical Results for Penta- and Hexasaccharides	131

# Acknowledgements

Although I am the sole author of this thesis, I am by no mean the sole contributor. Many people have supported me with their encouragement, wisdom and belief that I could complete my research.

Firstly, I would like to thank my supervisor Jim Scrivens for giving me the opportunity to study for a PhD under his supervision. He has been a constant source of support, guidance and exciting new ideas providing focus to my research.

I would also like to thank all of my colleagues past and present in the biological mass spectrometry and proteomics group: Charlie, Elle, Fran, George, Gill, Jonathon, Matt, Nisha, Sarah, Sue and Vib.

Special thanks go Kostas for his support as a post-doc and a friend.

The work undertaken has been supported by many colleagues and collaborators, who I would also like to thank: Kevin Giles and Bob Bateman at Waters for access to the prototype TWIM-MS instrument; Megan Grabenauer, Anna Erickson at UCSB for performing DCIM-MS and molecular modelling experiments; and a great many thanks go to David Harvey for his generous donation of glycan samples and knowledge.

The biggest thank you goes to all of my family for their patience and support, especially Rob, and my parents, Anne and Jim.

# Declaration

I hereby declare that this thesis, submitted in partial fulfilment of the requirements for the degree of Doctor of Philosophy and entitled “The use of recently developed mass spectrometry approaches for the characterisation of biological mixtures”, represents my own work and has not been previously submitted to this or any other institution for any degree, diploma or other qualification. Work undertaken by my collaborators is explicitly stated where appropriate.

Richard J. Holland

September 2009

# Summary

The thesis describes a number of examples of the use of recently developed mass spectrometry experimental approaches to characterise biologically important mixtures. The recently introduced field of ambient ionisation mass spectrometry has been utilised in the rapid, sensitive, information rich characterisation of pharmaceutical formulations. Little, or no, sample treatment was required and the experiments were shown to provide detailed information on active ingredients in the presence of a number of other components. A number of ambient ionisation approaches including DART, DESI and DAPCI were compared and advantages and disadvantages of each approach outlined and discussed.

The exciting technology of ion mobility has recently been commercially interfaced with mass spectrometry (IMMS). This has been utilised in a series of fundamental experiments that probe the interaction of varied cations with isomeric oligomers of carbohydrates. The approach enables conformational changes to be rapidly measured over a wide (500-6000 Da) mass range. Changes in conformations were observed for multiply cationised species which agree with previously measured solution phase measurements.

The IMMS approach has also been used successfully to characterise a number of N-linked glycans released from glycoproteins. The experiments enable isomeric structures to be differentiated and present an opportunity to develop a rapid, high information content screen. Estimated cross sectional measurements have been calculated and found to be in good agreement with those obtained from conventional drift cell approaches.

# Abbreviations

## #

**3D** Three-Dimensional

## A

**AC** Alternating Current

**ADC** Analogue to Digital Converter

**APCI** Atmospheric Pressure Chemical Ionisation

**APGDDI** Atmospheric Pressure Glow Discharge Desorption Ionisation

**AP-MALDI** Atmospheric Pressure Matrix-Assisted Laser  
Desorption/Ionisation

**APTDI** Atmospheric Pressure Thermal Desorption

**ASAP** Atmospheric Solids Analysis Probe

**ATD** Arrival Time Distribution

## B

**B-PS** B-Pentasaccharide

## C

**CI** Chemical Ionisation

**CID** Collision-Induced-Decomposition

**CRM** Charged Residue Model



## **D**

<b>DAPCI</b>	Desorption Atmospheric Pressure Chemical Ionisation
<b>DAPPI</b>	Desorption Atmospheric Pressure Photoionisation
<b>DART</b>	Direct Analysis in Real Time
<b>DBDI</b>	Dielectric Barrier Discharge Ionisation
<b>DC</b>	Direct Current
<b>DCIM-MS</b>	Drift Cell Ion Mobility Mass Spectrometry
<b>DCIMS</b>	Drift Cell Ion Mobility Spectrometry
<b>DESI</b>	Desorption Electrospray Ionisation
<b>DeSSI</b>	Desorption Sonic Spray Ionisation
<b>DNA</b>	Deoxyribonucleic acid

## **E**

<b><i>E. coli</i></b>	<i>Escherichia coli</i>
<b>EASI</b>	Easy Ambient Sonic Spray Ionisation
<b>ECD</b>	Electron Capture Dissociation
<b>EESI</b>	Extractive Electrospray Ionisation
<b>EI</b>	Electron Ionisation
<b>ELDI</b>	Electrospray-Assisted Laser Desorption/Ionisation
<b>ESI</b>	Electrospray Ionisation
<b>ETD</b>	Electron Transfer Dissociation

## **F**

<b>FAB</b>	Fast Atom Bombardment
<b>FAMIS</b>	High-Field Asymmetric Wave Form Ion Mobility
<b>FTICR</b>	Fourier Transform Ion Cyclotron Resonance
<b>FWHM</b>	Full Width at Half Maximum

## **G**

<b>Gal</b>	Galactose
<b>GalNAc</b>	N-acetylgalactosamine
<b>GC</b>	Gas Chromatography
<b>Glc</b>	Glucose
<b>GlcNAc</b>	N-acetylglucosamine
<b>GPI</b>	Glycophosphatidylinositol

## **H**

<b>HDMS</b>	High Definition Mass Spectrometry
<b>HPAEC</b>	High pH Anion Exchange Chromatography

## **I**

<b>IEM</b>	Ion Evaporation Model
<b>IM</b>	Ion Mobility
<b>IMMS</b>	Ion Mobility-Mass Spectrometry
<b>IMS</b>	Ion Mobility Separator
<b>IMS-MS/MS</b>	Ion Mobility Spectrometry-Tandem Mass Spectrometry
<b>IR LADESI</b>	Infrared Laser Assisted Desorption Electrospray Ionisation
<b>IRMPD</b>	Infrared Multiphoton Dissociation
<b>Iso-B-PS</b>	Iso-B-Pentasaccharide

## **J**

<b>JeDI</b>	Jet Desorption Electrospray Ionisation
-------------	--

## **L**

<b>LC</b>	Liquid Chromatography
<b>LC-MS/MS</b>	Liquid Chromatography-Tandem Mass Spectrometry

<b>LD/APCI</b>	Laser Desorption/Atmospheric Pressure Chemical Ionisation
<b>LD/ESI</b>	Laser Desorption/Electrospray Ionisation
<b>LDTD</b>	Laser Diode Thermal Desorption
<b>LMJ-SSP</b>	Liquid Microjunction Surface-Sampling Probe
<b>LNDFH I</b>	Lacto-N-Difucohexaose I
<b>LNDFH II</b>	Lacto-N-Difucohexaose II
<b>LNFP I</b>	Lacto-N-Fucopentaose I
<b>LNFP V</b>	Lacto-N-Fucopentaose V
<b><u>M</u></b>	
<i>m/z</i>	Mass to Charge Ratio
<b>MALDESI</b>	Matrix-Assisted Laser Desorption Electrospray Ionisation
<b>MALDI</b>	Matrix Assisted Laser Desorption/Ionisation
<b>Man</b>	Mannose
<b>MCP</b>	Microchannel Plate
<b>mRNA</b>	Messenger ribonucleic acid
<b>MS</b>	Mass Spectrometry
<b>MS/MS</b>	Tandem Mass Spectrometry
<b><u>N</u></b>	
<b>ND-EESI</b>	Neutral Desorption-Extractive Electrospray Ionisation
<b>N-linked</b>	Asparagine-linked
<b>NMR</b>	Nuclear Magnetic Resonance
<b>NSAID</b>	Non-Steroidal Anti Inflammatory
<b><u>O</u></b>	
<b>oa-TOF</b>	Orthogonal Axis Time Of Flight
<b>O-linked</b>	Serine or threonine-linked

## **P**

<b>PAD</b>	Post Amperometric Detection
<b>PADI</b>	Plasma-assisted desorption/ionisation
<b>PAGE</b>	Poly acrylamide gel electrophoresis
<b>PNGaseF</b>	Peptide N-glycosidase F
<b>poly-Glc</b>	Polyglucose
<b>PTM</b>	Post-translational modification

## **Q**

<b>Q-TOF</b>	Quadrupole-Time of Flight
--------------	---------------------------

## **R**

<b>RF</b>	Radio Frequency
<b>RNA</b>	Ribonucleic acid

## **S**

<b><i>S. cerevisiae</i></b>	<i>Saccharomyces cerevisiae</i>
<b>SDS</b>	Sodium Dodecyl Sulfate
<b>SRIG</b>	Stacked Ring Ion Guide
<b>SSSP</b>	Sealing Surface-Sampling Probe

## **T**

<b>TD/APCI</b>	Thermal Desorption/Atmospheric Pressure Chemical Ionisation
<b>TDC</b>	Time to Digital Converter
<b>TOF</b>	Time Of Flight
<b>tRNA</b>	Transfer Ribonucleic Acid
<b>T-Wave</b>	Travelling Wave

<b>TWIG</b>	Travelling Wave Ion Guide
<b>TWIMS</b>	Travelling Wave Ion Mobility Spectrometry
<b><u>U</u></b>	
<b>UCSB</b>	University of California, Santa Barbara

# **Chapter 1:**

# **Introduction**

## **Analytical biochemistry**

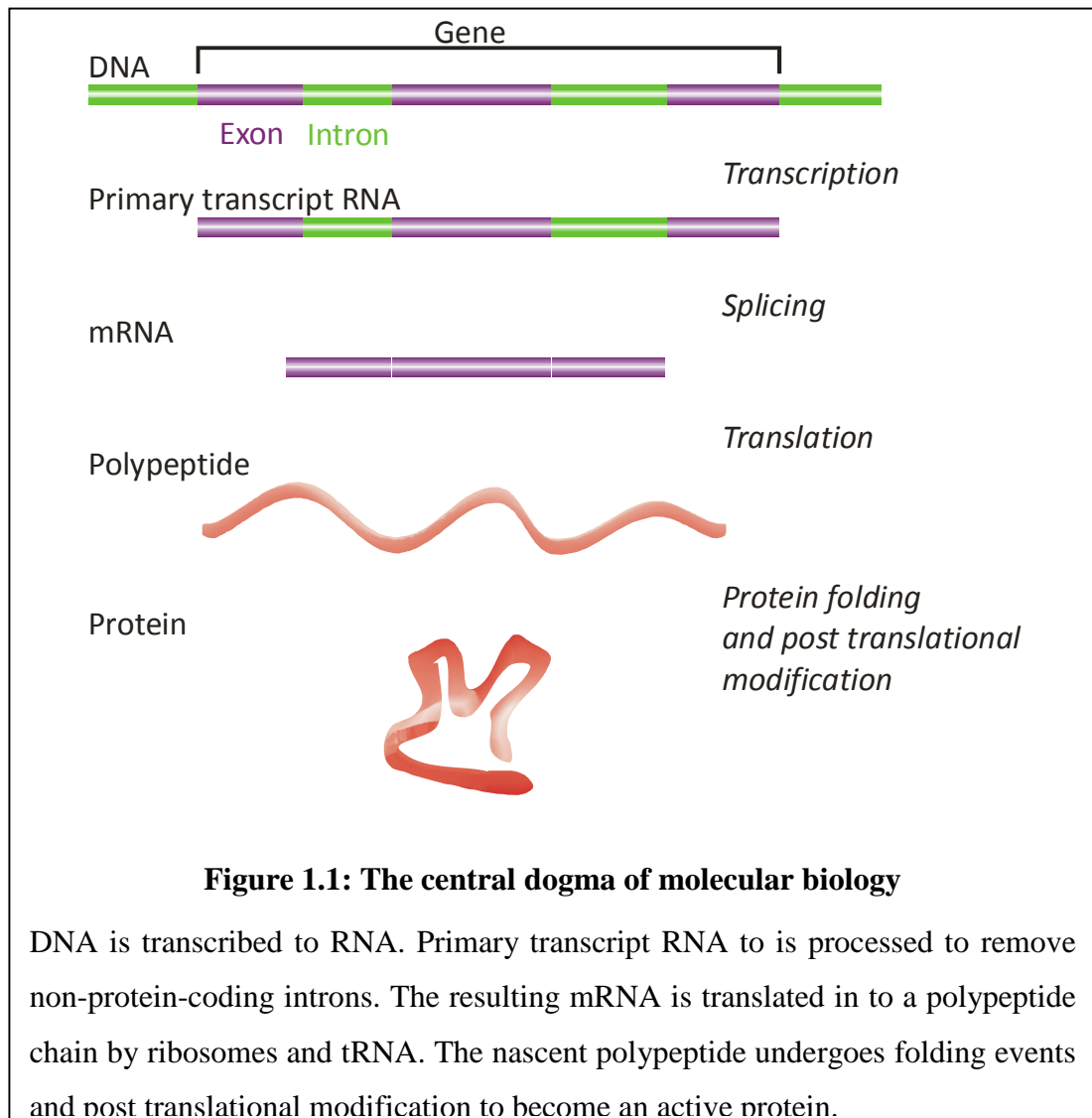
There is a persistent requirement to develop new methods and improved instrumentation for use in the study of molecules in biological systems. An ideal analytical technique is sensitive, selective, rapid, reproducible and provides a high level of information about a sample. Current techniques have a trade-off between one or more of these properties.

This thesis examines emerging techniques and technologies and assesses their amenability to improving the throughput in analysis of molecules of biological importance. The following introduction will focus on the instrumentation and techniques in the research described here.

Genomics is the study of the genetic complement of a cell or organism. Since the completion of the first genome sequences there has been a great drive to predict and annotate all of the potential genes and protein coding regions they contain. The genetic material contained in most cells is static, and while providing a complete blueprint for an organism, it does not allow the prediction of the temporal or spatial expression of its gene products.

Proteomics is the study of the protein complement of a cell, tissue or organism. Where DNA is predominantly an information storage molecule, proteins are the driving force behind almost all biochemical reactions. The most important property a polypeptide chain requires before it is a functional protein is the correct three-dimensional structure. The correct 3D structure is required for all proteins to function but there are many proteins that need an additional stage of post-translational modification to become active. There are more than 400 different post-translational

modifications (PTMs) that have been observed including: phosphorylation, glycosylation and disulphide bonds.



While protein primary structure (the amino acid sequence) and, to a certain extent, secondary structure ( $\alpha$ -helices and  $\beta$ -sheets) can be obtained from sequencing the genome, computational approaches cannot, for the most part, be used to predict higher order structure or the presence post-translational modifications in the biologically active molecule. With a greater number of proteins being characterised through the use of modern techniques, it is becoming more apparent that PTMs have very important roles and require detailed investigation.



## **Glycosylation**

Glycosylation is the covalent attachment of carbohydrate structures to the side chains of amino acids in a polypeptide chain. It is one of the most common forms of PTM present in eukaryotic systems with more than 50% of all proteins having some form of glycosylation (Apweiler *et al.*, 1999). A wide range of roles have been ascribed to the presence of glycans. These include presentation (or masking) of molecular determinants for recognition by cells, microorganisms, or other biological molecules; modulation of the half-life of glycoproteins; and physical/structural roles (Varki, 1993; Haltiwanger and Lowe, 2004; Ohtsubo and Marth, 2006; Sharon, 2006).

## **Glycans in cancer**

Glycans presented on the surface of a cell are known to have roles in host cell-cell interaction and recognition. Cell malignancy has been observed to result in presentation of a different profile of glycans on the surface of the cell (Kim and Varki, 1997). Detection of the changes in glycosylation profile as a means of cancer diagnosis is widely practiced. Current approaches use antibodies to glycan structures known to be presented in certain cancers (Waldmann, 1991). The drawbacks of this approach are the requirement of an antibody specific to the glycan marker, and potential binding of the antibody to closely related glycan structures that have no role in malignancy or tumorigenesis. Thus, more specific detection methods are required.

## **Glycosylation in pharmaceuticals**

The presence of glycosylation in pharmaceuticals ranges from minor carbohydrate moieties attached to small-molecule drugs (e.g. streptomycin, erythromycin and oseltamivir (Tamiflu<sup>TM</sup>)), to large glycoproteins (e.g. erythropoietin, antibodies and glycosidases). Glycopeptide and protein pharmaceuticals are a significant challenge

to produce by *in vitro* chemical synthesis approaches, and so are produced in recombinant bacterial or eukaryotic cell lines. These biopharmaceuticals can be used as treatments for a wide range of diseases, but their overall efficacy and safety can be highly dependent on the presence (or absence) of native PTMs. Development in recombinant technologies have allowed the production of some human-like protein glycosylation patterns, however, a range of factors during the manufacturing process can dramatically affect the downstream quality and activity of the protein. Figures 1.2 – 3 show the distribution of recombinant biopharmaceuticals currently approved for human use, and the production systems used to grow them. The trend towards using mammalian cell (predominantly chinese hamster ovary cell) based production systems is increasing due to the human-like post-translational modification patterns that can be achieved. There are concerns about the comparability in the glycosylation profiles of the endogenous molecules and different batches of the same product (Yuen *et al.*, 2003), rapid batch to batch characterisation and quality control of biopharmaceuticals is therefore of the utmost importance. Existing approaches to characterise glycoproteins and peptides are discussed later in this chapter.

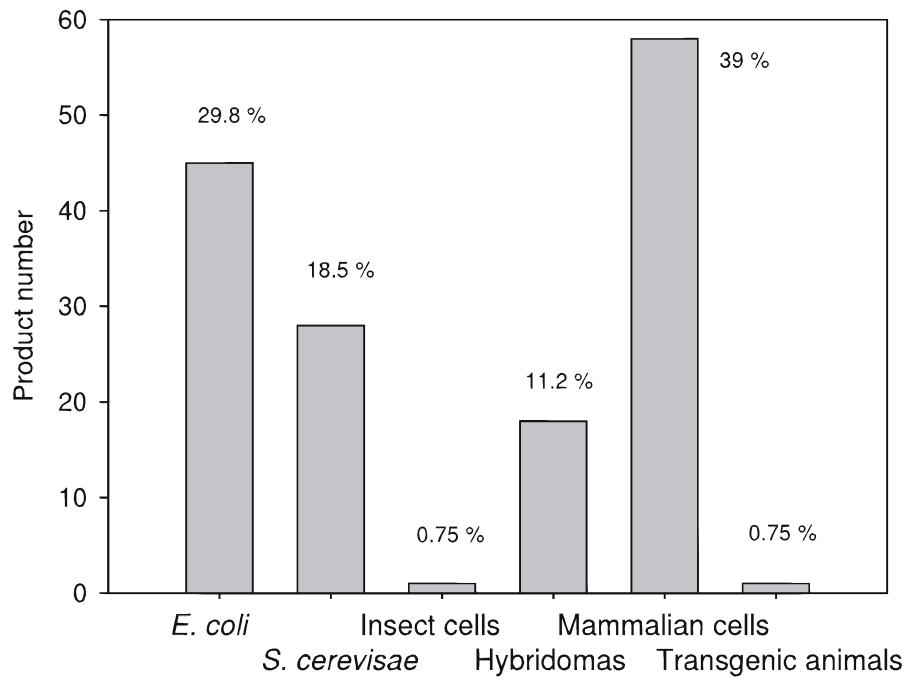


**Figure 1.2: Number (and percentage values) of recombinant proteins approved as biopharmaceuticals in different production systems**

From (Ferrer-Miralles *et al.*, 2009)

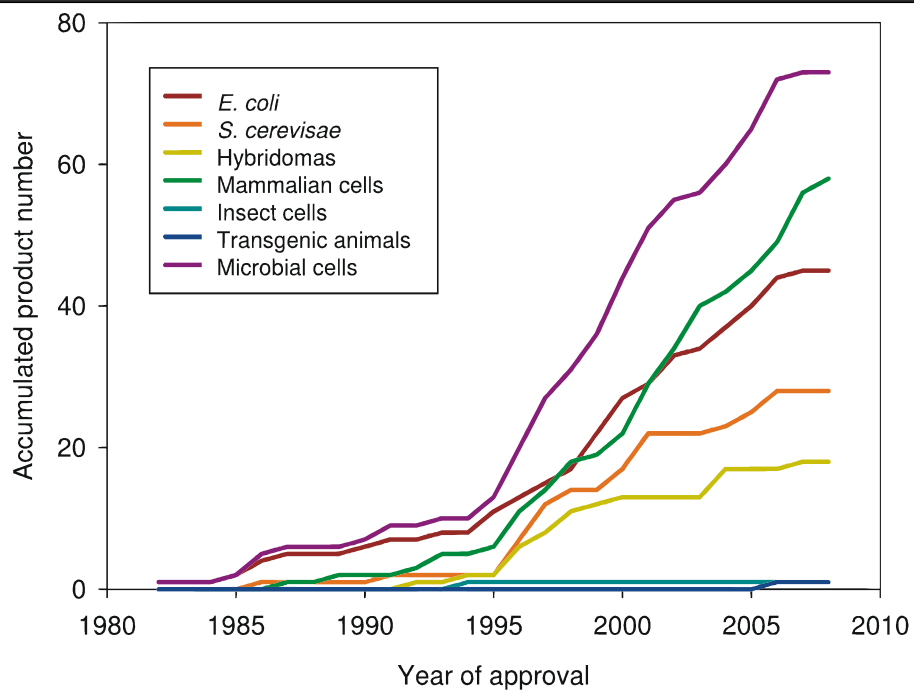


**Figure 1.3: Accumulated number of recombinant biopharmaceuticals obtained in different production systems, in front of year of their first time approval**

Products from *E. coli* and *S. cerevisiae* are presented together under the category of microbial cells. From (Ferrer-Miralles *et al.*, 2009)

## **Glycan structure**

Mammalian glycans consist of 10 common monosaccharide units that are used to build up the complex oligosaccharide structures. In contrast with nucleic and amino acids, which only form linear structures due to presence of only one linkage site for oligomerisation, monosaccharides can connect via any of their hydroxyl groups, resulting in a diverse set of linkages that can form either linear or branched structures. This is further complicated by the stereochemistry at the linkage site due to anomericity of the reducing sugar. Two mannose residues can theoretically be connected in 8 different configurations, although, in biological systems, only a limited number of these linkages have been observed to occur. Additional modification by sulfation, phosphorylation and acetylation combined with the stereochemical and structural diversity provides a major analytical challenge.

Glycans can range from single monosaccharide subunits, to large, complex oligosaccharides and occur in four main types: glycosphosphatidylinositol (GPI) anchors, N-linked, O-linked, and free oligosaccharides.

## **GPI Anchors**

GPI anchors are a glycan bridge between phosphatidylinositol and phosphoethanolamine, an amide linkage on the carboxyl terminus of a protein. Their main role is to anchor proteins to the phospholipid bilayer of a cell membrane.

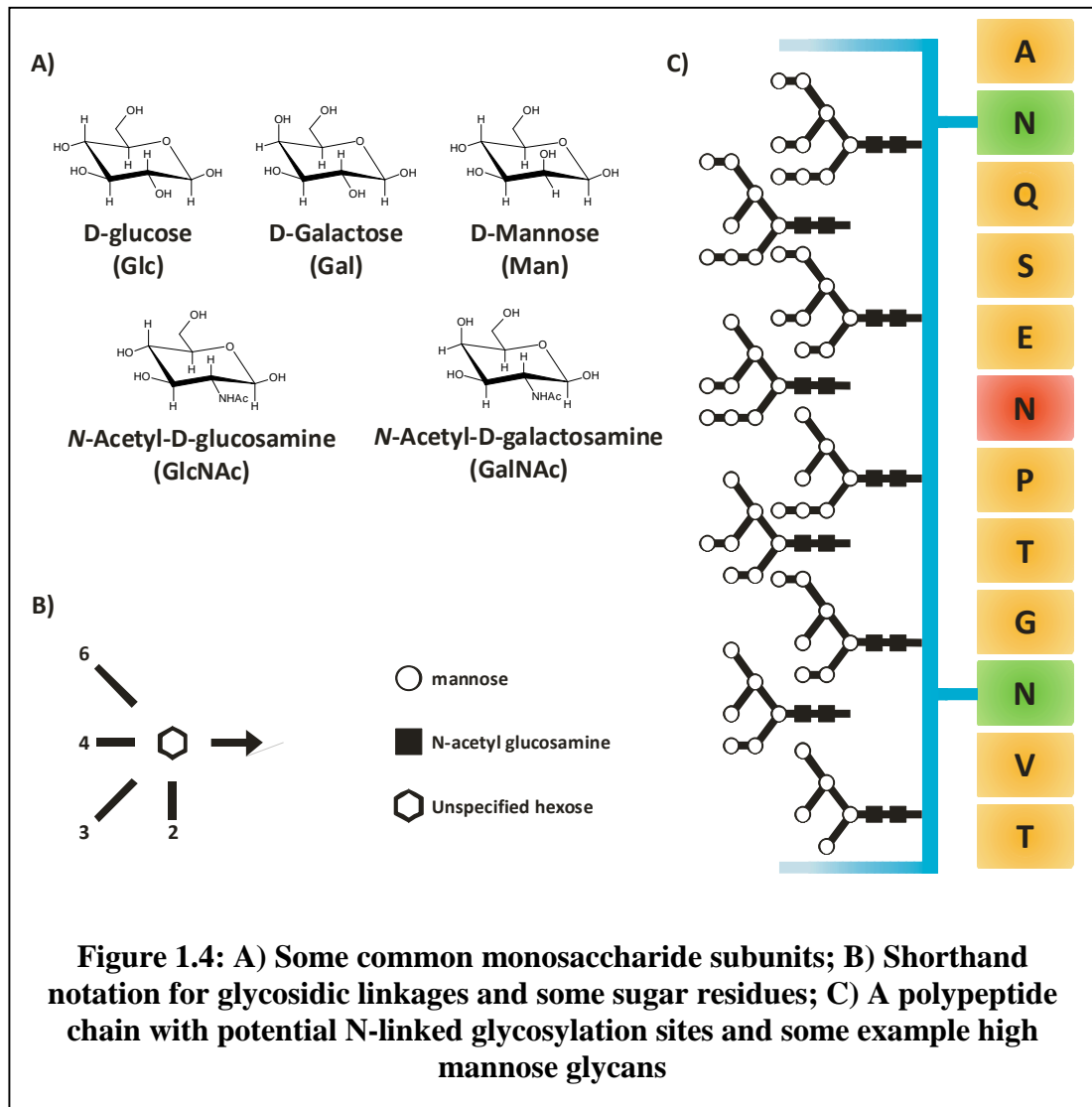
## **N-linked glycosylation**

N-linked glycosylation is the covalent attachment of an oligosaccharide chain to an asparagine residue in a polypeptide chain. N-glycans share a common pentasaccharide core and can be divided into three general classes: high mannose type, complex type and hybrid type. The high mannose type contains only mannose

residues beyond the pentasaccharide core, complex type glycans contain a mixture of monosaccharide subunits, and hybrid type contain features of both complex type and high mannose glycans. Potential N-linked glycosylation sites can be predicted from the genome as they require a consensus sequence in the polypeptide chain of Asn-X-Ser/Thr, where X is any amino acid except proline. Although these potential glycosylation sites can be predicted, not all of them are occupied by glycans *in vivo*, and contribute to the heterogeneous composition of glycoproteins (microheterogeneity) (Raman *et al.*, 2005; Budnik *et al.*, 2006; Hossler *et al.*, 2007).

### **O-linked glycosylation**

O-linked glycans are frequently linked to the polypeptide via *N*-acetylgalactosamine (GalNAc) to the hydroxyl group of serine or threonine residues. O-glycans can be a single monosaccharide, or long highly sulfated structures. O-glycosylation sites (unlike N-linked) do not have a consensus sequence that can be elucidated from the protein primary structure.



## Current strategies in glycan characterisation

### Identifying glycoproteins

The first stage in glycan characterisation requires the identification and isolation of glycosylated proteins.

Traditional biochemical colourimetric assays for carbohydrates in solution (e.g. phenol-sulphuric acid assay) are not sensitive enough to detect the presence of glycans at the concentrations relevant to biological systems. It has therefore been necessary to develop more sensitive techniques to identify the presence of glycoconjugates.

The periodic acid-Schiff staining procedure is capable of identifying the presence of glycosylated proteins in a sodium dodecyl sulfate-polyacrylamide gel electrophoresis (SDS-PAGE) gels, but it is not completely specific for carbohydrates and requires a relatively large amount of protein (50- 250  $\mu$ g) to be loaded on to the gel to bring the carbohydrate concentration up to detectable levels. Fluorescent stains and markers can be more sensitive for the detection of glycosylation, but all of these techniques covalently modify the glycoproteins making them inadequate for the analysis of fine structural detail, and can make quantitative analysis difficult. When a gel is stained specifically for the carbohydrate component, numerous additional species may also be present but would remain unstained. A common procedure which allows characterisation of the native glycoprotein after detection is to run duplicate SDS-PAGE gels, of which one is used for carbohydrate detection. A second is retained and only the protein component stained, leaving the native glycan intact. The number of glycoproteins identified using SDS-PAGE approaches can be a significant under-representation of the total number of glycoconjugates present in a cell or tissue lysate. This is due to the inherent challenges in solubilising hydrophobic, membrane associated proteins (Geyer and Geyer, 2006).

Lectins are carbohydrate-binding proteins that are not enzymes or antibodies, but can bind to specific carbohydrate residues and motifs (Lis and Sharon, 1998; Sharon and Lis, 2004) Lectin affinity chromatography is a technique which can separate and enrich glycosylated proteins (Merkle *et al.*, 1987). A protein or peptide mixture is passed through the chromatography column containing lectins bound to the stationary phase. Interaction of the carbohydrate moieties of glycoconjugates with the lectins causes them to be retained on the column. Incubation with competing sugar molecules can be used to elute the glycoproteins or peptides. A limitation of

this technology is that each lectin binds a specific subset of carbohydrates. Therefore a lectin column has a bias towards glycoproteins containing specific glycan structures. This can result in the loss of novel glycans.

## **Glycan release methods**

Most of the techniques for glycan analysis require the oligosaccharide to be released from the underlying peptide. Both enzymatic and chemical methods are available to release intact oligosaccharides for further analysis.

### **Enzymatic release**

The most common enzymatic release of N-linked glycans is by treatment with peptide N-glycosidase F (PNGase F) (Anthony *et al.*, 1987). Its enzymatic activity is specific for the cleavage of the amide bond between the GlcNAc residue and the asparagine of the polypeptide chain. As a result of the treatment, the oligosaccharide is released providing a free reducing terminus (which may be used for labelling and derivatisation at a later stage), and the asparagine is converted to an aspartic acid. PNGase F treatment is the preferred technique as it leaves the oligosaccharide and the peptide intact for further analysis. PNGase F cannot release O-linked glycans; N-linked glycans with an  $\alpha$ 1-6 linked fucose on the GlcNAc adjacent to the polypeptide; or glycans on the amino- or carboxy-terminus of a peptide chain.

An alternative family of enzymes that perform oligosaccharide release are endo- $\beta$ -N-acetylglucosidases (e.g. Endo H (Trimble *et al.*, 1987) and Endo F). These enzymes cleave the glycosidic bond between the two GlcNAc residues at the reducing terminus of an N-linked glycan. The point of cleavage yields an oligosaccharide which has lost one GlcNAc residue from the reducing terminus, and the peptide with the second GlcNAc residue still attached to the asparagine side chain.



There is currently no enzyme with O-glycanase activity which can be used against all O-linked glycans. Enzymatic release of O-linked glycans is not generally attempted but can to a certain extent be achieved by sequential treatments with endoglycosidases of different carbohydrate specificities. This may yield an intact peptide for site mapping, but will not produce an intact oligosaccharide for complete structure determination.

### **Chemical release**

Two forms of chemical release have been developed to overcome the limitations of the enzymatic release techniques: hydrazinolysis and  $\beta$ -elimination.

Hydrazinolysis uses anhydrous hydrazine to release both N- and O-linked glycans (Patel *et al.*, 1993). By varying the conditions of the reaction, it is possible to selectively release N-linked glycans; sequentially release N- followed by O-linked; or release all at the same time. The hydrazine treatment will cleave many of the amide bonds in the peptide rendering it useless for further studies, and will break any N-acyl groups in the oligosaccharide (e.g. N-acyl groups present in GlcNAc). It is necessary to re-N-acetylate the cleaved groups using acetic anhydride. Some structural information can be lost as a result of hydrazinolysis due to loss of components like N-glycolyl-neuramic acid.

Alkaline borohydride treatment ( $\beta$ -elimination) of glycoproteins under carefully controlled conditions can selectively release only the O-linked glycans. This release method modifies the reducing terminus so it loses the capacity to be further derivatised (e.g. addition of fluorescent labels). Modification of the glycosylation site also occurs making the technique amenable to site mapping studies.

## **Compositional analysis**

Compositional analysis is routinely carried out using two main techniques: high pH anion exchange chromatography with pulsed amperometric detection (HPAEC-PAD) (Hardy, 1994) and gas chromatography-mass spectrometry (GC-MS).

HPAEC-PAD has become a routine compositional analysis tool as it is a relatively simple and sensitive technique and does not require the derivitisation of samples prior to analysis. Carbohydrates typically have a high  $pK_a$  values in the 12-14 range. Monosaccharides and oligosaccharides, when placed in a sufficiently basic environment will become negatively charged due to the formation of oxyanions. The carbohydrate samples can be retained on an anion exchange column where they are eluted by reducing the pH of the surrounding solution. The elution time is recorded by pulsed amperometric detection. There is good correlation between  $pK_a$  and their elution order.

GC-MS is a sensitive technique for monosaccharide composition analysis allowing detection of subnanomole amounts (Merkle *et al.*, 1994). Composition analysis is carried out by the cleavage of the oligosaccharide to give monosaccharides. The monosaccharides are then derivatised to make volatile compounds which can then be introduced in to the GC-MS for analysis.

## **Sequence analysis**

Sequence information for an oligosaccharide can be obtained using a number of techniques including exoglycosidase treatment and mass spectrometry.

Exoglycosidases are enzymes which remove sugar subunits from the non-reducing terminals of an oligosaccharide (Jacob *et al.*, 1994). A purified oligosaccharide is

incubated with a high concentration of a specific exoglycosidase before being subjected to chromatographic analysis. A change in the retention time of the oligosaccharide can be attributed to the removal of one or more monosaccharides. Sequential incubation and analysis can be used to perform stepwise degradation of the glycan to provide sequence and some linkage information. This method is time consuming and requires large amounts of purified glycan samples.

As a result of developments in instrumentation resulting in low pico- femtomolar sensitivity, mass spectrometry is becoming a powerful tool in the analysis of oligosaccharides. Matrix assisted laser desorption/ionisation (MALDI) mass spectrometry (MS) offers high throughput, high mass range and contaminant resistant profiling and composition analysis of complex mixtures of glycans. This type of MALDI-MS experiment yields only intact masses of glycans, and cannot be used to determine definitive composition or sequence of analysed carbohydrates. Chromatographic separations coupled to tandem mass spectrometry can allow a greater degree of structural information to be elucidated including the potential identification of carbohydrate composition, sequence and stereochemistry at the expense of analysis speed (Harvey, 2001).

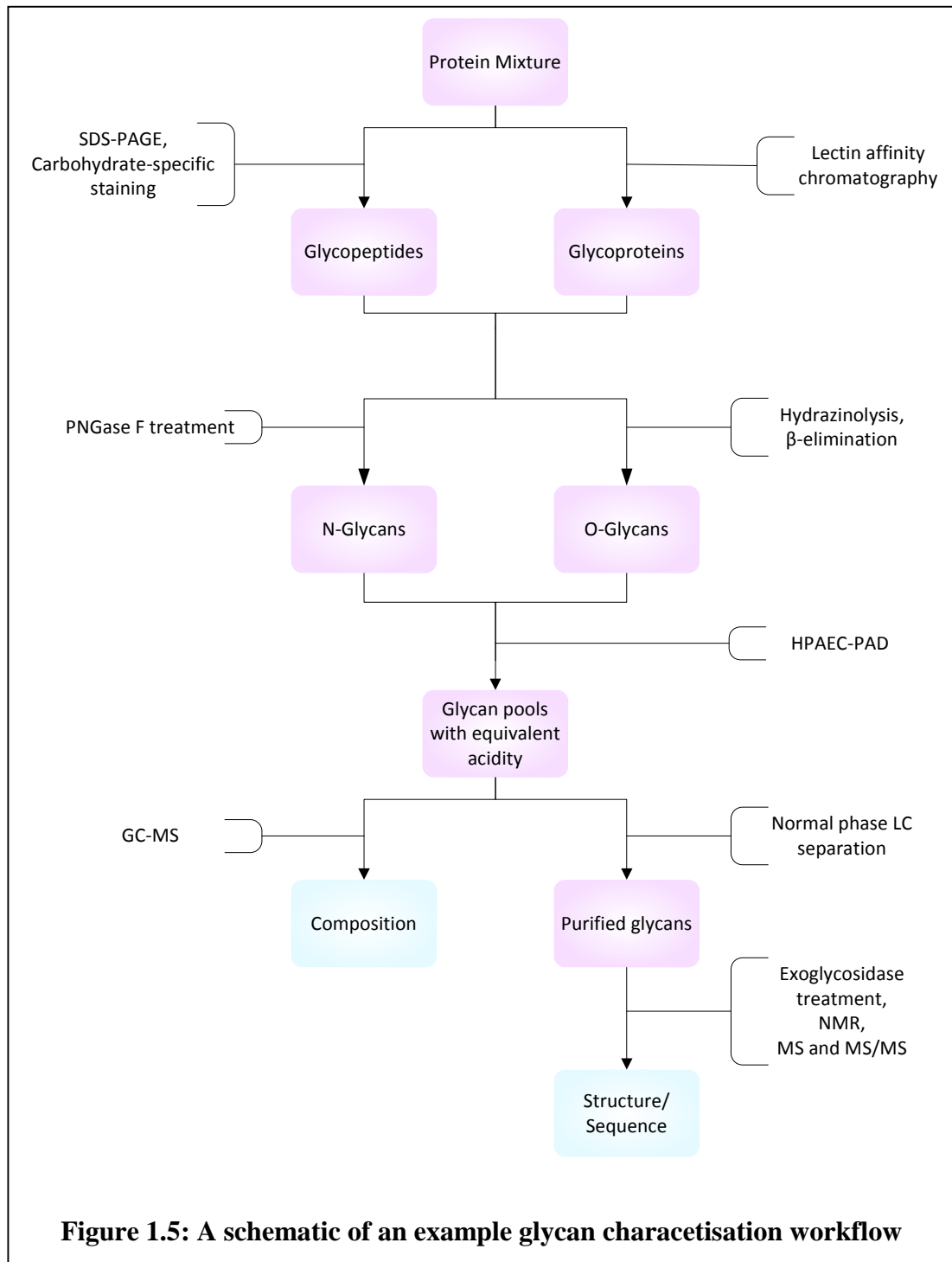
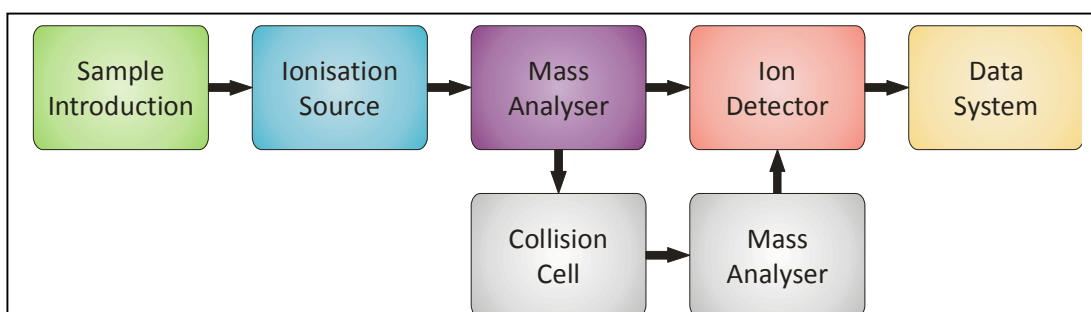


Figure 1.5 shows an example workflow for characterisation of glycans from a protein mixture. The timescale for carrying out each of these processes ranges from hours (chromatography separations), to overnight incubation (PNGase F treatment). These

strategies have a low rate of throughput, and require relatively large amounts of sample to perform complete glycan characterisation.

## Introduction to mass spectrometry

Mass spectrometry is a powerful analytical technique that can offer both high sensitivity and selectivity. The basic function of a mass spectrometer is to separate ions based on their mass-to-charge ratio ( $m/z$ ). This is achieved by ionisation of the sample, separation of ions of differing ( $m/z$ ) and subsequently detecting and recording their relative abundance. A mass spectrometer is therefore comprised of an ionisation source, an inlet, a mass analyser and a detector. Variations on each stage allow the production of a wide range of mass spectrometers which are suitable for different applications.



**Figure 1.6: A schematic block diagram of a mass spectrometer**

Sections in grey are only used during tandem mass spectrometry experiments.

## Ionisation

Ionisation of analytes can be carried out in a number of ways. Common ionisation methods include Electron ionisation (EI), Chemical Ionisation (CI), Fast Atom Bombardment (FAB), Matrix-assisted Laser Desorption/Ionisation (MALDI),

Electrospray Ionisation (ESI) and Atmospheric Pressure Chemical Ionisation (APCI). Only ESI will be discussed here. A more detailed account of other methods can be found elsewhere (de Hoffmann and Stroobant, 2007).

### **Electrospray Ionisation (ESI)**

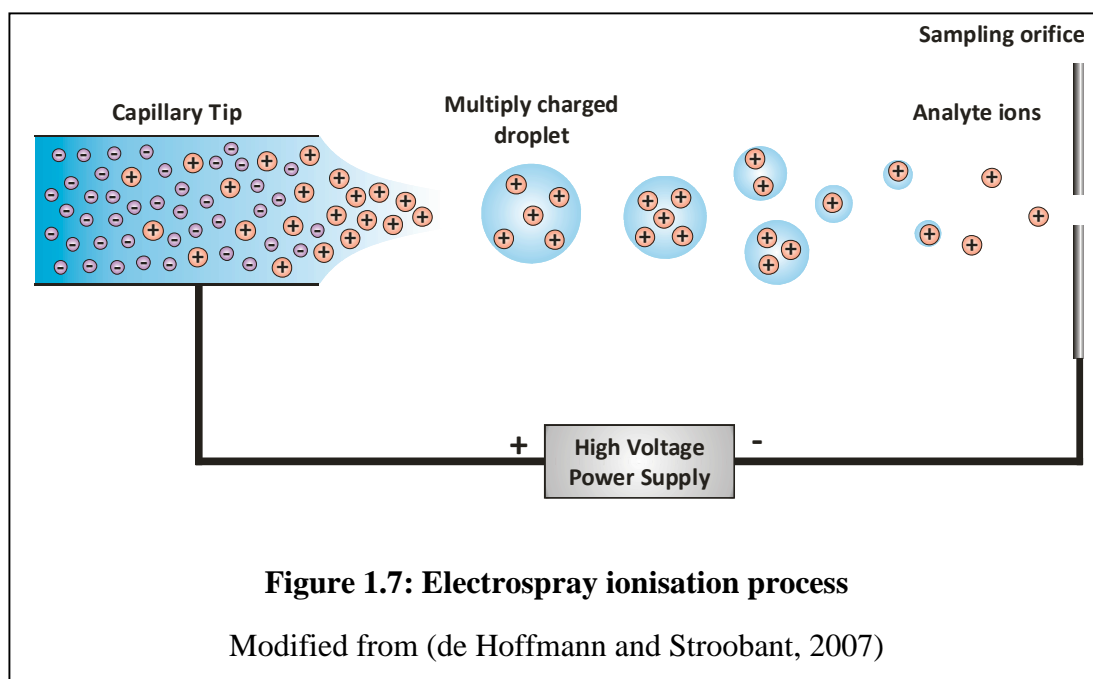
Electrospray Ionisation was first reported by Dole (Dole *et al.*, 1968) in the late 1960's, and was subject to major improvements in the 1980's by Fenn and co-workers (Yamashita and Fenn, 1984, 1984).

The analyte is dissolved in a volatile solvent before the solution is introduced in to the source region by means of a conductive capillary held at high potential difference relative to the walls of the ion source. In positive mode, the migration of positive ions to the surface of the liquid causes an instability as Coulombic repulsive forces overcome the liquid's surface tension. This results in the formation of a mist of positively charged droplets. There are a number of proposed mechanisms for the generation of analyte ions from these charged droplets. Two main mechanisms are the charged residue model (CRM) and the ion evaporation model (IEM).

In the CRM mechanism, solvent evaporation causes an increase in charge density at the surface of the droplets until it reaches a critical point known as the Rayleigh limit. At this point, the electrostatic repulsion of the ions is greater than that of the surface tension causing fission of the droplet. The resultant smaller droplets undergo multiple rounds of desolvation and fission until droplets containing only one solute molecule are formed. Analyte ions are then ejected in to the gas phase by electrostatic repulsion (Dole *et al.*, 1968).

The IEM mechanism proposes that, as the solvent evaporates from the charged droplets, it becomes electrostatically favourable for analyte ions evaporate from the droplet surface (Iribarne and Thomson, 1976).

The ions then enter the analyser region via a sampling orifice.



## Mass analysers

The mass analyser is the second major variable in the design of a mass spectrometer. Common mass analysers include ion traps, Orbitraps, time-of-flight (TOF), Fourier transform ion cyclotron resonance (FTICR), and quadrupoles. Quadrupole and time-of-flight analysers will be discussed here, detailed descriptions of other analyser types can be found elsewhere (de Hoffmann and Stroobant, 2007).

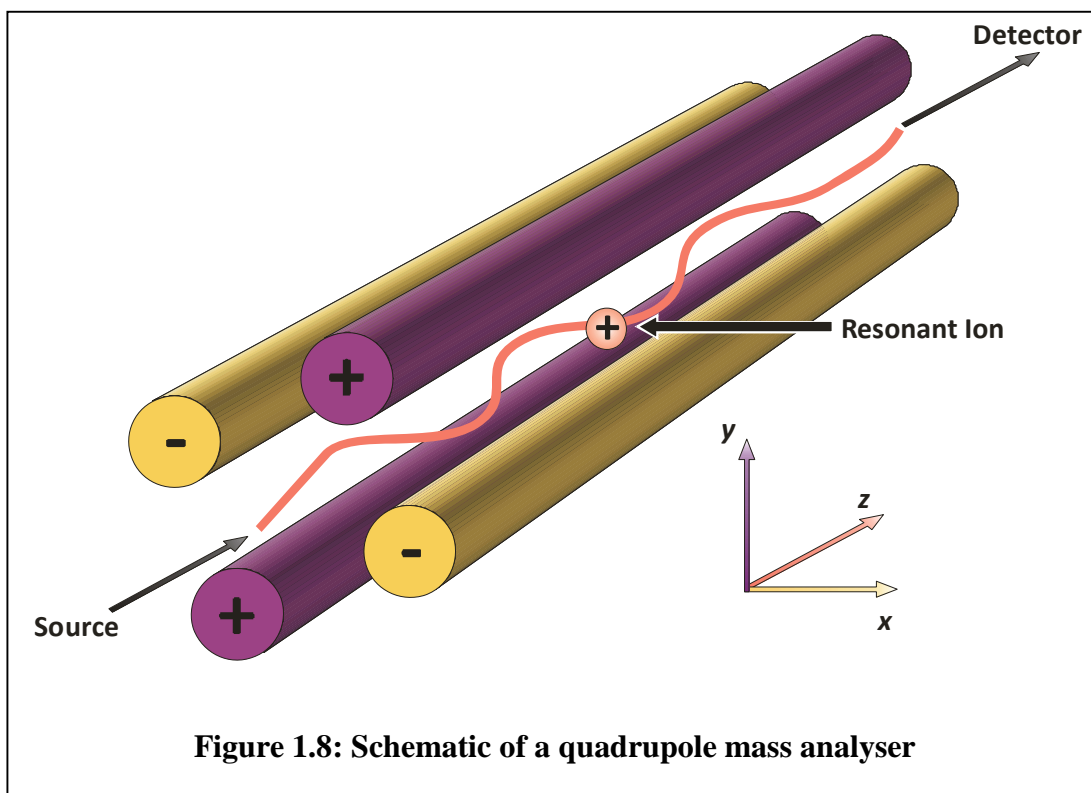
## Quadrupole

The quadrupole analyser (Paul and Steinwedel, 1953) (also known as a quadrupole mass filter) is a scanning analyser, producing a mass spectrum by sequentially scanning individual mass-to-charge ratios over a selected range.

The quadrupole comprises four cylindrical metal rods held in parallel in a square array. Ions generated in the source region of the instrument are transported in to the space between the rods. A direct current (DC) voltage and a radio frequency alternating current (AC) voltage (often referred to as the RF voltage) is applied to each diagonally opposed pair of rods. Each pair of rods receives a voltage of the same amplitude but opposite sign. This results in an electrostatic field which causes ions to oscillate in the  $x$  and  $y$  directions, while they traverse the length of the quadrupole region ( $z$ ). For a set DC/RF voltage, only ions of a specific  $m/z$  will be transmitted through the quadrupole region as they will maintain a stable oscillating trajectory. Ions outside of this  $m/z$  range have unstable trajectories and will undergo collisions with the quadrupole rods resulting in neutralisation of the ions.

A mass spectrum is obtained by increasing the RF and DC voltages simultaneously permitting ions of increased  $m/z$  to traverse the quadrupole to the detector. The intensity of the ion signal at the detector is then plotted versus the  $m/z$  being transmitted by the quadrupole.





Quadrupole analysers can be used in RF mode only. This allows all ions above a certain  $m/z$  (determined by the amplitude of the RF voltage) to traverse the quadrupole region. Ions transmitted in this way are systematically focused to the centre of the space between the rods, even after deflection due to collision with other ions. The resultant focussing effect is important for improving the transmission of ions after collisions.

### Time of Flight

Initially conceived as a linear analyser and first produced as a commercial instrument in this form (Wiley and McLaren, 1955). The development of the TOF analyser and hence its use in mainstream applications was significantly delayed until the early 1980's. There was a renewed interest in the technology when faster electronics became available that could be capable of handling the flow of data from the analyser.

Packets of ions (produced either by a pulsed ionisation source, or a transient application of focusing lenses) are introduced from the source region. The ions are accelerated by a potential ( $V_s$ ) and traverse a field-free region of a known distance ( $d$ ) before reaching the detector. The time taken for the ions to travel the length of the field-free region ( $t$ ) is converted to a mass-to-charge ratio using the relationship:

$$t^2 = \frac{m}{z} \left( \frac{d^2}{2V_s e} \right)$$

### 1.1

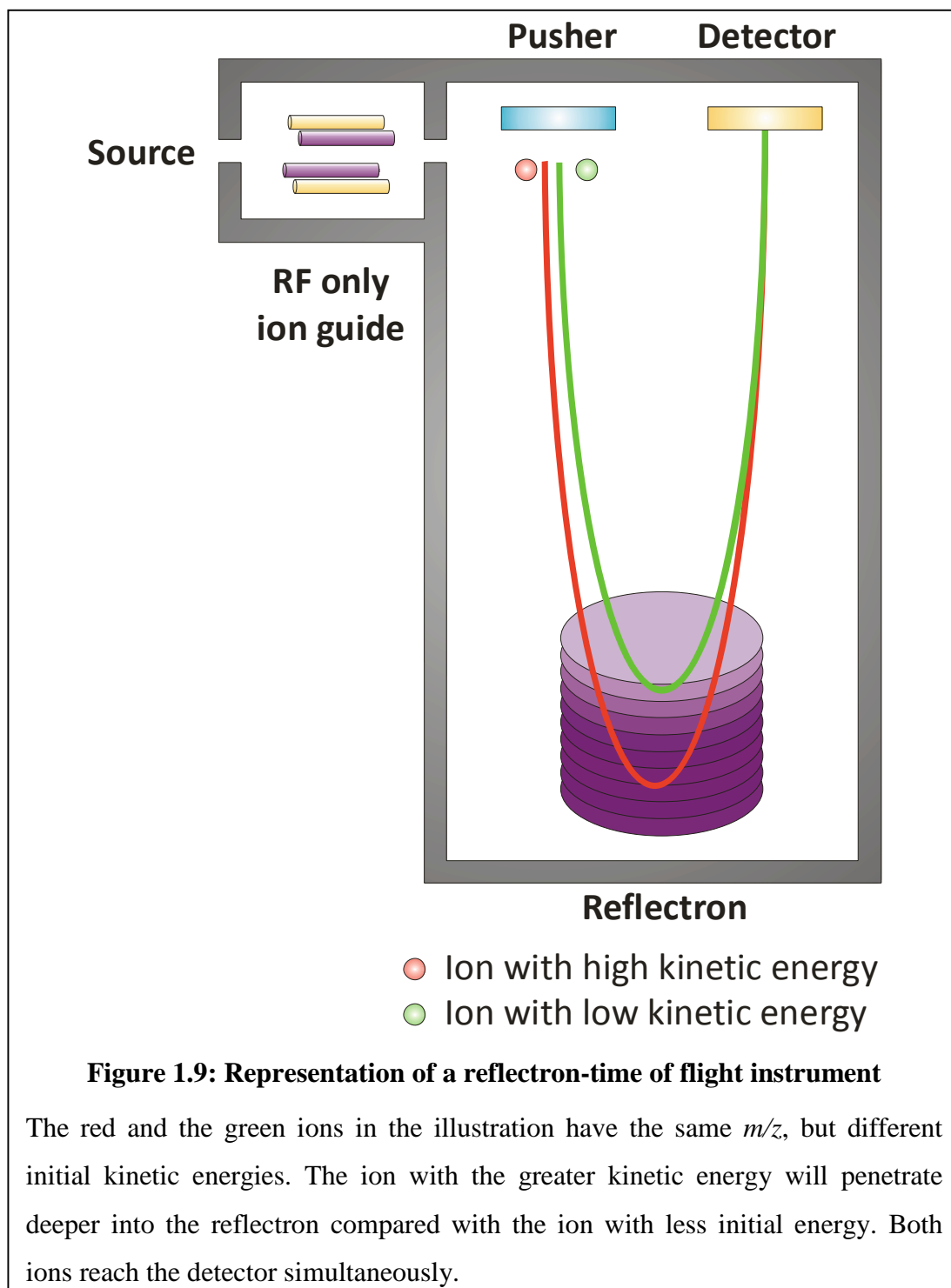
Benefits of this type of mass analyser include a potentially unlimited upper mass range, and very high sensitivity due to the high transmission efficiency. The main drawback of a linear TOF is a low resolution compared with some other analysers. This reduced resolution is due to a number of factors including the duration of the ion pulse, the volume of the ion packet and the initial kinetic energy of the ions.

The different initial kinetic energies of the ions results in different velocities for ions of the same  $m/z$ . The resultant spread of arrival times causes broadening of the mass spectral peak. One method of overcoming this problem is the use of a reflectron. A reflectron is comprised of a series of ring electrodes which act as an ion mirror, deflecting the packet of ions back in to the field-free flight tube, slightly off their original axis. This has two benefits for resolution, firstly, the distance travelled in the field-free region is doubled, causing better spatial separation of ions of different  $m/z$  and secondly, the correction of the kinetic energy dispersion of ions of the same  $m/z$ . Ions with greater initial kinetic energy will have a higher velocity. When they encounter the electrostatic field of the reflectron, they will penetrate deeper than an ion of lower kinetic energy. The reflected ions of the same  $m/z$  then have the same

arrival time at the detector. This increase in resolution is however at the expense of some sensitivity and the introduction of a kinetic energy range limitation.

An additional method for reducing the spread of initial kinetic energies of ions before analysis in a TOF, is to use delayed pulsed extraction. It is more commonly used in instruments with pulsed ion sources (e.g. MALDI). Immediately after formation, ions are allowed to expand in to a field free region in the source. After a delay of up to several microseconds, a voltage pulse is applied to an electrode grid to extract the ions from the source region. This helps to even out the kinetic energy spread of the ions as those that have spent longer in the source region receive more energy than those that have travelled further from the extraction electrode (Vestal *et al.*, 1995).

For a TOF analyser to be coupled to a continuous ion source such as ESI, an interface for sampling the ion beam must be used. Orthogonal injection can be used to generate packets of ions which are directed off axis from the source beam to a detector or reflectron (Dawson and Guilhaus, 1989). Ions enter a field-free region of the orthogonal accelerator before a transient injection voltage is applied to a pusher plate. The ions then traverse the field-free flight tube (via a reflectron, if present) to the detector. In practice, the pulsed electric field applied to the pusher plate operates at a frequency of several kilohertz. Any ions not sampled to the analyser are lost.



## Detectors

Various types of detector can be used to detect ions after mass separation. Some detectors that have been employed include: photographic plates, Faraday cups, electron multipliers, photon multipliers and array detectors.

A widely used detector is a microchannel plate (MCP). An MCP is made of an array of small electron multiplier channels, approximately 4-25  $\mu\text{m}$  in diameter and a few millimetres long. The input side of the plate is held at -1 to 2 kV relative to the output side. Ions collide with a conversion dynode on the surface of the plate. The dynode emits electrons which are directed in to the channels by a semiconductor coating. The channels act as continuous dynodes resulting in the multiplication of electrons. Amplifications in electron numbers of  $10^4$  can be achieved by a simple channel or up to  $10^8$  with the use of multiple plates. The cascade of electrons is collected at an anode and the current measured. A single ion will only activate a few channels so it is possible to detect multiple ions simultaneously. The MCP channels require a period of time to recover after detecting an ion before they can be activated again (dead time). It is therefore important to not saturate the detector with signals as subsequent ions may not be detected.

### **Data systems**

A modern mass spectrometer generally has a data system which is required for control of the mass spectrometer, and acquisition and processing of the data recorded by the mass spectrometer. A data acquisition system is required to convert analogue signals recorded by the mass spectrometer in to digital signals that can be processed by the data system. Different data acquisition systems are used in different types of mass spectrometer.

### **Analogue to digital converter**

An analogue to digital converter (ADC) is commonly used in conjunction with scanning analysers like quadrupoles. An ADC records the amplitude of the voltage from the detector at regular time intervals. The sampling frequency of the ADC

depends on the scan speed of the mass analyser (mass range per unit time) and the desired resolution. If scan speed or resolution is increased, the sampling rate of the ADC must be increased. For a quadrupole scanning 1000 mass units in 1 s, with 10 data points per peak, the sampling frequency must be at least 10 kHz. The sampling frequency required for TOF instruments (capable of 50 mass units in 1  $\mu$ s) must be at least 500 MHz. As the volume of data is dependant on the number of data points recorded, and not number of ions detected, the rate of data transfer and data storage capacity requires the use of a summing memory which accumulates data for a period of time before forwarding to the data system.

### **Time to digital converter**

An alternative method of converting analogue signals to digital signals which is often used in a TOF instrument is a time to digital converter (TDC). In contrast with an ADC which records voltage at a regular sampling frequency, a TDC counts voltage pulses that exceed a set amplitude threshold, and records the start and end time of the pulse. The list of recorded times are stored in a histogram memory. The volume of information transferred from the histogram memory is relatively small as the size of the list is proportional to the number of ions detected in that TOF cycle. The histogram memory can be used to sum the detected events from a number of flight cycles. As the TDC is a counting device, if two or more ions arrive at the detector simultaneously in one flight cycle, only one pulse is counted. This is also true for two ions arriving in rapid succession, as the TDC has a counting dead time after each ion event before it can register another count. Saturation of the detector in this way results in a reduction in mass accuracy. It is therefore more suited to applications detecting small quantities of ions for a long period of time.

## Tandem Mass Spectrometry

Single mass analyser mass spectrometers can be used to measure the molecular mass of an analyte, but if greater structural information is to be obtained, a tandem mass spectrometry experiment must be performed. Tandem mass spectrometry (MS/MS) couples two mass analysers, of the same or different types, allowing the isolation and fragmentation of selected  $m/z$  species in the first analyser and mass separation and detection using the second analyser.

A common method of fragmentation carried out in MS/MS experiments is collision-induced-dissociation (CID) (Jennings, 1968). Ions of selected  $m/z$  (precursor ions) enter a collision cell containing inert gas molecules. Collisions with the gas molecules cause the ions to fragment into a mixture of product ions and neutral fragments. The product ions are then analysed.

MS/MS experiments of two types can be performed, these are referred to as: in-space and in-time. An in-time experiment can be carried out in a mass analyser capable of trapping ions e.g. ion trap. RF and DC fields are applied to select an ion of a given  $m/z$ . Fragmentation of the ions can then be carried out by a number of methods including electron capture dissociation (ECD) (Zubarev *et al.*, 1998), electron transfer dissociation (ETD) (Syka *et al.*, 2004), infrared multiphoton dissociation (IRMPD), CID and others. The fragments are analysed by the same analyser.

In-space experiments use instruments where the mass analysers are arranged in sequence. An example of one of these instruments is a quadrupole – time-of-flight (Q-TOF) instrument. In a Q-TOF, ions of a particular  $m/z$  are selected by the quadrupole. The precursor ions undergo CID in a collision cell containing an inert gas such as argon. The product ions are then transmitted to the TOF analyser.

## **Ambient mass spectrometry**

Ambient mass spectrometry is described as mass spectrometric analysis with no or minimal sample preparation, using direct sampling and ionisation at ambient conditions (Venter *et al.*, 2008). Since the introduction of desorption electrospray ionisation (DESI) in 2004 (Takats *et al.*, 2004) there have been a number of other ambient ionisation sources developed including: direct analysis in real time (DART) (Cody *et al.*, 2005), desorption atmospheric pressure chemical ionisation (DAPCI) (Takats *et al.*, 2005), atmospheric pressure solids analysis probe (ASAP) (McEwen *et al.*, 2005), extractive electrospray (EESI) (Chen *et al.*, 2006), and neutral desorption extractive electrospray (ND-EESI) (Chen *et al.*, 2007). A comprehensive list of current ambient ionisation sources can be found in Table 1.



Table 1: A compilation of atmospheric pressure-surface sampling/ionisation techniques (Modified from (Van Berkel *et al.*, 2008))

Technique name	Acronym	Surface-sampling approach	Dominant process	ionisation	Selected references
Atmospheric pressure thermal desorption	APTDI	Thermal desorption	Liberation of organic salts from surface		(Chen <i>et al.</i> , 2006)
Thermal desorption/atmospheric pressure chemical ionisation	TD/APCI		APCI discharge	corona	(Ebejer <i>et al.</i> , 2005)
Atmospheric pressure solids analysis probe	ASAP				(McEwen <i>et al.</i> , 2005)
Laser diode thermal desorption	LDTD				(Wu <i>et al.</i> , 2007)
Desorption atmospheric pressure chemical ionisation	DAPCI				(Williams and Scrivens, 2005)
Direct analysis in real time	DART		APCI-like		(Cody <i>et al.</i> , 2005)
Desorption atmospheric pressure photoionisation	DAPPI		APPI		
Plasma-assisted desorption/ionisation	PADI		APCI-like		(Ratcliffe <i>et al.</i> , 2007)
Dielectric barrier discharge ionisation	DBDI				(Na <i>et al.</i> , 2007)
Atmospheric pressure glow discharge desorption ionisation	APGDDI				(Andrade <i>et al.</i> , 2008)
Laser ablation/atmospheric pressure chemical ionisation	LA/ICP	Laser (ablation)	Secondary ionisation by ICP		(Gunther and Hattendorf, 2005)

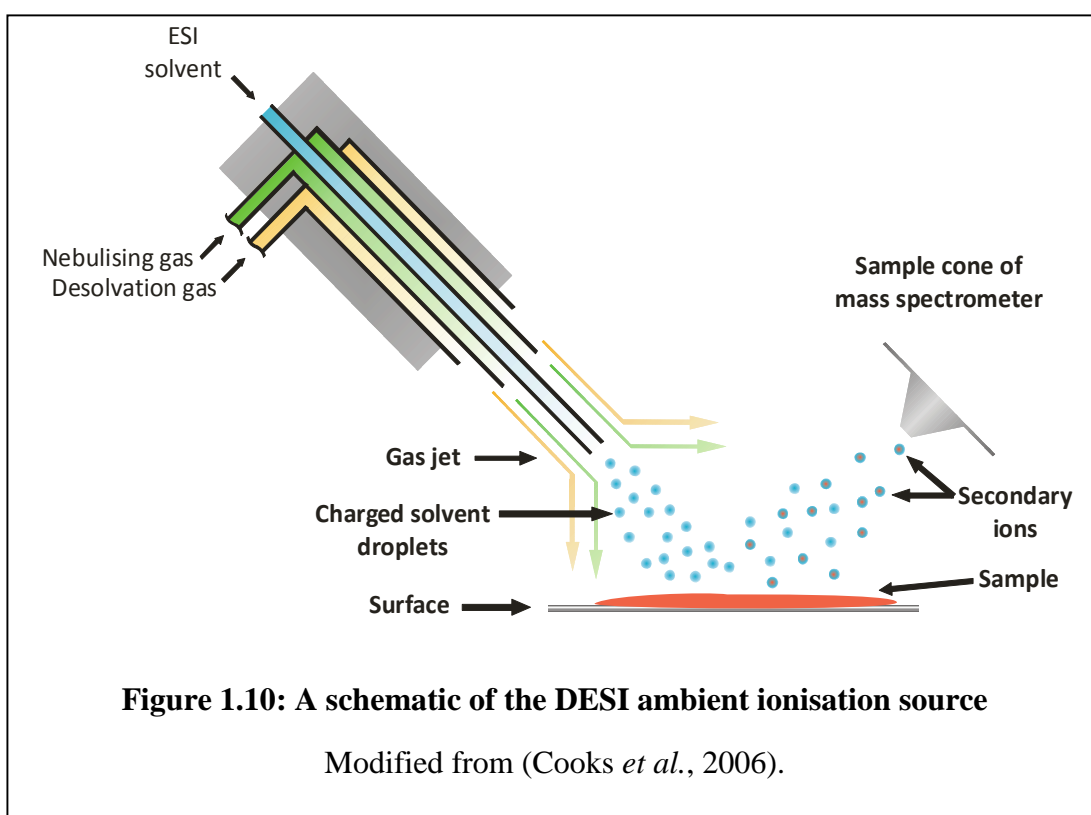
Table 1 (continued)

Technique name	Acronym	Surface-sampling approach	Dominant process	ionisation	Selected references
Laser desorption/atmospheric pressure ionisation	LD/APCI	Laser (ablation)	Secondary ionisation by APCI	ionisation	(Coon <i>et al.</i> , 2002)
Laser desorption/Electrospray ionisation	LD/ESI	Secondary ionisation by ESI			
Electrospray-assisted laser desorption/ionisation	ELDI				(Shiea <i>et al.</i> , 2005)
Laser ablation with electrospray ionisation	LAESI				(Nemes and Vertes, 2007)
Infrared laser assisted desorption electrospray ionisation	IR LADESI				
Matrix-assisted laser desorption electrospray ionisation	MALDESI				(Sampson <i>et al.</i> , 2006)
Atmospheric pressure matrix-assisted desorption/ionisation	AP-MALDI	Matrix-assisted ionisation			(Creaser and Ratcliffe, 2006)
Desorption electrospray ionisation	DESI	Liquid and gas desorption	jet ESI-like		(Takats <i>et al.</i> , 2004)
Desorption sonics spray ionisation	DeSSI		SSI-like		(Haddad <i>et al.</i> , 2006)
Easy ambient sonic spray ionisation	EASI				(Haddad <i>et al.</i> , 2008)
Jet desorption electrospray ionisation	JeDI		ESI-like		
Neutral desorption extractive electrospray ionisation	NDEESI		Secondary ionisation by ESI		(Chen <i>et al.</i> , 2007)
Liquid microjunction surface-sampling probe	LMJ-SSP	Liquid surface-sampling probe	ESI, APCI – discharge	corona	(Van Berkel <i>et al.</i> , 2002)
Sealing surface-sampling probe	SSSP		ESI		(Luftmann, 2004)

## ESI related ambient ionisation sources

### Desorption electrospray ionisation

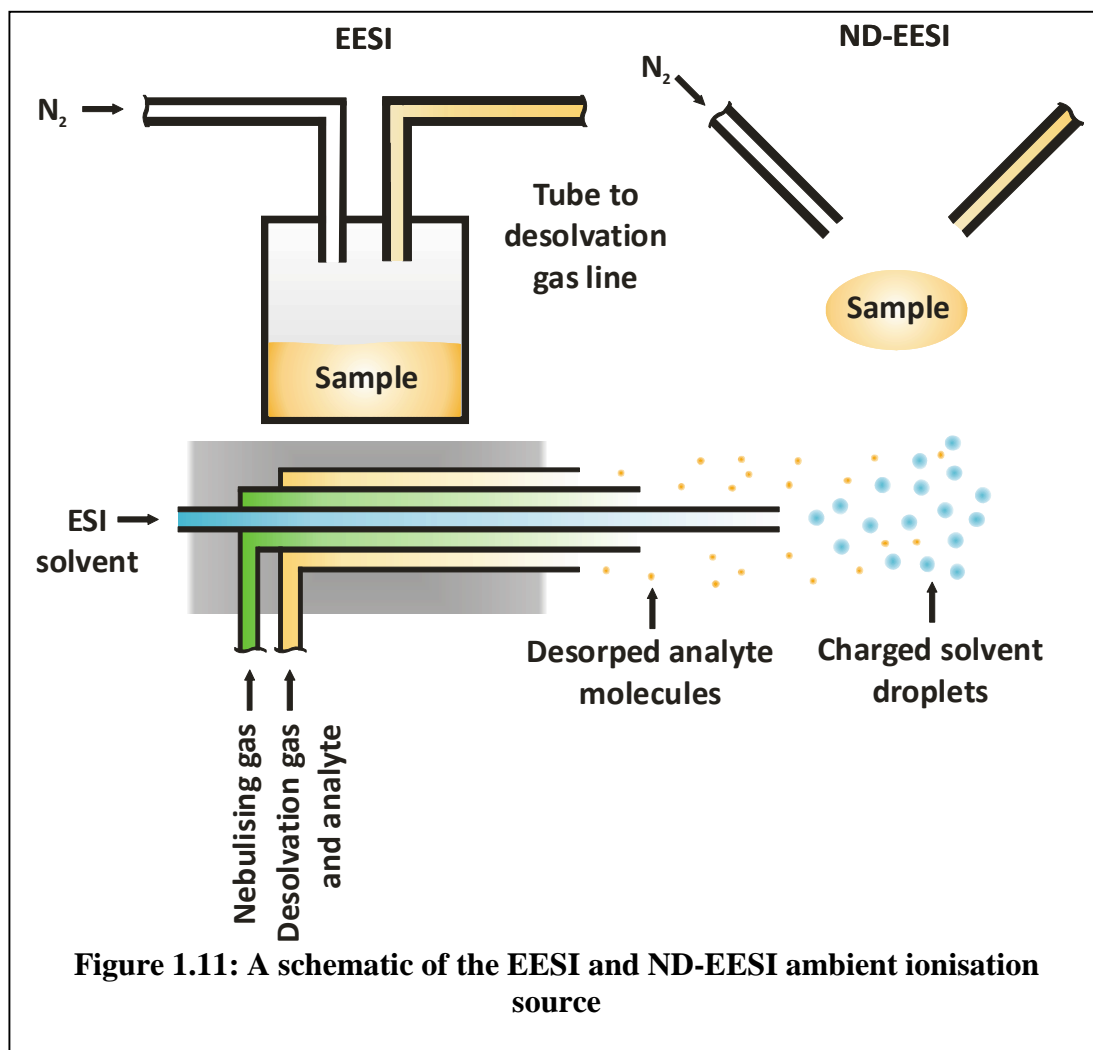
DESI is a variation on ESI whereby the analyte sample is not pre-dissolved in the ESI solvent, but is instead held in the path of the ESI spray between the capillary and the source inlet. A suggested mechanism for ionisation during a DESI experiment has been proposed by Venter *et al.* (Venter *et al.*, 2008). Aqueous droplets less than 10  $\mu\text{m}$  in diameter impact the sample surface. Initial droplets pre-wet the surface causing analyte molecules to dissolve. Later-arriving droplets impact the surface solvent layer resulting in its disruption and formation of offspring droplets containing dissolved analyte. Charging of the analyte molecules then progresses by ESI mechanisms.



Non destructive sampling of a wide variety of surface types including: glass, cardboard, paper, leather and skin has been achieved. Using a confined diameter solvent beam, it is possible to obtain spatially resolved chemical information with DESI, allowing sensitive imaging under ambient conditions (Venter *et al.*, 2008). DESI imaging of phospholipids in rat brain tissue sections has been achieved with a spatial resolution of < 500  $\mu\text{m}$ . The advantages of DESI imaging compared with the existing MALDI imaging technique are higher throughput, and no requirement to pre-treat the surface with matrices. The disadvantages of the DESI imaging approach are lower spatial resolution (250 – 500  $\mu\text{m}$  compared with 25 – 200  $\mu\text{m}$  in MALDI imaging (Liam and Ron, 2007)), and only the surface or near-surface compounds will be analysed as the solvent beam does not penetrate in to the sample.

### **Extractive electrospray ionisation and neutral desorption extractive electrospray ionisation**

EESI and the closely related ND-EESI also use an ESI related setup for ambient sample analysis. Both techniques use a nitrogen gas flow directed at a sample to generate an aerosol of  $\text{N}_2$  and analyte molecules. For EESI, the sample is a liquid or volatile compounds in an enclosed vessel. ND-EESI samples exposed surfaces, either solid or liquid. The analyte aerosol is the sampled in to the desolvation gas line of an un-modified ESI source (Chen *et al.*, 2007). ESI solvent is ionised at the capillary tip before it is allowed to mix with the desolvation gas/analyte aerosol. The precise mechanism of ionisation of the analyte molecules is not currently known, however it has been proposed that analytes are extracted from neutral droplets, into charged droplets where they then encounter an ESI-like mechanism.

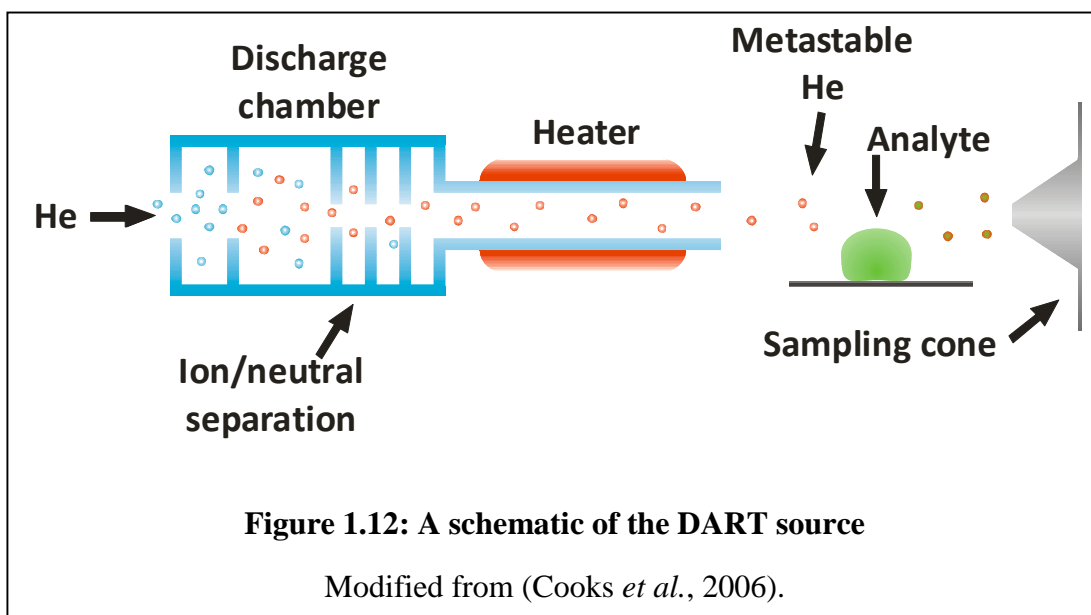


### APCI related ambient ionisation sources

APCI is an ionisation method that uses gas-phase ion-molecule reactions at atmospheric pressure to generate charged analyte ions. Analytes dissolved in a solvent are nebulised by nitrogen at a high flow rate. Droplets are then heated causing evaporation of the solvent. The hot gas and sample leave the source probe and are directed to a corona discharge electrode. Ionisation occurs due to proton transfer or adduct formation from neutral metastable molecules formed in the electric field.

## Direct analysis in real time

The DART source uses the flow of helium gas through a corona discharge field to form reactive species used to ionise analyte molecules. In the proposed mechanism by Cody *et al.*, metastable helium atoms are generated when the gas is passed through the corona discharge field. These neutral metastable atoms react with ambient water and oxygen to produce ionising species which are carried to the sample surface by a stream of heated gas. Analyte ions generated by reaction with the ionising species are then sampled in to the mass spectrometer (Venter *et al.*, 2008).



## Desorption atmospheric pressure chemical ionisation

In DAPCI, a solvent is nebulised and heated as with APCI. The stream of heated nitrogen gas and solvent vapour are then directed over the sample surface where analyte molecules are thermally desorbed in to the gas phase. The gaseous analyte molecules are then ionised in the corona discharge field by an APCI like mechanism.

## **Atmospheric solids analysis probe**

ASAP is a thermal desorption method similar to that in DAPCI. Molecules on the sample surface are desorbed using a stream of heated nitrogen gas without any additional solvent. The analyte molecules are subsequently ionised in the corona discharge field and then sampled in to the mass spectrometer.

## **Ion mobility spectrometry**

Ion mobility spectrometry is an analytical technique currently employed for the detection of drugs, explosives and chemical warfare agents. The ion mobility approach uses the migration of analyte ions under the influence of an electrostatic field through a drift cell containing an inert buffer gas. Separations of the ions result from interactions with the buffer gas. The separation is dependant on the mass, charge and shape of the analyte ion.

Ion mobility spectrometry can be carried out in three different methods: drift cell ion mobility spectrometry (DCIMS), high-field asymmetric wave form ion mobility (FAIMS), and travelling wave ion mobility spectrometry (TWIMS). A description of FAIMS can be found elsewhere (Guevremont and Purves, 1999).

### **DCIMS**

DCIMS separates ions based on their different velocities attained when accelerated through a drift tube, filled with a neutral gas, by a constant electric field ( $E$ ) (Cohen and Karasek, 1970). The drift tube has a constant electric field generated by a series of electrodes. An ion achieves a quasi-constant velocity ( $v_d$ ) due to the acceleration by the field, and retardation by collisions with the neutral gas. The ion mobility ( $K$ ) is the ratio of  $v_d$  to electric field strength  $E$ .

$$K = \frac{v_d}{E}$$

## 1.2

The ion mobility is usually expressed as reduced mobility ( $K_0$ ) which is the mobility of the ion at standard temperature and pressure ( $P_0$  of 760 Torr and  $T_0$  of 273.15 K) so that:

$$K_0 = K \frac{PT_0}{TP_0} = K \frac{P \times 273.15}{T \times 760}$$

## 1.3

Using kinetic theory (Edward and Earl, 2005), the reduced mobility  $K_0$  can be related to the collision cross section of the ion species by the following equation:

$$K_0 = \frac{3ze}{16N_0} \times \frac{1}{\sigma} \sqrt{\left(\frac{2\pi}{\mu k_B T}\right)}$$

## 1.4

Where  $z$  is the number of charges,  $e$  is the electronic charge,  $N_0$  is the buffer gas number density at standard temperature and pressure,  $\mu$  is the reduced mass of the buffer gas and the ion,  $k_B$  is Boltzmann's constant,  $T$  is the effective temperature and  $\sigma$  is the average collision integral or collision cross section. The average collision cross section can be obtained by averaging all possible collision geometries (Clemmer and Jarrold, 1997). Exact calculation of an average collision cross section is not trivial and many models have been proposed (Lee *et al.*, 1995; von Helden *et al.*, 1995; Wessel *et al.*, 1996; von Helden *et al.*, 2002). Approaches pioneered by Bowers and co-workers have been used to relate theoretical average collision cross



sections with those obtained experimentally. This approach uses molecular dynamics calculations to generate three-dimensional structures of molecules, minimising these structures to determine lowest-energy conformation of these molecules, and using programs (Wyttbach *et al.*, 1997) to calculate theoretical cross sections. These calculations have been shown to be in good agreement with experimental observations (Wyttbach *et al.*, 1996).

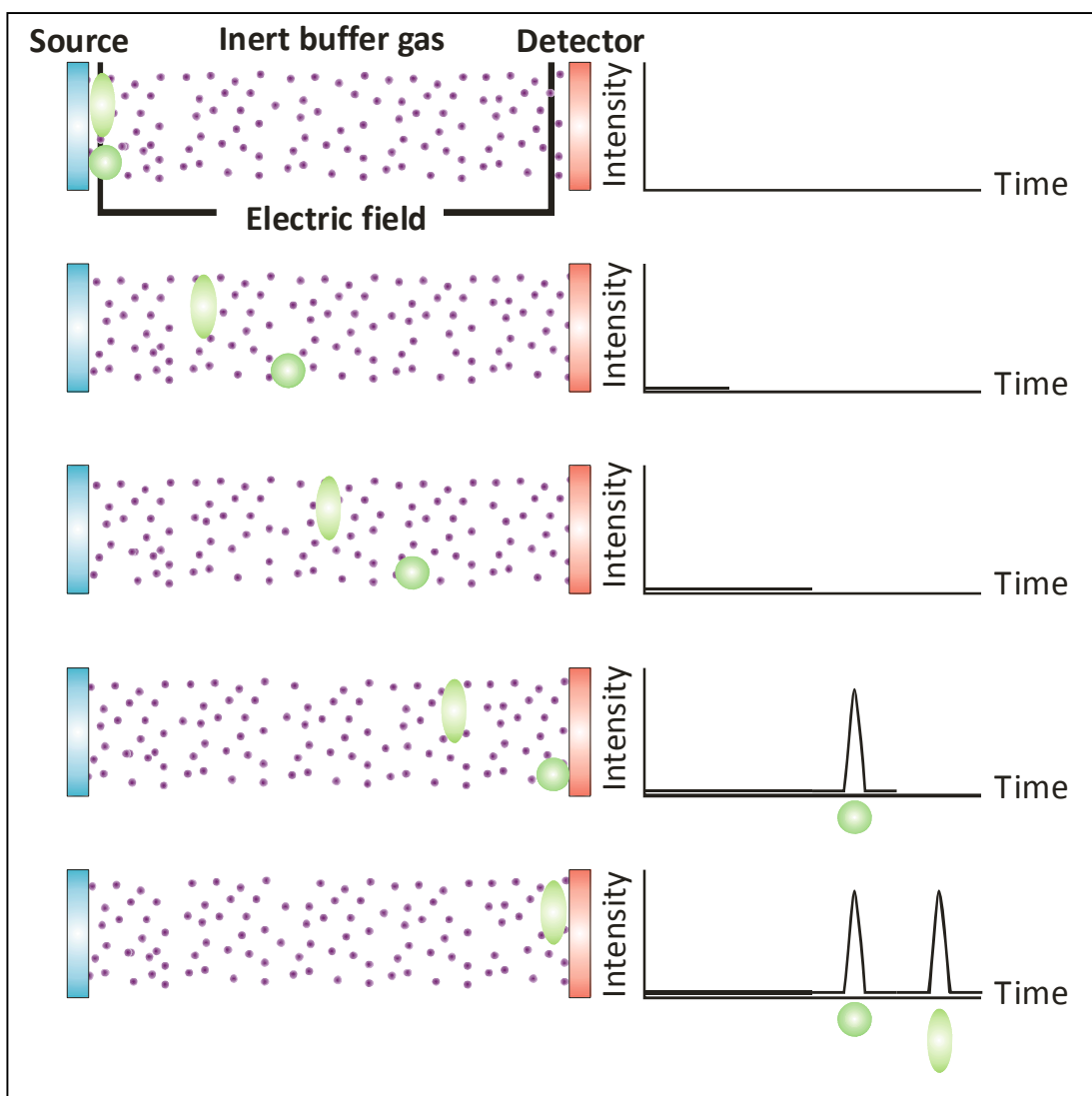


**Figure 1.13: A representation of DCIMS**

The two green ions have the same  $m/z$  but different cross sections. The more compact ion encounters fewer interactions with the buffer gas (purple) than the extended ion. This results in a greater velocity, and earlier arrival time at the

## **DCIM-MS**

Ion mobility (IM) has been coupled with a range of mass spectrometers. Ionisation sources including ESI (Wittmer *et al.*, 1994; Wu *et al.*, 1998) and MALDI (von Helden *et al.*, 1995) have been used to generate ions for IM analysis. Mass analysers including quadrupoles (Shelimov *et al.*, 1997), TOF (Srebalus *et al.*, 1999), and FTICR (Bluhm *et al.*, 2000) have been used to perform mass analysis after IM separation.

DCIMS approaches have been used to study a wide variety of molecules including polymers (Wytenbach *et al.*, 1997; Gidden *et al.*, 2002), peptides (Wytenbach *et al.*, 1996), proteins and nucleic acids (Gidden and Bowers, 2003).

The main limitation of DCIM-MS instruments described to date is a lack of sensitivity and ease of use. All instruments described have been constructed by research groups and so have limitations compared to commercial alternatives.

## **TWIMS**

In comparison with DCIMS, where a constant electric field is applied to the drift tube, travelling wave ion mobility spectrometry (TWIMS) uses a travelling voltage wave to propel ions through a mobility cell containing neutral gas molecules. The travelling wave (T-Wave) is generated by applying transient DC voltages to electrodes in a stacked ring ion guide (SRIG). A SRIG is composed of a series of ring electrodes that are arranged orthogonally to the axis of ion transmission. Opposite phases of RF voltage are applied to pairs of adjacent electrodes. This generates a radially-confining potential barrier preventing ion loss by diffusion to the

wall of the SRIG. Ions are propelled through the SRIG by superimposing a DC potential on the RF potential applied to one pair of adjacent electrodes. This potential moves along ring electrode pairs across the length of the SRIG at regular time intervals generating a series of T-Waves. A SRIG operated in this configuration will be referred to as a travelling wave ion guide (TWIG).

## TWIM-MS

The Synapt HDMS (high definition mass spectrometry) system (Waters corp., Milford, USA) is the first commercial instrument to incorporate ion mobility separation.

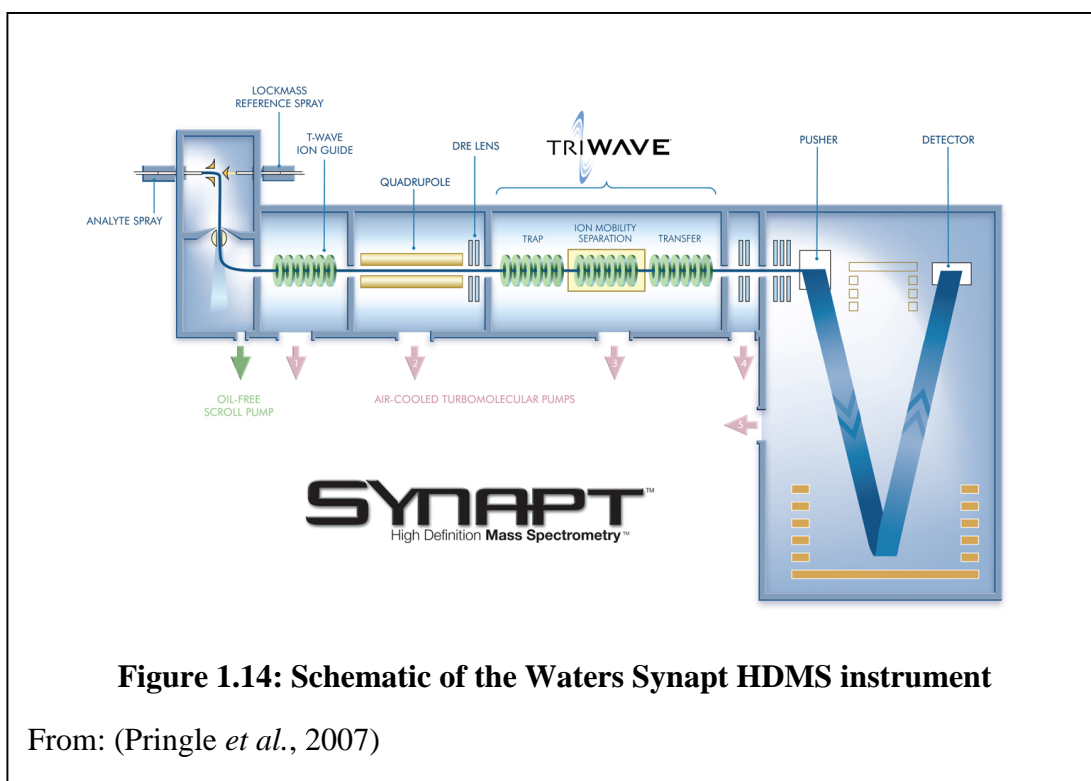


**Figure 1.14: Schematic of the Waters Synapt HDMS instrument**

From: (Pringle *et al.*, 2007)

The Synapt HDMS incorporates a series of three TWIGs ('TriWave' device) for ion mobility separation within a Q-TOF instrument. The 'TriWave' device is positioned between the quadrupole and the (oa)-TOF. The first TWIG is referred to as the trap, the second is the ion mobility separator (IMS), and the third is the transfer TWIG.

The final electrode pair of the trap TWIG is DC-only. When the voltage is raised, it does not allow the passage of ions, causing them to accumulate in the TWIG. At the start of an ion mobility separation cycle, the amplitude of the voltage on this gate is lowered, typically for 100  $\mu\text{s}$ , releasing a packet of ions in to the IMS region for separation. The transfer TWIG maintains the mobility separation of the ions while delivering them to the oa-TOF.

The IMS region of the Synapt HDMS is at high pressure relative to the other regions of the instrument. It can be operated at pressures of up to 1 mbar using a range of gases (but most commonly, nitrogen). The T-Wave in this region has a repeat pattern of 6 electrode pairs which means that the DC pulse is applied to the 1<sup>st</sup> and 7<sup>th</sup> pairs of electrodes, then it is applied to the 2<sup>nd</sup> and 8<sup>th</sup> pairs etc. The velocity of the wave is derived from the distance between electrode pairs divided by the time the DC pulse remains in each pair. The velocity is given in metres per second and the operating range is from 200 to 600  $\text{m s}^{-1}$ .

Mobility separation of ions is achieved because ions with high mobility are driven through the IMS region by the T-Wave and exit faster. Ions with a lower mobility roll over the wave top and require subsequent waves to propel them further resulting in a later exit time. The amplitude of the T-Wave voltage (T-Wave height) must be optimised to ensure all ions from a single packet exit the mobility separator before the next packet is injected, while maintaining sufficient mobility separation of the ions.

To record the arrival time distribution (ATD) of the mobility separated ions, the oa-TOF acquisition is synchronised with the gated release of ions from the trap TWIG in to the mobility cell. For each packet of ions, 200 orthogonal axis pushes

(mass spectra) of the TOF analyser are recorded. The overall mobility separation time is:  $200 \times t_p$  where  $t_p$  is the pusher period. 200 mass spectra obtained from the next packet of ions are added to the data from the previous gated release. This is repeated until a desired signal-to-noise ratio for the mass spectrum is obtained.

The major advantage of this method of mobility acquisition is the recording of both arrival time information and mass spectral data of all ions in the mass spectrum.

### **Tandem MS on the Synapt HDMS**

An additional feature of the Synapt HDMS instrument is the ability to perform CID in the trap and/or transfer TWIGs, with or without prior  $m/z$  selection on the quadrupole. This allows: i) the mobility separation of product ions (trap only CID), ii) fragmentation of mobility separated ions (transfer only CID), iii) and an MS<sup>3</sup> experiment where ions are fragmented in the trap, product ions are mobility separated, and further fragmentation performed in the transfer TWIG.

The advantages of this type of instrument configuration include: i) high sensitivity. Introduction of the TriWave device does not compromise sensitivity of the Q-TOF instrument. ii) Excellent reproducibility. The reproducibility is better than  $\pm 1$  scan (in the 200 collected per ion packet injection). iii) Versatility. The ability to perform a range of mobility and MS/MS experiments provides an analytical technique of significant flexibility.

The major limitation of the Synapt HDMS instrument is the inability to directly calculate average collision cross sections from the measured drift times. Cross section estimation is however possible using calibration standards with established cross sections.

## **Cross section calibration**

The path taken by an ion traversing the mobility cell in a TWIMS device is complex and, currently, not fully understood. Therefore, the direct calculation of average collision cross sections for ions of interest is not possible. The calibration of the TWIMS device to obtain estimated average collision cross sections has been demonstrated (Ruotolo *et al.*, 2005; Wildgoose *et al.*, 2006; Ruotolo *et al.*, 2008; Scarff *et al.*, 2008; Williams and Scrivens, 2008; Thalassinou *et al.*, 2009).

A detailed method for the cross section calibration can be found in Chapter 3. The most common calibration approach relies on using the Synapt HDMS to measure the mobility of compounds of known cross section values, and to derive estimates of cross section of unknown compounds from a calibration curve.

## **Aims and objectives**

The development of new ambient ionisation sources and travelling-wave-based ion mobility mass spectrometry experiments have resulted in improved approaches for the analysis of a range of compound classes.

The requirement for rapid, sensitive and selective analysis of carbohydrates and glycoconjugates is increasing due to the greater understanding of their significance in biological systems, and their increased use as therapeutic agents.

This project focused on evaluating the use of selected ambient ionisation approaches in the analysis of pharmaceutical formulations, and investigating the potential of shape selective separations in the analysis of carbohydrates.

The aims of the project were to:

Assess the amenability of recently developed ambient ionisation approaches to the analysis of a range of pharmaceutical formulations, including the glycosylated antibiotic: erythromycin (Chapter 2). Improvements in the rate of sample analysis could provide a method of rapid batch to batch characterisation of small molecule pharmaceuticals.

Investigate the shape selective separation of two isomeric glucose polymers, (dextran and maltodextrin) ionised using a range of alkali metal cations, using a recently commercialised travelling-wave-based ion mobility mass spectrometer. Arrival time data obtained from the ion mobility separation will also be used to generate estimated collision cross sections for the molecules (Chapter 3).

Employ the shape selective separation potential of the Synapt HDMS in the rapid analysis of glycans released from glycoproteins and oligosaccharides commonly found in milk (Chapter 4). Rapid, reproducible ion mobility separations of glycan mixtures could result in a method of obtaining glycosylation profiles for individual proteins or protein mixtures in biopharmaceutical analysis or diagnostic testing.

## References

- Andrade, F. J., Shelley, J. T., Wetzal, W. C., Webb, M. R., Gamez, G., Ray, S. J. and Hieftje, G. M.** (2008). "Atmospheric pressure chemical ionization source. 2. Desorption-ionization for the direct analysis of solid compounds." *Analytical Chemistry* **80**(8): 2654-2663.
- Anthony, L., Plummer, J. T. H. and Victor, G.** (1987). Peptide-N4-(N-acetyl-[beta]-glucosaminy) asparagine amidase and endo-[beta]-n-acetylglucosaminidase from *Flavobacterium meningosepticum*. *Methods in Enzymology*, Academic Press. **Volume 138**: 770-778.
- Apweiler, R., Hermjakob, H. and Sharon, N.** (1999). "On the frequency of protein glycosylation, as deduced from analysis of the SWISS-PROT database." *Biochimica et Biophysica Acta (BBA) - General Subjects* **1473**(1): 4-8.
- Bluhm, B. K., Gillig, K. J. and Russell, D. H.** (2000). "Development of a Fourier-transform ion cyclotron resonance mass spectrometer-ion mobility spectrometer." *Review of Scientific Instruments* **71**(11): 4078-4086.
- Budnik, B. A., Lee, R. S. and Steen, J. A. J.** (2006). "Global methods for protein glycosylation analysis by mass spectrometry." *Biochimica et Biophysica Acta (BBA) - Proteins & Proteomics* **1764**(12): 1870-1880.
- Chen, H., Yang, S., Wortmann, A. and Zenobi, R.** (2007). "Neutral desorption sampling of living objects for rapid analysis by extractive electrospray



ionization mass spectrometry." *Angewandte Chemie-International Edition* **46**(40): 7591-7594.

**Chen, H., Zheng, O. Y. and Cooks, R. G.** (2006). "Thermal production and reactions of organic ions at atmospheric pressure." *Angewandte Chemie-International Edition* **45**(22): 3656-3660.

**Chen, H. W., Lai, J. H., Zhou, Y. F., Huan, Y. F., Li, J. Q., Zhang, X., Wang, Z. C. and Luo, M. B.** (2007). "Instrumentation and characterization of surface desorption atmospheric pressure chemical ionization mass Spectrometry." *Chinese Journal of Analytical Chemistry* **35**(8): 1233-1240.

**Chen, H. W., Venter, A. and Cooks, R. G.** (2006). "Extractive electrospray ionization for direct analysis of undiluted urine, milk and other complex mixtures without sample preparation." *Chemical Communications*(19): 2042-2044.

**Chen, H. W., Wortmann, A. and Zenobi, R.** (2007). "Neutral desorption sampling coupled to extractive electrospray ionization mass spectrometry for rapid differentiation of biosamples by metabolomic fingerprinting." *Journal of Mass Spectrometry* **42**(9): 1123-1135.

**Clemmer, D. E. and Jarrold, M. F.** (1997). "Ion mobility measurements and their applications to clusters and biomolecules." *Journal of Mass Spectrometry* **32**(6): 577-592.

**Cody, R. B., Laramee, J. A. and Durst, H. D.** (2005). "Versatile new ion source for the analysis of materials in open air under ambient conditions." *Analytical Chemistry* **77**(8): 2297-2302.

- Cohen, M. J. and Karasek, F. W.** (1970). "Plasma chromatography: a new dimension for gas chromatography and mass spectrometry." *Journal of Chromatographic Science* **8**(6): 330-&.
- Cooks, R. G., Ouyang, Z., Takats, Z. and Wiseman, J. M.** (2006). "Ambient mass spectrometry." *Science* **311**(5767): 1566-1570.
- Coon, J. J., McHale, K. J. and Harrison, W. W.** (2002). "Atmospheric pressure laser desorption/chemical ionization mass spectrometry: a new ionization method based on existing themes." *Rapid Communications in Mass Spectrometry* **16**(7): 681-685.
- Creaser, C. S. and Ratcliffe, L.** (2006). "Atmospheric pressure matrix-assisted laser desorption/ionisation mass spectrometry: A review." *Current Analytical Chemistry* **2**(1): 9-15.
- Dawson, J. H. J. and Guilhaus, M.** (1989). "Orthogonal-acceleration time-of-flight mass spectrometer." *Rapid Communications in Mass Spectrometry* **3**(5): 155-159.
- de Hoffmann, E. and Stroobant, V.** (2007). *Mass Spectrometry: Principles and Applications*, John Wiley and Sons Ltd.
- Dole, M., Mack, L. L., Hines, R. L., Mobley, R. C., Ferguson, L. D. and Alice, M. B.** (1968). "Molecular Beams of Macroions." *The Journal of Chemical Physics* **49**(5): 2240-2249.
- Ebejer, K. A., Brereton, R. G., Carter, J. F., Ollerton, S. L. and Sleeman, R.** (2005). "Rapid comparison of diacetylmorphine on banknotes by tandem mass spectrometry." *Rapid Communications in Mass Spectrometry* **19**(15): 2137-2143.
- Edward, A. M. and Earl, W. M.** (2005). *Transport Properties of Ions in Gases*.

- Ferrer-Miralles, N., Domingo-Espin, J., Corchero, J. L., Vazquez, E. and Villaverde, A.** (2009). "Microbial factories for recombinant pharmaceuticals." *Microbial Cell Factories* **8**: 8.
- Geyer, H. and Geyer, R.** (2006). "Strategies for analysis of glycoprotein glycosylation." *Biochimica et Biophysica Acta (BBA) - Proteins & Proteomics* **1764**(12): 1853-1869.
- Gidden, J. and Bowers, M. T.** (2003). "Gas-phase conformations of deprotonated trinucleotides (dGTT<sup>-</sup>, dTGT<sup>-</sup>, and dTTG<sup>-</sup>): The question of zwitterion formation." *Journal of the American Society for Mass Spectrometry* **14**(2): 161-170.
- Gidden, J., Bowers, M. T., Jackson, A. T. and Scrivens, J. H.** (2002). "Gas-phase conformations of cationized poly(styrene) oligomers." *Journal of the American Society for Mass Spectrometry* **13**(5): 499-505.
- Guevremont, R. and Purves, R. W.** (1999). "Atmospheric pressure ion focusing in a high-field asymmetric waveform ion mobility spectrometer." *Review of Scientific Instruments* **70**(2): 1370-1383.
- Gunther, D. and Hattendorf, B.** (2005). "Solid sample analysis using laser ablation inductively coupled plasma mass spectrometry." *Trac-Trends in Analytical Chemistry* **24**(3): 255-265.
- Haddad, R., Sparrapan, R. and Eberlin, M. N.** (2006). "Desorption sonic spray ionization for (high) voltage-free ambient mass spectrometry." *Rapid Communications in Mass Spectrometry* **20**(19): 2901-2905.
- Haddad, R., Sparrapan, R., Kotiaho, T. and Eberlin, M. N.** (2008). "Easy ambient sonic-spray ionization-membrane interface mass spectrometry for direct analysis of solution constituents." *Analytical Chemistry* **80**(3): 898-903.

- Haltiwanger, R. S. and Lowe, J. B.** (2004). "Role of glycosylation in development." *Annual Review of Biochemistry* **73**(1): 491-537.
- Hardy, M. R.** (1994). "Methods and Reviews - Methods for the Analysis of Glycoprotein Carbohydrates." *ABRF News* **5**(1).
- Harvey, D. J.** (2001). "Identification of protein-bound carbohydrates by mass spectrometry." *Proteomics* **1**(2): 311-328.
- Hossler, P., Mulukutla, B. C. and Hu, W.-S.** (2007). "Systems Analysis of N-Glycan Processing in Mammalian Cells." *PLoS ONE* **2**(8): e713.
- Iribarne, J. V. and Thomson, B. A.** (1976). "On the evaporation of small ions from charged droplets." *The Journal of Chemical Physics* **64**(6): 2287-2294.
- Jacob, G. S., Scudder, P. and William, J. L. a. G. W. H.** (1994). Glycosidases in structural analysis. *Methods in Enzymology*, Academic Press. **Volume 230**: 280-299.
- Jennings, K. R.** (1968). "Collision-induced decompositions of aromatic molecular ions." *International Journal of Mass Spectrometry and Ion Physics* **1**(3): 227-235.
- Kim, Y. J. and Varki, A.** (1997). "Perspectives on the significance of altered glycosylation of glycoproteins in cancer." *Glycoconjugate Journal* **14**(5): 569-576.
- Lee, S., Wyttenbach, T., Vohhelden, G. and Bowers, M. T.** (1995). "Gas-phase conformations of  $\text{Li}^+$ ,  $\text{Na}^+$ ,  $\text{K}^+$ , and  $\text{Cs}^+$  complexed with 18-crown-6." *Journal of the American Chemical Society* **117**(40): 10159-10160.
- Liam, A. M. and Ron, M. A. H.** (2007). "Imaging mass spectrometry." *Mass Spectrometry Reviews* **26**(4): 606-643.

- Lis, H. and Sharon, N.** (1998). "Lectins: Carbohydrate-Specific Proteins That Mediate Cellular Recognition " *Chemical Reviews* **98**(2): 637-674.
- Luftmann, H.** (2004). "A simple device for the extraction of TLC spots: direct coupling with an electrospray mass spectrometer." *Analytical and Bioanalytical Chemistry* **378**(4): 964-968.
- McEwen, C. N., McKay, R. G. and Larsen, B. S.** (2005). "Analysis of solids, liquids, and biological tissues using solids probe introduction at atmospheric pressure on commercial LC/MS instruments." *Analytical Chemistry* **77**(23): 7826-7831.
- Merkle, R. K., Cummings, R. D. and Victor, G.** (1987). Lectin affinity chromatography of glycopeptides. *Methods in Enzymology*, Academic Press. **Volume 138**: 232-259.
- Merkle, R. K., Poppe, I. and William, J. L. a. G. W. H.** (1994). Carbohydrate composition analysis of glycoconjugates by gas-liquid chromatography/mass spectrometry. *Methods in Enzymology*, Academic Press. **Volume 230**: 1-15.
- Na, N., Zhao, M. X., Zhang, S. C., Yang, C. D. and Zhang, X. R.** (2007). "Development of a dielectric barrier discharge ion source for ambient mass spectrometry." *Journal of the American Society for Mass Spectrometry* **18**(10): 1859-1862.
- Nemes, P. and Vertes, A.** (2007). "Laser ablation electrospray ionization for atmospheric pressure, in vivo, and imaging mass spectrometry." *Analytical Chemistry* **79**(21): 8098-8106.
- Ohtsubo, K. and Marth, J. D.** (2006). "Glycosylation in Cellular Mechanisms of Health and Disease." *Cell* **126**(5): 855-867.

- Patel, T., Bruce, J., Merry, A., Bigge, C., Wormald, M., Parekh, R. and Jaques, A.** (1993). "Use of hydrazine to release in intact and unreduced form both N- and O-linked oligosaccharides from glycoproteins." *Biochemistry* **32**(2): 679-693.
- Paul, W. and Steinwedel, H.** (1953). "A new mass spectrometer without a magnetic field." *Journal Name: Zeitschrift fuer Naturforschung (West Germany) Divided into Z. Naturforsch., A, and Z. Naturforsch., B: Anorg. Chem., Org. Chem., Biochem., Biophys.,; Journal Volume: Vol: a8; Other Information: Orig. Receipt Date: 31-DEC-53; Medium: X; Size: Pages: 448-50.*
- Pringle, S. D., Giles, K., Wildgoose, J. L., Williams, J. P., Slade, S. E., Thalassinos, K., Bateman, R. H., Bowers, M. T. and Scrivens, J. H.** (2007). "An investigation of the mobility separation of some peptide and protein ions using a new hybrid quadrupole/travelling wave IMS/oa-ToF instrument." *International Journal of Mass Spectrometry* **261**(1): 1-12.
- Raman, R., Raguram, S., Venkataraman, G., Paulson, J. C. and Sasisekharan, R.** (2005). "Glycomics: an integrated systems approach to structure-function relationships of glycans." *Nat Meth* **2**(11): 817-824.
- Ratcliffe, L. V., Rutten, F. J. M., Barrett, D. A., Whitmore, T., Seymour, D., Greenwood, C., Aranda-Gonzalvo, Y., Robinson, S. and McCoustra, M.** (2007). "Surface analysis under ambient conditions using plasma-assisted desorption/ionization mass spectrometry." *Analytical Chemistry* **79**(16): 6094-6101.
- Ruotolo, B. T., Benesch, J. L. P., Sandercock, A. M., Hyung, S. J. and Robinson, C. V.** (2008). "Ion mobility-mass spectrometry analysis of large protein complexes." *Nature Protocols* **3**(7): 1139-1152.

- Ruotolo, B. T., Giles, K., Campuzano, I., Sandercock, A. M., Bateman, R. H. and Robinson, C. V.** (2005). "Evidence for macromolecular protein rings in the absence of bulk water." *Science* **310**(5754): 1658-1661.
- Sampson, J. S., Hawkrige, A. M. and Muddiman, D. C.** (2006). "Generation and detection of multiply-charged peptides and proteins by matrix-assisted laser desorption electrospray ionization (MALDESI) Fourier transform ion cyclotron resonance mass spectrometry." *Journal of the American Society for Mass Spectrometry* **17**(12): 1712-1716.
- Scarff, C. A., Thalassinou, K., Hilton, G. R. and Scrivens, J. H.** (2008). "Travelling wave ion mobility mass spectrometry studies of protein structure: biological significance and comparison with X-ray crystallography and nuclear magnetic resonance spectroscopy measurements." *Rapid Communications in Mass Spectrometry* **22**(20): 3297-3304.
- Sharon, N.** (2006). "Carbohydrates as future anti-adhesion drugs for infectious diseases." *Biochimica et Biophysica Acta (BBA) - General Subjects* **1760**(4): 527-537.
- Sharon, N. and Lis, H.** (2004). "History of lectins: from hemagglutinins to biological recognition molecules." *Glycobiology* **14**(11): 53R-62.
- Shelimov, K. B., Clemmer, D. E., Hudgins, R. R. and Jarrold, M. F.** (1997). "Protein structure in vacuo: Gas-phase confirmations of BPTI and cytochrome c." *Journal of the American Chemical Society* **119**(9): 2240-2248.
- Shiea, J., Huang, M. Z., Hsu, H. J., Lee, C. Y., Yuan, C. H., Beech, I. and Sunner, J.** (2005). "Electrospray-assisted laser desorption/ionization mass

spectrometry for direct ambient analysis of solids." *Rapid Communications in Mass Spectrometry* **19**(24): 3701-3704.

**Srebalus, C. A., Li, J. W., Marshall, W. S. and Clemmer, D. E.** (1999). "Gas phase separations of electrosprayed peptide libraries." *Analytical Chemistry* **71**(18): 3918-3927.

**Syka, J. E. P., Coon, J. J., Schroeder, M. J., Shabanowitz, J. and Hunt, D. F.** (2004). "Peptide and protein sequence analysis by electron transfer dissociation mass spectrometry." *Proceedings of the National Academy of Sciences of the United States of America* **101**(26): 9528-9533.

**Takats, Z., Cotte-Rodriguez, I., Talaty, N., Chen, H. W. and Cooks, R. G.** (2005). "Direct, trace level detection of explosives on ambient surfaces by desorption electrospray ionization mass spectrometry." *Chemical Communications*(15): 1950-1952.

**Takats, Z., Wiseman, J. M., Gologan, B. and Cooks, R. G.** (2004). "Mass spectrometry sampling under ambient conditions with desorption electrospray ionization." *Science* **306**(5695): 471-473.

**Thalassinos, K., Grabenauer, M., Slade, S. E., Hilton, G. R., Bowers, M. T. and Scrivens, J. H.** (2009). "Characterization of Phosphorylated Peptides Using Traveling Wave-Based and Drift Cell Ion Mobility Mass Spectrometry." *Analytical Chemistry* **81**(1): 248-254.

**Trimble, R. B., Trumbly, R. J., Maley, F. and Victor, G.** (1987). Endo-[beta]-N-acetylglucosaminidase H from *Streptomyces plicatus*. *Methods in Enzymology*, Academic Press. **Volume 138**: 763-770.



- Van Berkel, G. J., Pasilis, S. P. and Ovchinnikova, O.** (2008). "Established and emerging atmospheric pressure surface sampling/ionization techniques for mass spectrometry." *Journal of Mass Spectrometry* **43**(9): 1161-1180.
- Van Berkel, G. J., Sanchez, A. D. and Quirke, J. M. E.** (2002). "Thin-layer chromatography and electrospray mass spectrometry coupled using a surface sampling probe." *Analytical Chemistry* **74**(24): 6216-6223.
- Varki, A.** (1993). "Biological roles of oligosaccharides: all of the theories are correct." *Glycobiology* **3**(2): 97-130.
- Venter, A., Nefliu, M. and Cooks, R. G.** (2008). "Ambient desorption ionization mass spectrometry." *Trac-Trends in Analytical Chemistry* **27**(4): 284-290.
- Vestal, M. L., Juhasz, P. and Martin, S. A.** (1995). "Delayed extraction matrix-assisted laser desorption time-of-flight mass spectrometry." *Rapid Communications in Mass Spectrometry* **9**(11): 1044-1050.
- von Helden, G., Hsu, M. T., Gotts, N. and Bowers, M. T.** (2002). "Carbon cluster cations with up to 84 atoms: structures, formation mechanism, and reactivity." *The Journal of Physical Chemistry* **97**(31): 8182-8192.
- von Helden, G., Wyttenbach, T. and Bowers, M. T.** (1995). "Inclusion of a MALDI ion-source in the ion chromatography technique: conformational information on polymer and biomolecular ions." *International Journal of Mass Spectrometry and Ion Processes* **146**: 349-364.
- Waldmann, T. A.** (1991). "Monoclonal antibodies in diagnosis and therapy." *Science* **252**(5013): 1657-1662.
- Wessel, M. D., Sutter, J. M. and Jurs, P. C.** (1996). "Prediction of reduced ion mobility constants of organic compounds from molecular structure." *Analytical Chemistry* **68**(23): 4237-4243.

- Wildgoose, J. L., Giles, K., Pringle, S. D., Koeniger, S. J., Valentine, R. H., Bateman, R. H. and Clemmer, D. E.** (2006). *A comparison of travelling wave and drift tube ion mobility separations*. Proc. 54th ASMS Conf. Mass Spectrometry and Allied Topics, Seattle.
- Wiley, W. C. and McLaren, I. H.** (1955). "Time-of-Flight Mass Spectrometer with Improved Resolution." *Review of Scientific Instruments* **26**(12): 1150-1157.
- Williams, J. P. and Scrivens, J. H.** (2005). "Rapid accurate mass desorption electrospray ionisation tandem mass spectrometry of pharmaceutical samples." *Rapid Communications in Mass Spectrometry* **19**(24): 3643-3650.
- Williams, J. P. and Scrivens, J. H.** (2008). "Coupling desorption electrospray ionisation and neutral desorption/extractive electrospray ionisation with a travelling-wave based ion mobility mass spectrometer for the analysis of drugs." *Rapid Communications in Mass Spectrometry* **22**(2): 187-196.
- Wittmer, D., Luckenbill, B. K., Hill, H. H. and Chen, Y. H.** (1994). "Electrospray-ionization ion mobility spectrometry." *Analytical Chemistry* **66**(14): 2348-2355.
- Wu, C., Siems, W. F., Asbury, G. R. and Hill, H. H.** (1998). "Electrospray ionization high-resolution ion mobility spectrometry - Mass spectrometry." *Analytical Chemistry* **70**(23): 4929-4938.
- Wu, J., Hughes, C. S., Picard, P., Letarte, S., Gaudreault, M., Levesque, J. F., Nicoll-Griffith, D. A. and Bateman, K. P.** (2007). "High-throughput cytochrome P450 inhibition assays using laser diode thermal desorption-atmospheric pressure chemical ionization-tandem mass spectrometry." *Analytical Chemistry* **79**(12): 4657-4665.

- Wytttenbach, T., vonHelden, G., Batka, J. J., Carlat, D. and Bowers, M. T.** (1997). "Effect of the long-range potential on ion mobility measurements." *Journal of the American Society for Mass Spectrometry* **8**(3): 275-282.
- Wytttenbach, T., vonHelden, G. and Bowers, M. T.** (1996). "Gas-phase conformation of biological molecules: Bradykinin." *Journal of the American Chemical Society* **118**(35): 8355-8364.
- Yamashita, M. and Fenn, J. B.** (1984). "Electrospray ion source. Another variation on the free-jet theme." *The Journal of Physical Chemistry* **88**(20): 4451-4459.
- Yamashita, M. and Fenn, J. B.** (1984). "Negative ion production with the electrospray ion source." *The Journal of Physical Chemistry* **88**(20): 4671-4675.
- Yuen, C. T., Storrington, P. L., Tiplady, R. J., Izquierdo, M., Wait, R., Gee, C. K., Gerson, P., Lloyd, P. and Cremata, J. A.** (2003). "Relationships between the N-glycan structures and biological activities of recombinant human erythropoietins produced using different culture conditions and purification procedures." *British Journal of Haematology* **121**(3): 511-526.
- Zubarev, R. A., Kelleher, N. L. and McLafferty, F. W.** (1998). "Electron Capture Dissociation of Multiply Charged Protein Cations. A Nonergodic Process." *Journal of the American Chemical Society* **120**(13): 3265-3266.

## **Chapter 2:**

# **Ambient Ionisation of Pharmaceuticals**

## Introduction

A significant process in mass spectrometry based techniques is the generation of gas phase ions from a sample, and introducing them in to the mass spectrometer for analysis. Ionisation methods such as ESI and MALDI have helped to address the problems associated with ionising a range of compound classes including small molecules, lipids, carbohydrates, nucleic acids and proteins.

The recent development of a family of ambient ionisation techniques can allow the formation of gaseous ions under ambient conditions with minimal sample pre-treatment and can, in many cases, be performed on existing commercial instruments without significant modifications to hardware or software.

There has been rapid growth and continued interest in ambient mass spectrometry since DESI was first reported in 2004, with the development of more than twenty new ionisation sources being reported in the past five years.

Presented here are a series of experiments performed during a period of technique and application development immediately following the initial publications of some of the new ionisation sources.

Aspects of this work have been peer reviewed and published as the following article:

**Williams, J. P., Patel, V. J., Holland, R. and Scrivens, J. H.** (2006). "The use of recently described ionisation techniques for the rapid analysis of some common drugs and samples of biological origin." *Rapid Communications in Mass Spectrometry* **20**(9): 1447-1456.

## **Aims**

The aims of this work were to:

Evaluate the novel ambient ionisation sources: DESI, DAPCI, DART and ND-EESI and their potential applications in analysing a range of polar and weakly-polar, solid and ointment pharmaceutical formulations.

Couple DESI and DAPCI with accurate mass tandem mass spectrometry experiments to enhance the information content acquired for more confident assignments of observed fragments of unknown structure.

Use DESI, and DAPCI to detect the use of pharmaceutical drugs by detection after topical application, or oral administration with no sample pre-treatment.

## Materials and Methods

Pharmaceuticals used in this investigation and their active ingredients are listed in Table 2.1.

Table 2.1: Pharmaceutical formulations and their active ingredients

Pharmaceutical formulation	Manufacturer	Active ingredients
Tablets		
		300 mg aspirin
Anadin Extra	Wyeth consumer healthcare (UK)	45 mg caffeine 200 mg paracetamol
Solpadeine Max	GlaxoSmithKline (UK)	12.8 mg codeine phosphate 500 mg paracetamol
Ibuprofen	Galpharm Healthcare Ltd (UK)	500 mg ibuprofen
Metoclopramide	Sanofi-Aventis (UK)	10 mg metoclopramide
Erythromycin	Concept medical (UK)	500 mg erythromycin
Gels and ointments		
Ibuprofen	The mentholatum company Ltd. (UK)	5% w/w ibuprofen
Proctosedyl	Sanofi-Aventis (UK)	0.5% w/w chinchocaine 0.5% w/w hydrocortisone

Solvents: acetonitrile, methanol, formic acid and water were obtained from Sigma-Aldrich (Poole, UK).

Dry tobacco was obtained from a Marlboro Red cigarette (Philip Morris USA).

## **DART**

DART experiments were carried out on an AccuToF LC TOF mass spectrometer (JEOL, Peabody, MA, USA). A detailed description of the DART source can be found elsewhere (Cody *et al.*, 2005). The DART source was operated using helium gas and a corona discharge voltage of 2 kV to generate metastable reactive species to promote positive ionisation of samples. Orifice 1 of the source interface was set to 27 eV. This voltage can be increased or decreased to promote or reduce fragmentation of analyte ions. The gas temperature was maintained at 80 °C. The operating resolution of the instrument was approximately 6000 (full width at half maximum (FWHM)), and mass spectra were acquired over a  $m/z$  range of 50 – 500 at a rate of 0.5 spectra  $s^{-1}$ . For sample analysis, the helium gas flow was directed towards the sample surface before being sampled in to the mass spectrometer.

## **DESI**

DESI experiments were performed on a Q-TOF I instrument (Waters, Manchester UK). The Q-TOF I was operated in positive and negative mode with a capillary voltage of 3.5 kV and -3.2 kV respectively. The ion source block and nitrogen desolvation gas temperatures were set to 100 °C and 400 °C. The desolvation gas was set to a flow rate of 300 L  $h^{-1}$ . A cone voltage of 20 V was set for MS and MS/MS experiments. The collision energy used for MS/MS experiments was ramped between 10 and 25 eV during the acquisition. The TOF mass analyser was operated at a resolution of 6000 (FWHM), spectra were acquired over a  $m/z$  range of 50-500 or 50-1000 with an acquisition rate of 1 spectrum  $s^{-1}$ . For MS/MS experiments, argon was used as the collision gas. Samples were held with tweezers at an angle of



approximately 45 ° to the solvent spray and a distance of 5 mm from the source sampling cone.

The solvent used in negative mode was acetonitrile/H<sub>2</sub>O (1:1), with acetonitrile/H<sub>2</sub>O + 0.2% formic acid being used in positive mode. All solvents were infused at a rate of 10 μL min<sup>-1</sup> using a model 22 syringe pump (Harvard Apparatus, South Natick, MA, USA). No extensive modification of solvents, buffers or pH was carried out.

## **DAPCI**

DAPCI experiments were carried out on the Q-TOF I in both positive and negative modes of ionisation. The corona discharge pin was set to 3.5 kV and -3.0 kV in positive and negative modes respectively. The cone voltage was optimised between 10 and 25 V for each sample. The collision energy used for MS/MS experiments was ramped between 10 and 25 eV during the acquisition. The flow rate of nitrogen desolvation gas was set to 150 L h<sup>-1</sup>. The source and probe temperatures were set to 100 °C and 400 °C respectively. A solvent mixture of methanol and H<sub>2</sub>O (1:1), flowing at 10 μL min<sup>-1</sup> was infused in to the heated nebuliser probe where it was converted in to an aerosol. This aerosol was rapidly heated in a stream of nitrogen gas forming a vapour at the probe tip. The probe tip directly faced the sample surface positioned between the corona discharge pin and the sampling cone. Reagent ions formed in the corona discharge region reacted with desorbed analyte molecules from the sample surface to produce predominantly protonated or deprotonated molecular ions depending on ionisation mode.

### **Solventless DAPCI**

The same protocol for DAPCI was followed, but the experiments were performed with no solvent flowing in to the heated probe. This is similar in setup to the ASAP experiment previously described (McEwen *et al.*, 2005).

### **ND-EESI**

ND-EESI experiments were performed on a Q-TOF Ultima API US (Waters, Manchester, UK). All instrument conditions were the same as those used for DESI experiments. To perform neutral desorption sampling, a break in the nitrogen desolvation gas line was introduced. Nitrogen gas from this line was directed at the sample surface. Nitrogen and desorbed species from the sample surface were sampled in to the ESI probe through the remaining section of the desolvation gas line. The ESI solvent used in positive mode was methanol/H<sub>2</sub>O + 0.1% formic acid.

### **Sample Preparation**

Minimal sample pre-treatment was carried out. Tablet formulations were broken in half to expose a fresh, uncoated surface for analysis.

Gels, ointments and liquids were spotted on to matt finish cardboard or filter paper before being introduced to the ionisation source.

### **Accurate Mass Measurement on the Q-TOF I**

Instrumental mass drift was corrected for using a single internal reference lock mass in MS and MS/MS mode. As the analyte compounds are known molecules, the precursor ion selected for MS/MS experiments provided the internal reference lock mass. Data acquisition and processing were carried out using the digital dead-time correction algorithm embedded in the operating software, MassLynx V3.5 (Waters,

Manchester, UK). High ion counts generated during DAPCI and DESI techniques caused TDC dead-time saturation. The TDC correction software was used to display centroided peaks with the correct  $m/z$  and signal intensity.

## Results and Discussion

An investigation in to the amenability of ambient ionisation techniques to the rapid analysis of active ingredients in a number of formulations has been carried out. Four pharmaceutical tablets and two ointments have been analysed by means of DART, DESI, DAPCI and solventless DAPCI. One tablet formulation (erythromycin) has been analysed by DESI and ND-EESI.

In addition, human skin and urine were analysed post topical-application and injection of a non-steroidal anti-inflammatory (NSAID) drug.

Accurate mass MS/MS experiments have also been carried out to confirm the identity of active ingredients.

Mass spectra with a suitable signal to noise ratio for interpretation were acquired, in most cases in less than 5 s.

### Anadin Extra

Anadin Extra is a tablet formulation containing aspirin (an antipyretic, anti-inflammatory and analgesic), paracetamol (analgesic and antipyretic) and caffeine (a central nervous system stimulant).

Positive mode mass spectra for Anadin Extra ionised by DAPCI, DESI and DART are shown in Figure 2.1A-C. The protonated molecules for each active ingredient: caffeine ( $m/z$  195), paracetamol ( $m/z$  152) and aspirin ( $m/z$  181) were all observed by

DESI and DAPCI, but the protonated aspirin species was absent from the DART spectrum. The base peak in all spectra was due to caffeine.

Accurate mass measurement has been used to confirm the molecular formulae of the  $m/z$  163 ion, present in all three spectra, to correspond to that formed by loss of  $H_2O$  from protonated aspirin. DESI and DAPCI spectra contained ammoniated aspirin  $[M+NH_4]^+$  at  $m/z$  198, and sodiated aspirin  $[M+Na]^+$  at  $m/z$  203 present only in the DESI spectrum.

The accurate mass MS/MS spectrum of caffeine (ionised by DAPCI) is shown in Figure 2.1D. Elemental composition assignments for product ions observed are presented in Table 2.2.

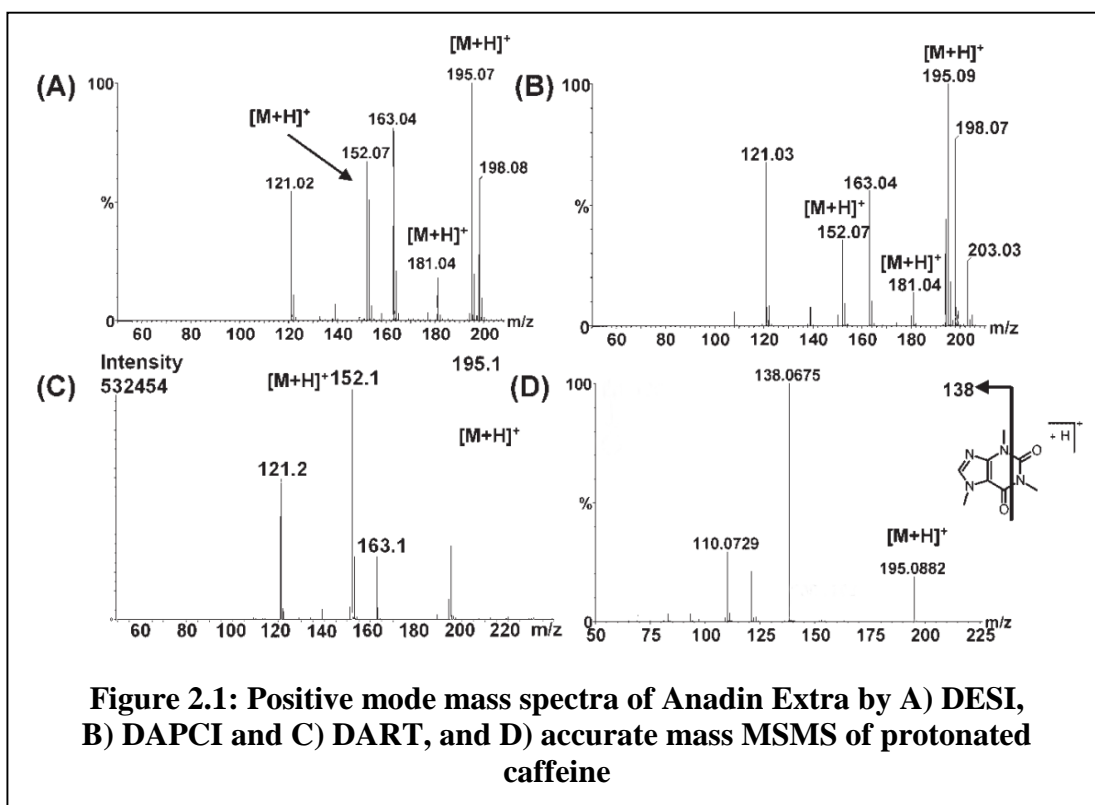


Table 2.2: Accurate masses of some DAPCI-MS/MS generated fragments of protonated caffeine

Measured mass	Molecular formula	Error (ppm)
138.0675	C <sub>6</sub> H <sub>8</sub> N <sub>3</sub> O	5.8
121.0293	C <sub>7</sub> H <sub>5</sub> O <sub>2</sub>	2.5
	C <sub>5</sub> H <sub>3</sub> N <sub>3</sub> O	14.0
110.0729	C <sub>5</sub> H <sub>8</sub> N <sub>3</sub>	10.0

### Solpadeine Max

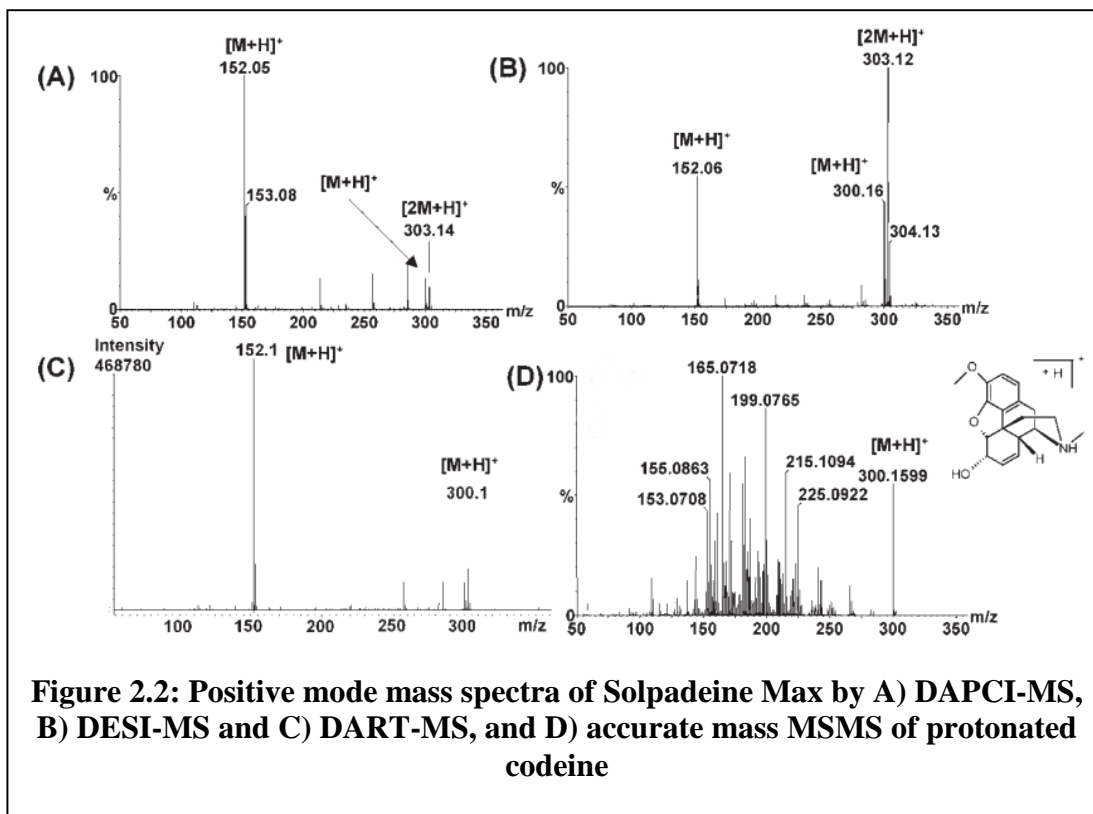
Solpadeine Max is a compound analgesic containing codeine phosphate and paracetamol and is used for the relief of minor pain. Codeine is an alkaloid opiate that has analgesic properties.

Positive mode mass spectra of Solpadeine Max ionised by DESI, DART and DAPCI are shown in Figure 2.2 A-C. Protonated paracetamol ( $m/z$  152) and protonated codeine ( $m/z$  300) are present in all three spectra. A paracetamol dimer  $[2M+H]^+$  ( $m/z$  303) is also present in all three spectra, and its formation is related to the area of the sample surface analysed. The ratio of monomer and dimer species can vary by the region of the tablet presented to the ionisation source.

Table 2.3: Accurate masses of some DAPCI-MS/MS generated fragments of protonated codeine

Measured mass	Molecular formula	Error (ppm)
266.1196	C <sub>17</sub> H <sub>16</sub> NO <sub>2</sub>	5.6
225.0922	C <sub>15</sub> H <sub>13</sub> O <sub>2</sub>	2.6
215.1094	C <sub>14</sub> H <sub>15</sub> O <sub>2</sub>	10.2
199.0765	C <sub>13</sub> H <sub>11</sub> O <sub>2</sub>	3.0
183.0800	C <sub>13</sub> H <sub>11</sub> O	-5.4

The MS/MS spectrum of codeine is shown in Figure 2.2 D. The product ion spectrum for protonated codeine is complex, but reproducible. The proposed formulae for some of the product ions observed are presented in Table 2.3.



## Metocolopramide

Metoclopramide is an antiemetic and gastroprokinetic that is predominantly used to treat nausea, vomiting and to facilitate gastric emptying in patients with gastroparesis.

Metoclopramide has been analysed using DAPCI in both positive ion, and negative ion modes. Positive mode DART spectra have also been acquired.

The deprotonated molecular species has been observed in negative mode ( $m/z$  298 and 300) with signal intensities in a ratio of 3:1, consistent with the presence of a chlorine atom Figure 2.3 A. The protonated active ingredient ( $m/z$  300 and 302) was

the base peak in both DAPCI and DART positive mode mass spectra Figure 2.3 B and E.

Accurate mass MS/MS of metoclopramide has been performed on both the  $[M+H]^+$  and  $[M-H]^-$  species. The spectra are displayed in Figure 2.3 C and D. The elemental composition assignments for some product ions are presented in Tables 2.4 and 2.5. The deprotonated molecule appears to fragment by the unusual loss of a methyl radical, resulting in the formation of an odd-electron radical anion of  $m/z$  283. This ion undergoes further fragmentation to  $m/z$  211, the loss of the diethylamine moiety (confirmed by accurate mass measurement).

Figure 2.3 D shows the accurate mass MS/MS spectrum obtained for protonated metoclopramide. The spectrum shows ions at  $m/z$  227 and 184, in agreement with results published from liquid chromatography-tandem mass spectrometry (LC-MS/MS) studies of this compound (Abdel-Hamid and Sharma, 2004).

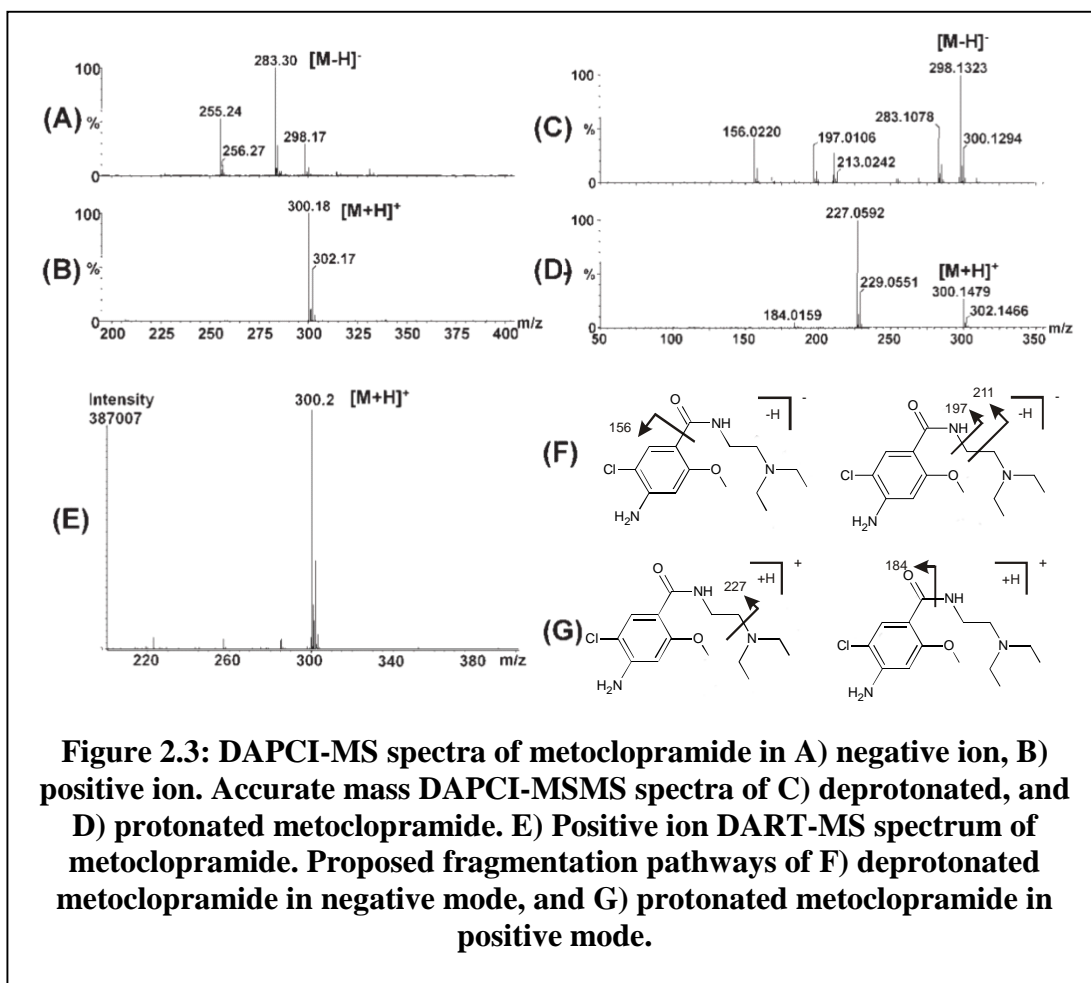


Table 2.4: Accurate masses of some DAPCI-MS/MS generated fragments of deprotonated metoclopramide

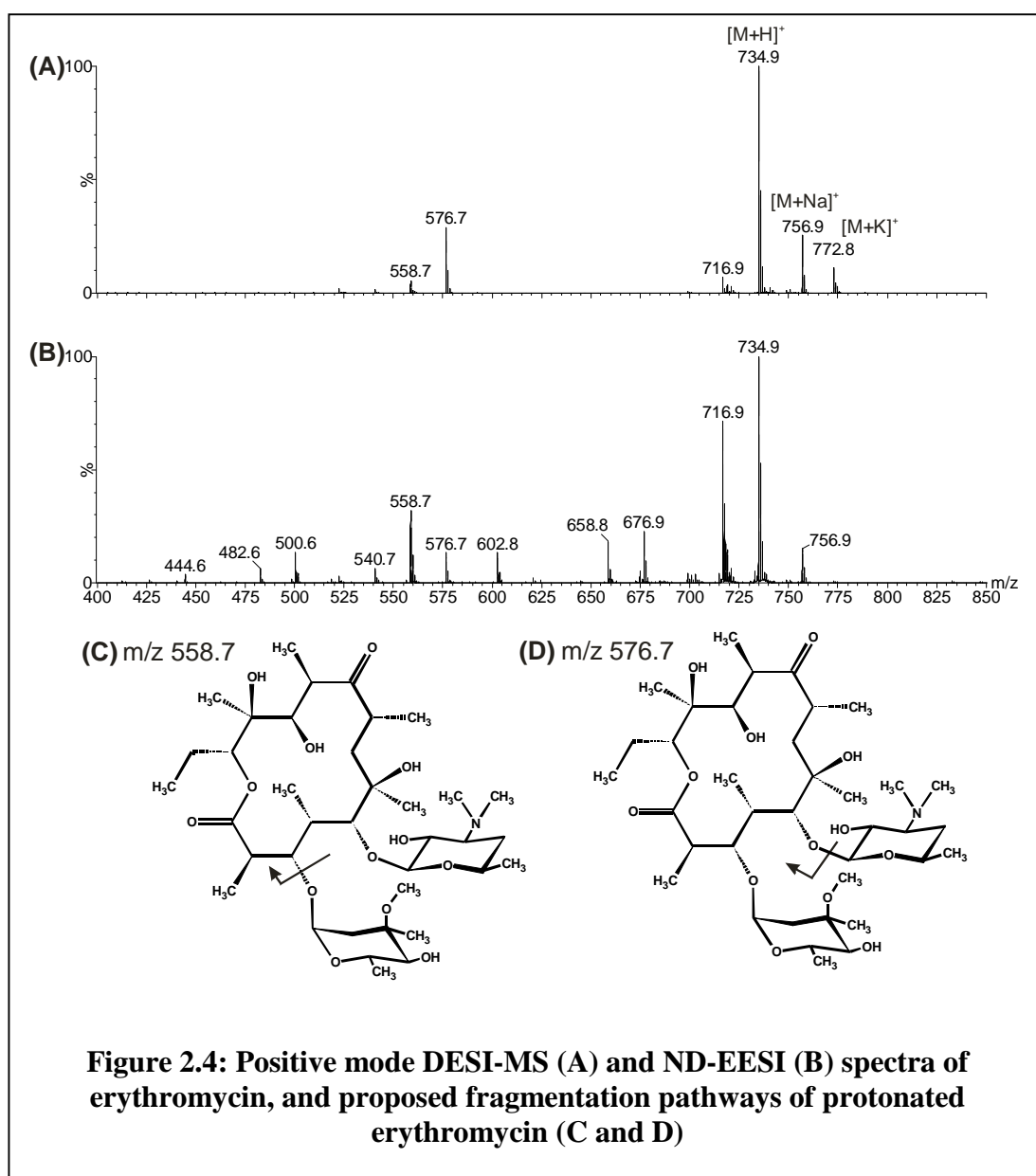
Measured mass	Molecular formula	Error (ppm)
283.1078	C <sub>13</sub> H <sub>18</sub> ClN <sub>3</sub> O <sub>2</sub>	-3.5
211.0258	C <sub>9</sub> H <sub>8</sub> ClN <sub>2</sub> O <sub>2</sub>	-7.6
197.0160	C <sub>8</sub> H <sub>6</sub> ClN <sub>2</sub> O <sub>2</sub>	-6.1
156.0220	C <sub>7</sub> H <sub>7</sub> ClNO	2.6



Table 2.5: Accurate masses of some DAPCI-MS/MS generated fragments of protonated metoclopramide

Measured mass	Molecular formula	Error (ppm)
227.0592	C <sub>10</sub> H <sub>12</sub> ClN <sub>2</sub> O <sub>2</sub>	2.2
184.0159	C <sub>8</sub> H <sub>7</sub> ClNO <sub>2</sub>	-3.3

## Erythromycin



Erythromycin is a broad spectrum, macrolide antibiotic containing a lactone ring and two sugar moieties: L-cladinose and D-desosamine. It is produced for commercial use from a strain of actinomycete called *Saccharopolyspora erythraea*. Positive mode mass spectra of erythromycin ionised by DESI and ND-EESI are shown in Figure 2.4. The base peak in both spectra is  $[M+H]^+$ , but significant amounts of  $[M+Na]^+$  and  $[M+K]^+$  species are also present. Peaks at  $m/z$  576.8 and 558.7 are indicative of loss of D-desosamine and L-cladinose respectively. The ND-EESI spectrum contains more species than the DESI spectrum, these may be due to additional components or an increase in fragmentation of the erythromycin during ND-EESI ionisation.

### Nicotine from Tobacco

Nicotine is a naturally occurring alkaloid present in the tobacco plant. Dried tobacco from a commercial cigarette was analysed by means of positive ion mode DAPCI, DESI and DART. The mass spectra acquired are shown in Figure 2.5 A-C.

At a low cone voltage, a single ion at  $m/z$  163 (corresponding to protonated nicotine) was observed by DESI and DAPCI. The higher cone voltage used on the DART source resulted in in-source fragmentation of the protonated nicotine species. The fragmentation pattern observed by this method is very similar to that obtained by DAPCI-MS/MS of  $m/z$  163 (Figure 2.5 D). Elemental composition assignments for observed product ions of protonated nicotine are listed in Table 2.6.

The protonated molecule fragments by the loss of 31 Da to form an ion at  $m/z$  132. Accurate mass measurement confirms this loss to be  $CH_3NH_2$  from the methyl-substituted pyrrolidine ring. The base peak in the spectrum,  $m/z$  130, is formed by loss of  $H_2$  from  $m/z$  132. Other ions at  $m/z$  117 and 106 are possibly formed from the

$m/z$  132 species by the loss of a methyl radical and  $C_2H_2$  molecule respectively. The methyl radical loss has been reported previously (Byrd *et al.*, 2005). Other easily recognised product ions resulting from cleavage of the bond between the methyl-substituted pyrrolidine ring and the pyridine ring are found at  $m/z$  84 and 80 respectively.

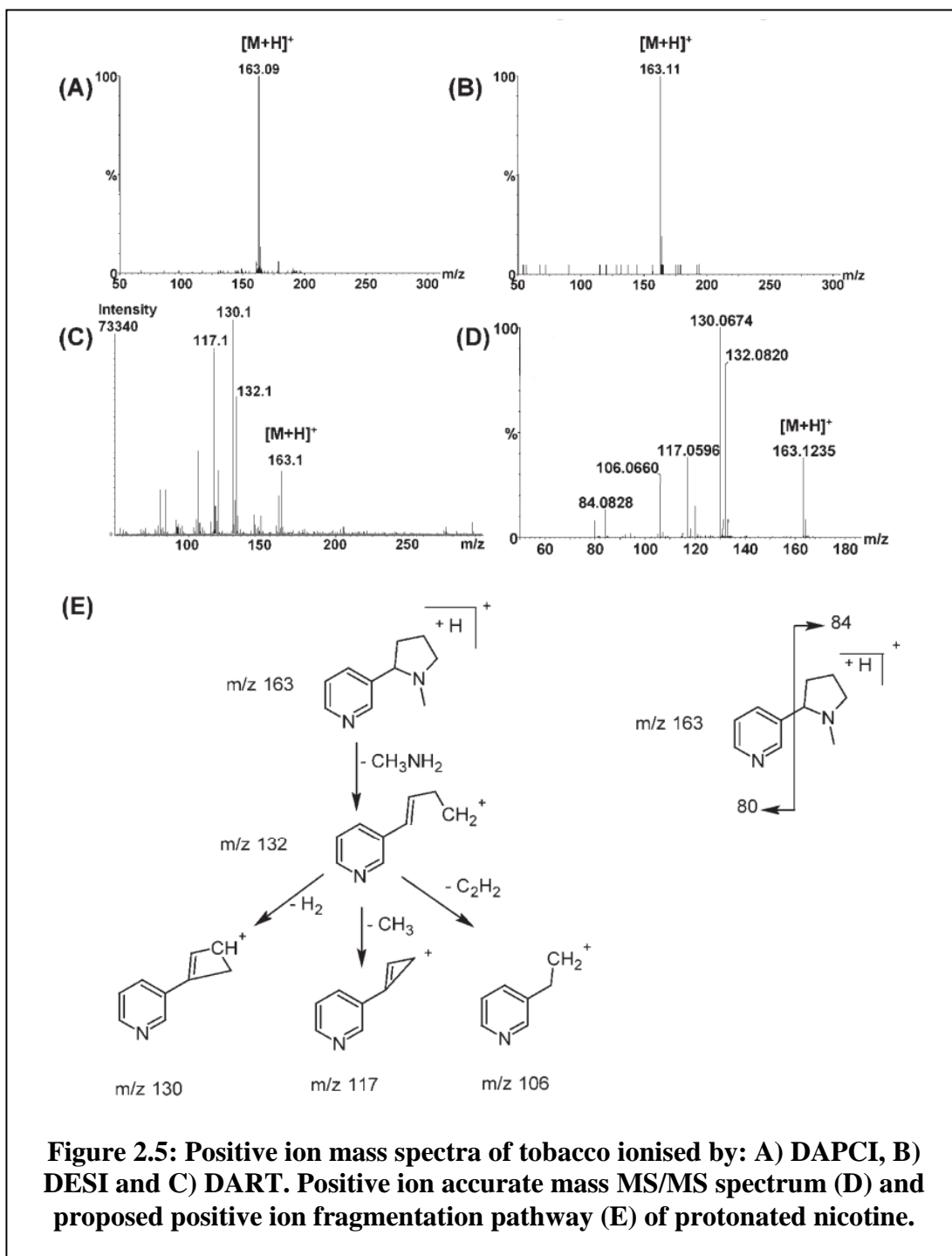


**Figure 2.5: Positive ion mass spectra of tobacco ionised by: A) DAPCI, B) DESI and C) DART. Positive ion accurate mass MS/MS spectrum (D) and proposed positive ion fragmentation pathway (E) of protonated nicotine.**

A proposed fragmentation scheme is shown in Figure 2.5 E, and is similar to the scheme previously proposed (Byrd). Accurate mass MS/MS also supports this hypothesis.

Table 2.6: Accurate masses of some DAPCI-MS/MS generated fragments of protonated nicotine

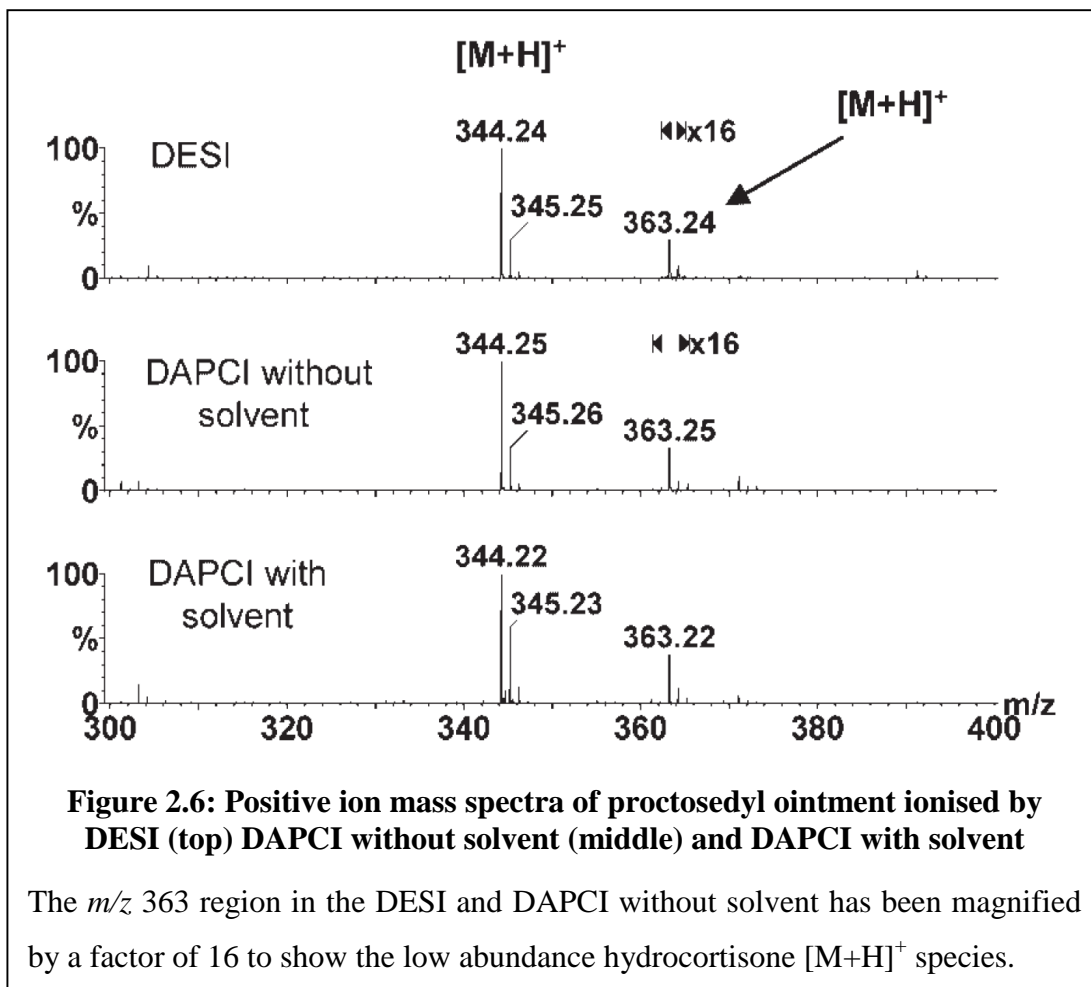
Measured mass	Molecular formula	Error (ppm)
132.0820	C <sub>9</sub> H <sub>10</sub> N	5.3
130.0674	C <sub>9</sub> H <sub>8</sub> N	13.1
117.0596	C <sub>8</sub> H <sub>7</sub> N	15.4
106.0660	C <sub>7</sub> H <sub>8</sub> N	2.8
84.0828	C <sub>5</sub> H <sub>10</sub> N	17.8
80.0542	C <sub>5</sub> H <sub>6</sub> N	52.5

### Proctosedyl ointment

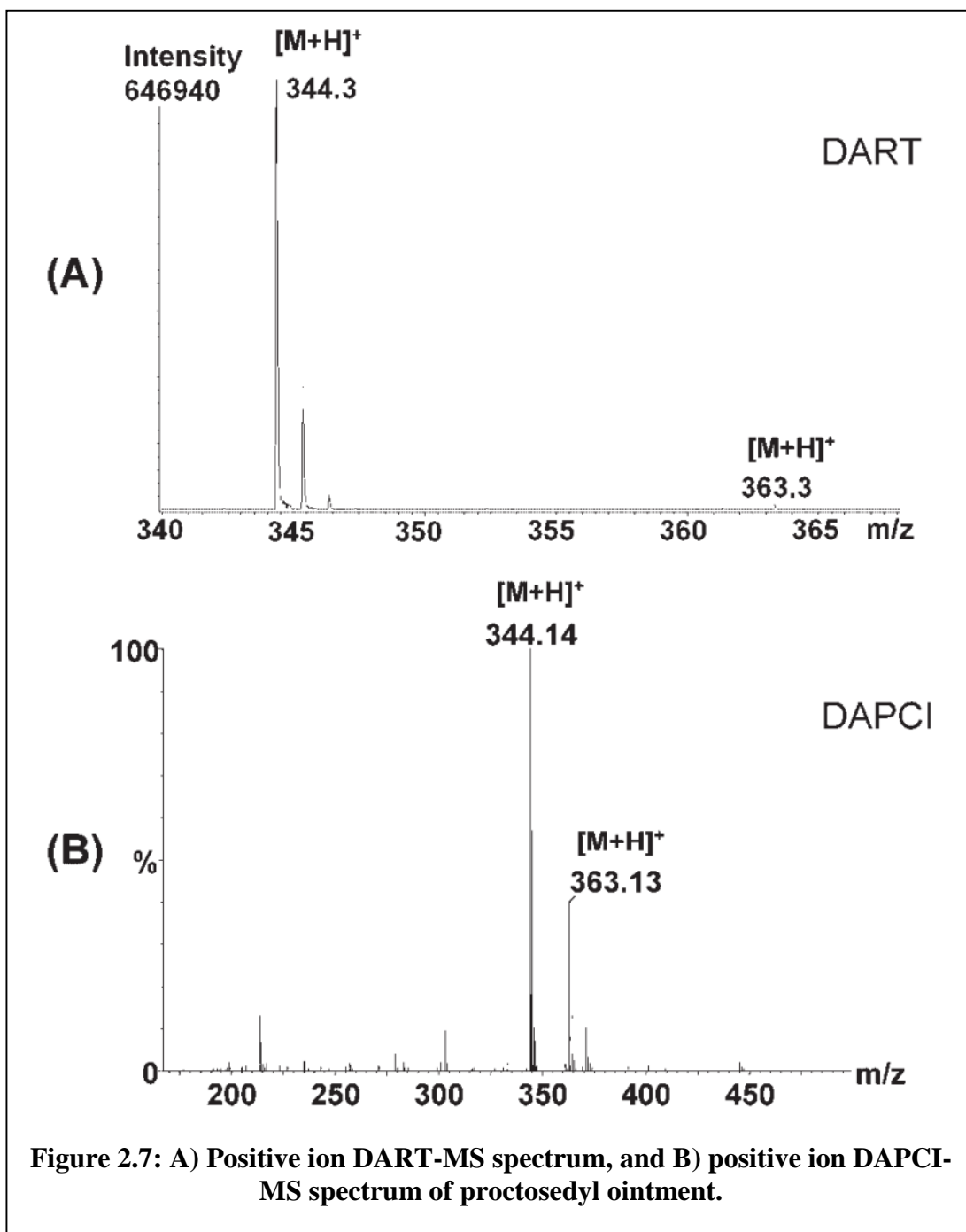
Proctosedyl contains two active ingredients, cinchocaine hydrochloride (a topical anaesthetic) and hydrocortisone (a corticosteroid hormone). Figure 2.6 shows the mass spectra of proctosedyl ionised in positive mode by DESI, DAPCI and solventless DAPCI. Protonated hydrocortisone ( $m/z$  363) is present in all three spectra, but the signal intensity when ionised by DESI and solventless DAPCI is significantly lower than when analysed by means of DAPCI with solvent. The cinchocaine hydrochloride protonates well ( $m/z$  344) by all three methods.

Figure 2.7 shows a comparison of proctosedyl ointment ionised by DAPCI with solvent, and DART. The DART ionisation method generates abundant protonated cinchocaine hydrochloride species, but only a very weak hydrocortisone signal.

Negative ion DAPCI and positive ion DAPCI spectra of proctosedyl are shown in Figure 2.8 A and B. An intense signal for cinchocaine hydrochloride can be observed in the negative mode spectrum ( $m/z$  342), but hydrocortisone is absent.



Accurate mass MS/MS of protonated and deprotonated cinchocaine hydrochloride are shown in Figure 2.8 C and D. Elemental compositions of some observed product ions are presented in tables 2.7 and 2.8. The base peak in the  $[M-H]^-$  MS/MS spectrum at  $m/z$  200 is formed by the loss of  $C_7H_{14}N_2O$  from the molecular ion. Further fragmentation of the  $m/z$  200 species occurs to form the ion at  $m/z$  144. The proposed fragmentation pathway is shown in Figure 2.8 E and F.



Positive mode MS/MS of protonated cinchocaine hydrochloride yields a base peak at  $m/z$  271. This ion is formed from the loss of  $C_4H_{11}N_1$  and can undergo further fragmentation to  $m/z$  251 by loss of  $C_4H_8$  (supported by accurate mass measurement). Proposed fragmentation pathways for these two ions are shown in Figure 2.8 E and

F, and probable elemental compositions for other ions in the MS/MS spectrum are listed in tables 2.7 and 2.8.

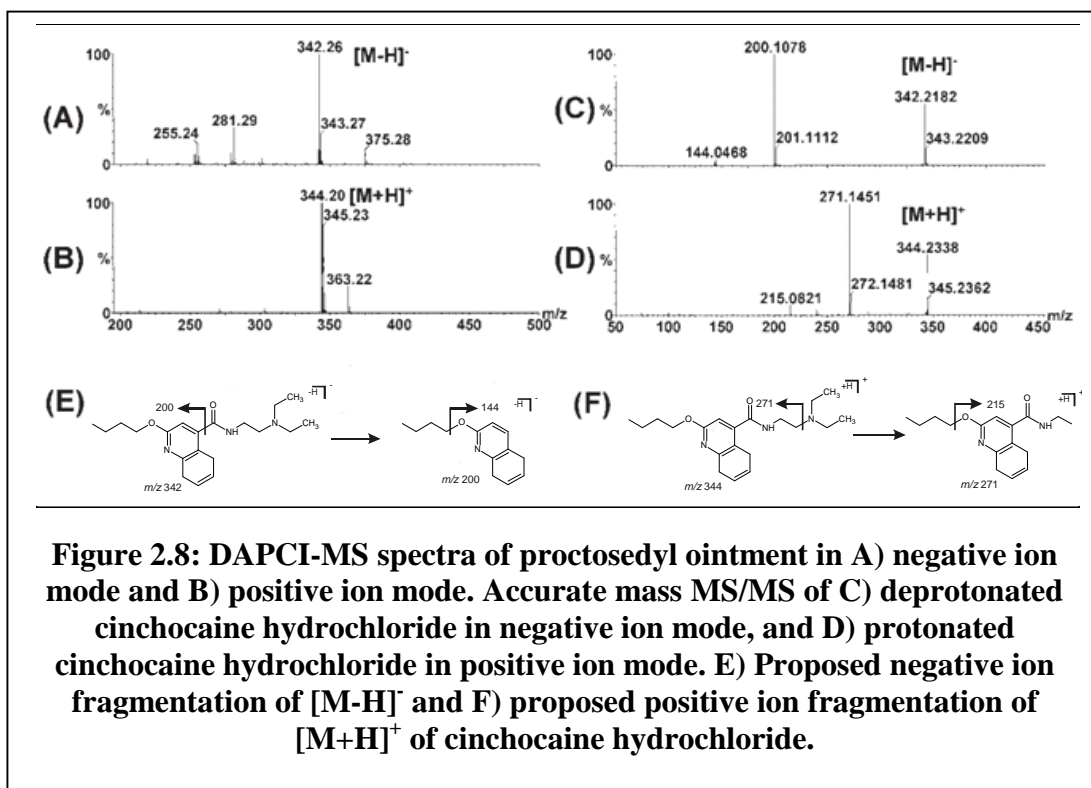


Table 2.7: Accurate masses of some DAPCI-MS/MS generated fragments of deprotonated cinchocaine hydrochloride

Measured mass	Molecular formula	Error (ppm)
200.1078	$C_{13}H_{14}NO$	1.5
144.0468	$C_9H_6NO$	13.2

Table 2.8: Accurate masses of some DAPCI-MS/MS generated fragments of protonated cinchocaine hydrochloride

Measured mass	Molecular formula	Error (ppm)
271.1451	$C_{16}H_{19}N_2O_2$	1.5
215.0821	$C_{12}H_{11}N_2O_2$	0.0

## Detection of Ibuprofen Gel From Skin

Ibuprofen is a non-steroidal anti-inflammatory drug that acts as an antipyretic, analgesic and anti-inflammatory.

A thin layer of ibuprofen gel was applied to the surface of a human finger. The gel was gently massaged until absorbed. Negative ion DESI with a reduced desolvation temperature (100 °C) was used to detect the drug at the point of application. Figure 2.9 shows the DESI-MS spectrum of ibuprofen 20 minutes after application to the skin. The deprotonated ibuprofen ( $m/z$  205) is the base peak in the spectrum.

Accurate mass MS/MS of the deprotonated ibuprofen species results in a single fragment ion at  $m/z$  161.1321, consistent with a proposed loss of  $\text{CO}_2$ .

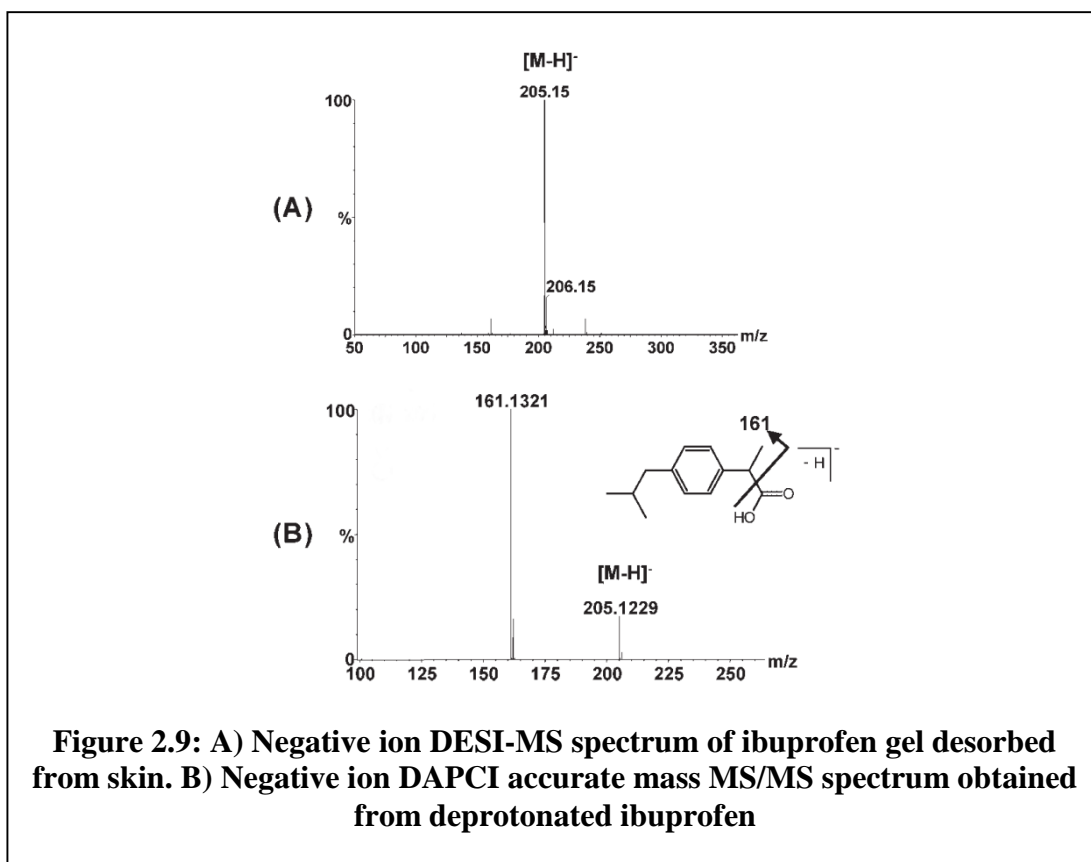


**Figure 2.9: A) Negative ion DESI-MS spectrum of ibuprofen gel desorbed from skin. B) Negative ion DAPCI accurate mass MS/MS spectrum obtained from deprotonated ibuprofen**



## Detection of ibuprofen metabolites from human urine

The development of a rapid screen for drugs and drug metabolites from urine is simplified by the use of DESI and DAPCI. ESI-MS cannot be used in the direct analysis of urine due to its inherent intolerance of salts. Time consuming desalting or extraction of metabolites from whole urine must be performed before analysis by ESI.

After ingestion, a number of modifications to ibuprofen are made, including: hydroxylation, carboxylation and glucuronidation (Glowka and Karazniewicz, 2005).

A sample of human urine was obtained 60 minutes after oral administration of two 200 mg ibuprofen tablets. Negative ion mode DAPCI was used for the detection of ibuprofen metabolites in the urine sample. Urine was spotted on to a piece of filter paper before being introduced in to the DAPCI source.

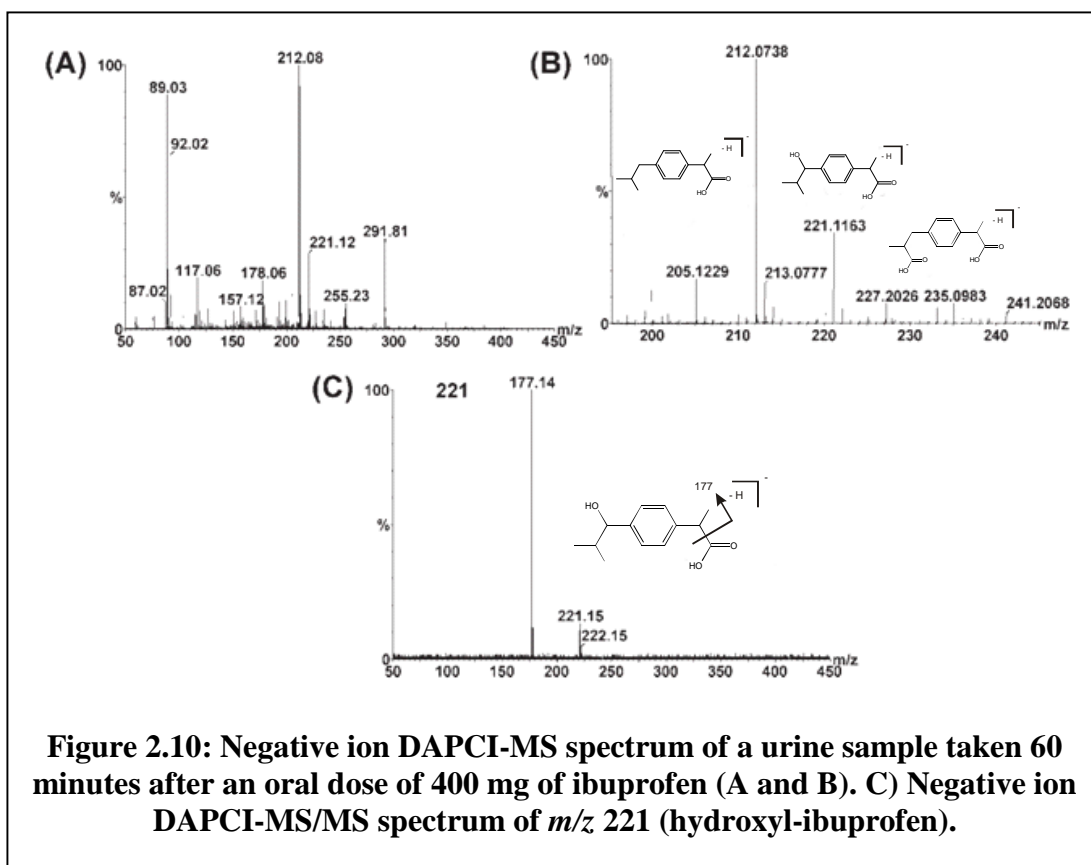


Figure 2.10A shows the negative ion mass spectrum obtained without any pre-treatment of the urine sample. The sample contains a number of ions that may be ascribed to endogenous components, including tentative assignments of deprotonated: pyruvic acid ( $m/z$  87), lactic acid ( $m/z$  89), methylmalonic acid ( $m/z$  117), xanthine ( $m/z$  151) and hippuric acid ( $m/z$  178).

The accurate mass spectrum obtained using deprotonated ibuprofen as a lock mass is shown in Figure 2.10 B. Two species corresponding to deprotonated hydroxyl-ibuprofen ( $m/z$  221) and carboxy-ibuprofen ( $m/z$  235) were detected. No glucuronide metabolites were detected.

MS/MS of the deprotonated hydroxyl-ibuprofen resulted in a single product ion at  $m/z$  177 through the loss of  $\text{CO}_2$  shown in Figure 2.10C.

## Conclusions

DART, DESI and DAPCI (with and without solvent) have been demonstrated as a means of ionising a range of molecules of pharmaceutical interest, with little or no sample pre-treatment. Significant differences between the ionisation approaches were observed. Compounds of moderate to low polarity were more amenable to ionisation by DAPCI (with and without solvent) than by DESI or DART.

The previously described approach of ASAP was found to be very similar to solventless DAPCI.

DESI and DAPCI have been shown to provide a robust means of interrogating the active ingredients in a variety of pharmaceutical formulations. Sampling is rapid and ionisation occurs almost instantly. The orientation and positioning of the sample surface in DESI and DAPCI seems to be more critical than with the DART source.

The use of a Q-TOF I instrument with elevated resolution and full scan sensitivity has improved selectivity and specificity of the DAPCI technique originally described by Cooks and co-workers (Takáts *et al.*, 2005). The high information content has allowed probable elemental compositions and fragmentation pathways to be proposed.

DESI was shown to be able to detect ibuprofen from the surface of skin with good sensitivity. DAPCI has been demonstrated to be effective in the detection of ibuprofen and its metabolites in urine after ingestion despite the high levels of endogenous salts present.

Development of these new ionisation techniques offers significant advantages for a number of analytical areas including rapid characterisation of pharmaceuticals, and forensic detection of drugs and drug metabolites from skin and urine.

## References

**Abdel-Hamid, M. E. and Sharma, D.** (2004). "Simultaneous quantification of doxorubicin, lorazepam, metoclopramide, ondansetron, and ranitidine in mixtures by liquid chromatography-tandem mass spectrometry." *Journal of Liquid Chromatography & Related Technologies* **27**(4): 641-660.

**Byrd, G. D., Davis, R. A. and Ogden, M. W.** (2005). "A rapid LC-MS-MS method for the determination of nicotine and cotinine in serum and saliva samples from smokers: Validation and comparison with a radioimmunoassay method." *Journal of Chromatographic Science* **43**(3): 133-140.

**Cody, R. B., Laramee, J. A. and Durst, H. D.** (2005). "Versatile New Ion Source for the Analysis of Materials in Open Air under Ambient Conditions." *Analytical Chemistry* **77**(8): 2297-2302.

**Glowka, F. K. and Karazniewicz, M.** (2005). "High performance capillary electrophoresis method for determination of ibuprofen enantiomers in human serum and urine." *Analytica Chimica Acta* **540**(1): 95-102.

**McEwen, C. N., McKay, R. G. and Larsen, B. S.** (2005). "Analysis of Solids, Liquids, and Biological Tissues Using Solids Probe Introduction at Atmospheric Pressure on Commercial LC/MS Instruments." *Analytical Chemistry* **77**(23): 7826-7831.

**Takáts, Z., Cotte-Rodriguez, I., Talaty, N., Chen, H. and Cooks, R. G. (2005).**

"Direct, trace level detection of explosives on ambient surfaces by desorption ionization mass spectrometry." *Chemical Communications*: 1950-1952.

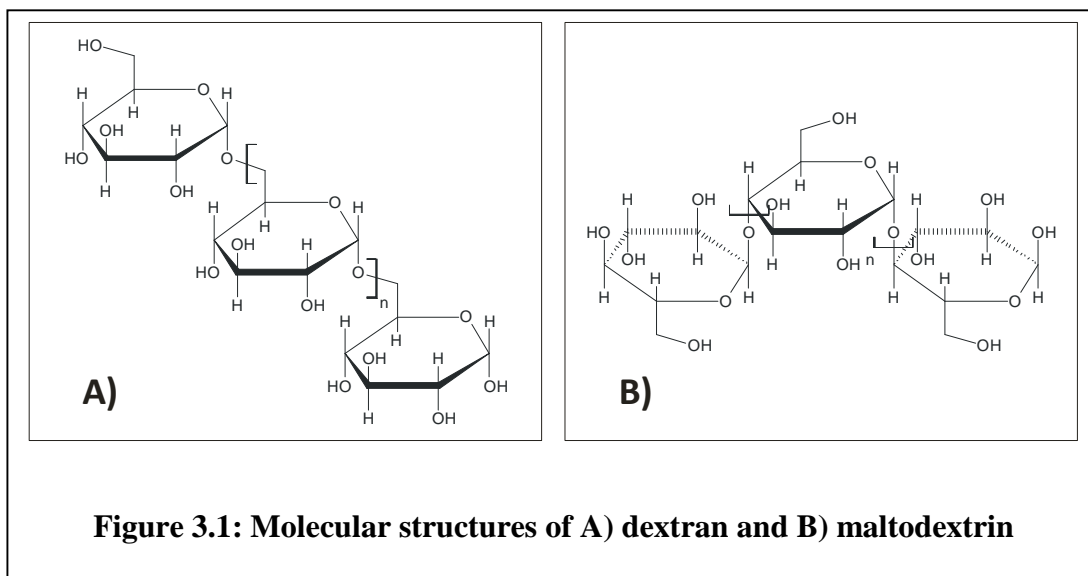
## **Chapter 3:**

### **Shape Selective Studies of Isomeric**

### **Glucose Homopolymers**

## Glucose Homopolymers

Dextran and maltodextrin are two glucose homopolymers (poly-Glc) which differ in chemical structure only by the glycosidic linkage type present.



### Dextran

Dextran is a linear  $\alpha$  1-6 linked glucose polymer (Figure 3.1A) synthesised by the bacterium *Leuconostoc mesenteroides*. Dextran has a wide range of clinical applications including the use of 40-70 kDa solutions as emergency blood replacement, and plasma substitution. Lower molecular weight dextrans are combined with iron to form a complex which is highly efficient at delivering iron to patients with anaemic iron deficiency. Dextran can also be used as a molecular weight calibrant in mass spectrometry due to the well defined molecular weight distribution of commercially available samples.

## Maltodextrin

Maltodextrin is an  $\alpha$  1-4 linked glucose polymer (Figure 3.1B) derived from the hydrolysis of starch. Maltodextrin is predominantly used in the food industry as a thickening agent. It is easily digested to glucose in the body.

Both dextran and maltodextrin have the ability to form complexes with metal ions and their regular structures make them suitable model systems for studying carbohydrate-based shape selective interactions with cations.

## Previous Studies of Poly-Glc Structures

Previous studies on dextran and maltodextrin have been carried out using a range of analytical techniques and modelling approaches.

Results from X-ray diffraction (Bluhm and Zugenmaier, 1981) and nuclear magnetic resonance (NMR) (Brant *et al.*, 1995) measurements have indicated that maltodextrin in crystalline form, or in solution, maintains a structured and more compact helical conformation than dextran oligomers of equivalent length. The absence of a similar structure in the dextran chain is thought to be due to the much greater conformational freedom associated with the  $\alpha$  1-6 glycosidic bond (Tvaroska and Kozár, 1981).

Investigations of cation binding affinities and resultant ionisation efficiencies of linear and cyclic poly-Glc by MALDI-MS have been carried out by multiple groups (Bashir *et al.*, 2003; Choi *et al.*, 2009). Alkali metal ions:  $\text{Li}^+$ ,  $\text{Na}^+$ ,  $\text{K}^+$ ,  $\text{Rb}^+$ ,  $\text{Cs}^+$  have been demonstrated to coordinate to carbohydrate polymers with varying binding affinities.

Further work by Bashir *et al.* (Bashir *et al.*, 2004) investigated the fragmentation of poly-Glc oligomers during analysis by MALDI-MS/MS. CID experiments on



poly-Glc oligomers resulted in abundant glycosidic bond cleavages and some pyranose ring cleavage of dextran. It was also reported that the degree of fragmentation of poly-Glc compounds during MALDI in-source decay fragmentation experiments is related to the stability of their solution phase structure (as obtained through NMR studies by (Vetter and Thorn, 1992)). Polymers with more constrained conformations or defined secondary structures (e.g. maltodextrin and cyclodextrins) yielded fewer fragment ions than those with ill-defined secondary structure.

Ion mobility mass spectrometry has been utilised in the study of cation attachment to a number of oligomeric systems including polystyrene (Gidden *et al.*, 2000), polyethylene glycol and polypropylene glycol (Gidden *et al.*, 2002). These studies indicate that different oligomeric systems can incorporate varying cation binding mechanisms and that cation type can influence the number of atoms that are involved with cation interaction. In these studies no systematic attempt was made to investigate the effect of oligomer number on cation binding.

## **Objectives**

The aim of this study was to investigate the conformational changes that occur when a range of cations are bound to oligomeric carbohydrate systems. Two closely related carbohydrate systems were employed and a wide range of selected cation species studied.

The Synapt HDMS ion mobility instrument was used to probe conformational variation with: carbohydrate isomer, oligomer length (molecular weight) and cation used for sample ionisation.

Estimated cross sections of ion mobility-resolved, arrival time distributions for poly-Glc oligomers complexed with alkali metal cations were calculated to provide instrument-independent values for comparison of mobility separated species.

## Materials

Dextran 5000 was purchased from Fluka (Dorset, U.K.). Maltodextrin, metal salts (lithium chloride, sodium chloride, potassium chloride, rubidium chloride and caesium iodide), proteins (serum albumin (bovine), cytochrome C (equine), aldolase (rabbit), transferrin (human), myoglobin (equine), creatine phosphokinase (rabbit), haemoglobin (rabbit) and trypsin) and Nafion-117 membrane were obtained from Sigma-Aldrich (Dorset, U.K.). Hydrochloric acid was obtained from Fisher Scientific (Loughborough, U.K.). Methanol and water were of LC/MS grade purchased from Mallinckrodt Baker (U.S.A). Borosilicate glass nano-flow capillaries were purchased from Waters (Waters, Manchester, U.K.).

## Experimental

### Cation Attachment

To ensure that the selected cation was dominant in the experiments, a cation exchange membrane, Nafion-117, was used to form complexes between the cation of interest and the poly-Glc sample (Börnsen *et al.*, 1995).

Nafion-117 membrane was prepared for cation exchange by incubation in concentrated hydrochloric acid at 95 °C for two hours. The membrane was then washed with distilled water to remove any remaining acid. A piece of Nafion membrane was floated on the surface of 0.1 M HCl solution (for sample protonation)

or 0.1 M alkali metal salt solution (LiCl, NaCl, KCl, RbCl, CsI for respective sample cationisation).

Poly-Glc samples were dissolved in water to a concentration of 2 mg mL<sup>-1</sup>. 10 µL aliquots were spotted on to the surface of the prepared Nafion-117 membrane. After 30 minutes, samples were removed from the membrane surface, mixed in a 1:1 ratio with methanol, and placed in to a nano-flow capillary for analysis.

### **TWIM-MS Analysis**

TWIM-MS analysis was performed in a hybrid quadrupole/ion mobility/orthogonal acceleration time-of-flight mass spectrometer (Synapt HDMS, Waters, Manchester, U.K.) operated in positive ion electrospray mode. Samples were infused by means of borosilicate glass nano-flow capillaries typically at a flow rate of 100 – 200 nL min<sup>-1</sup>. The source temperature was 120 °C, the capillary voltage was operated at 1.2 kV, and the cone voltage was kept at 50 V throughout all experiments. The gas in the TriWave IMS region was nitrogen, operated at flow rates from 24 - 42 mL min<sup>-1</sup> (4.55 - 7.61 × 10<sup>-1</sup> mbar respectively). The T-Wave height was fixed at either 8 or 12 V whilst the IMS gas cell pressure was optimised. During the wave height optimisation, the IMS gas cell flow was maintained at 30 mL min<sup>-1</sup>. The T-Wave velocity was fixed for all experiments at 300 m sec<sup>-1</sup>. The *m/z* acquisition range was from 100 to 3000 and mass spectra were obtained at a rate of 1 spectrum s<sup>-1</sup>. Ion mobility separation experiments take place in 18 ms and are divided in to 200 time bins of 90 µs. Each time bin contains mass spectral information for all ions detected in that period.

Ion mobility separation conditions were optimised using the [dextran +  $n\text{Cs}$ ] <sup>$n+$</sup>  sample to achieve an ion mobility separation of ions, while ensuring all ions had left the IMS TWIG before the next gated release of ions from the trap TWIG.

### **Cross Section Calibration and Estimation**

The cross section calibration method used (Thalassinos *et al.*, 2009) is a modified version of that proposed by Wildgoose *et al.* (Wildgoose *et al.*, 2006). Calibrant molecules of known cross section are analysed on the Synapt HDMS under the same experimental conditions as the unknown samples under investigation. The time bin (scan number) in which the calibrant arrives is converted to an arrival time by multiplying by the oa-TOF pusher period. This arrival time is corrected for mass dependent and mass independent flight time ( $t(d)''$ ). The mass independent time is the time taken to traverse the IMS and transfer TWIGs and does not depend on  $m/z$ . The mass dependent time is the time from the ion leaving the transfer TWIG to it arriving at the detector. This time is proportional to the square root of the  $m/z$  of the ion. The published cross sections for the calibrant ions are scaled by taking in to account the reduced mass and charge state of the ion ( $\Omega'$ ). A plot of  $t(d)''$  versus  $\Omega'$  is made, and a curve fitted to the data. Typically a power series curve is appropriate for proteins, and a linear series for peptides. The equation of this line, together with the  $t(d)''$  of the unknown samples are used to calculate estimated cross sections. A suitable calibrant for cross section estimation should bracket the mobilities of the unknown samples, not their cross sections (Shvartsburg and Smith, 2008).

The calibration compounds used were doubly sodiated dextran oligomers, and doubly protonated peptides from a number of proteins (serum albumin (bovine), cytochrome C (equine), aldolase (rabbit), transferrin (human), myoglobin (equine),

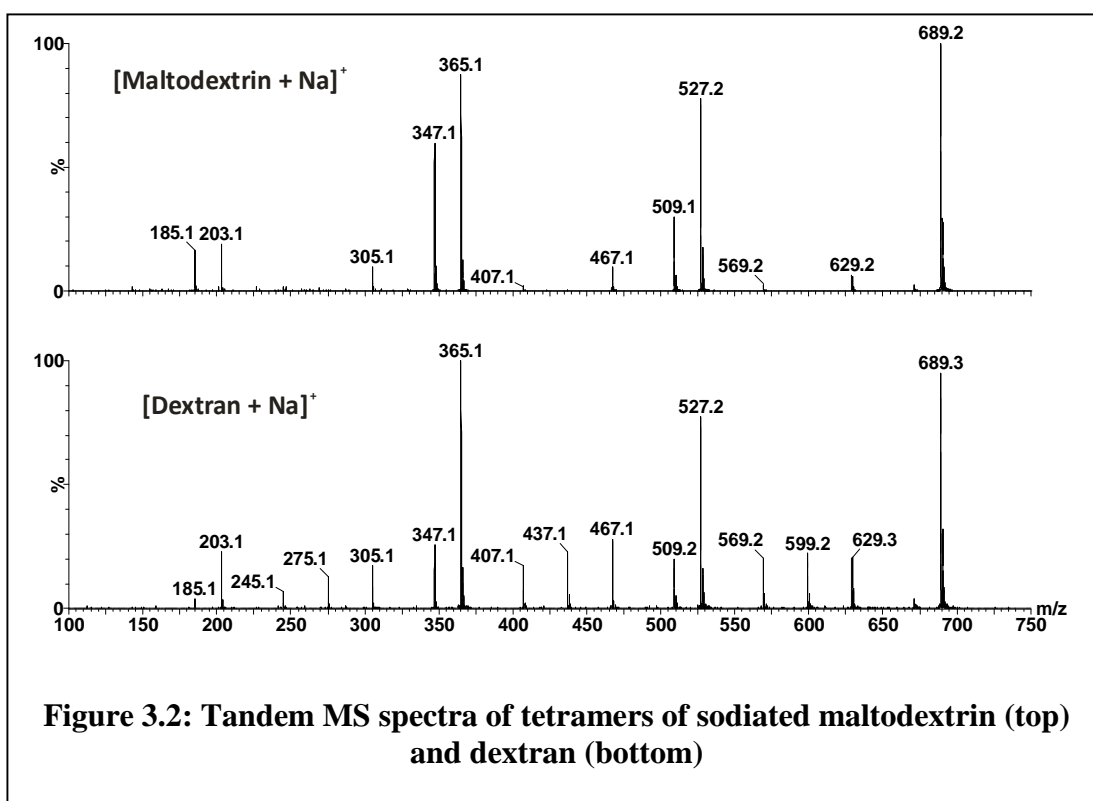
creatine phosphokinase (rabbit), haemoglobin (rabbit)) digested with trypsin. Cross sections for doubly protonated tryptic peptides have been obtained from a published database (Valentine *et al.*, 1999). Cross sections for doubly charged dextran oligomers were measured by means of DCIM-MS by collaborators at the University of California, Santa Barbara (UCSB). DCIM-MS was not been used for measurement of all other poly-Glc cross sections due to considerations of speed, sensitivity and ease of use of instrumentation.

## Results and Discussion

### Product Ion Mass Spectra

Figure 3.2 shows the product ion spectra produced from the sodium attachment ions of the tetramers  $m/z$  689,  $[M+Na]^+$  of maltodextrin and dextran. Using the Domon and Costello nomenclature (Domon and Costello, 1988) carbohydrates are labelled A, B, C from the non-reducing end and X, Y, Z from the reducing end. Since the samples studied here are homopolymers we are unable to assign uniquely the identity of the ring involved. A and X ions are produced by cleavage across the glycosidic ring and are labelled by assigning each bond a number and counting clockwise. As may be expected from the isomeric nature of the two compounds, the major fragment ions, at  $m/z$  527, 365 and 203 are common. These fragments are formed from the cleavage of the inter-ring glycosidic bonds and indicate a repeat unit of  $m/z$  162. The peaks at  $m/z$  629, 569, 467, 407 and 305 are again common to both spectra and are formed by intra-ring cross cleavage. Using the above nomenclature these may be labelled  $^{0,4}X_4$ ,  $^{0,2}X_4$ ,  $^{0,4}X_3$ ,  $^{0,2}X_3$ ,  $^{0,4}X_2$  and  $^{0,2}X_2$  respectively. The peaks at  $m/z$  671, 509, 347 and 185 are formed by water loss with glycosidic ring cleavage and are again seen in both spectra. Under the conditions of the MS/MS experiment there are

a series of ions which are present in the dextran product ion spectrum but are either very weak, or absent, in the maltodextrin product ion spectrum. The ions are found at  $m/z$  599, 437, and 275. These ions also correspond to intra-ring cross cleavage fragmentations and can be designated  $^{0,3}X_4$ ,  $^{0,3}X_3$  and  $^{0,3}X_2$  respectively. These ions presumably reflect the three dimensional structural variation of the two oligomers and enable them to be differentiated at the single molecule level. It is not possible however to utilise this information to comment on the details of the differences.



### Cross Section Calibration

Two cross section calibrations have been produced, one using  $[\text{dextran} + 2\text{Na}]^{2+}$  oligomers, and the other using doubly protonated tryptic peptides. The dextran  $t(d)''$  versus  $\Omega'$  plot was fitted with a power series trend line for use in cross section estimation (Figure 3.3). For the plot of  $t(d)''$  versus  $\Omega'$  for the tryptic peptides (Figure 3.4) a linear trend line was more appropriate.

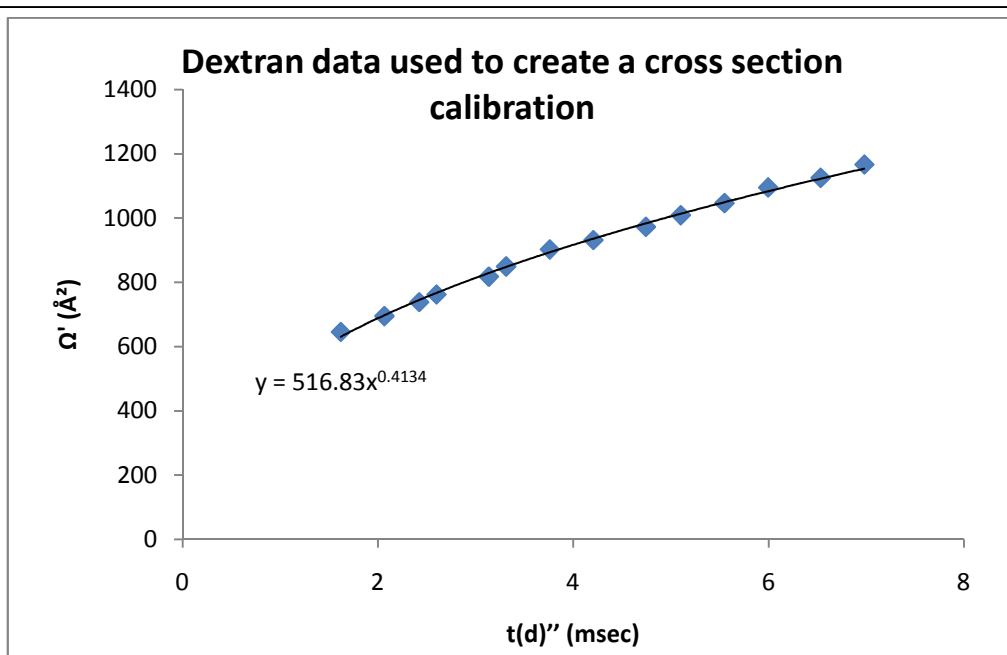


**Figure 3.3: A plot of corrected arrival times against corrected absolute cross sections for 14 dextran oligomers**

The dextran oligomers used for this calibration are all  $[\text{dextran} + 2\text{Na}]^{2+}$ .

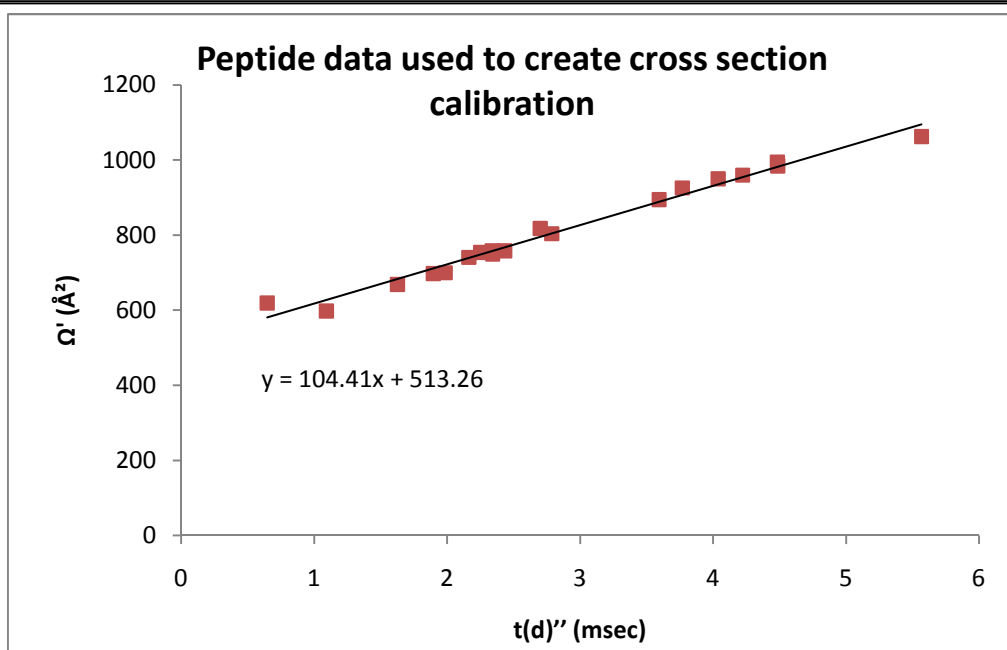


**Figure 3.4: A plot of corrected arrival times against corrected absolute cross sections for 19 tryptic peptides**

Tryptic peptides from serum albumin (bovine), cytochrome C (equine), aldolase (rabbit), transferrin (human), myoglobin (equine), creatine phosphokinase (rabbit), haemoglobin (rabbit) are all doubly charged.

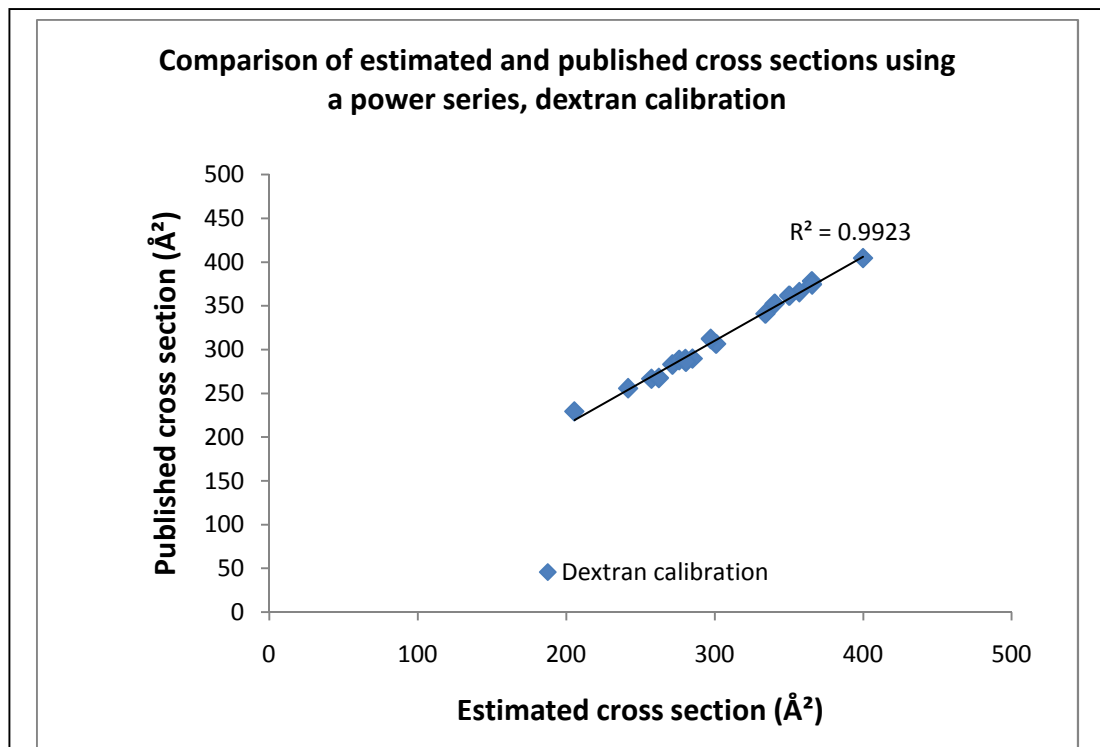


**Figure 3.5:** A comparison of published absolute and estimated cross sections for 19 tryptic peptides estimated using a dextran based calibration

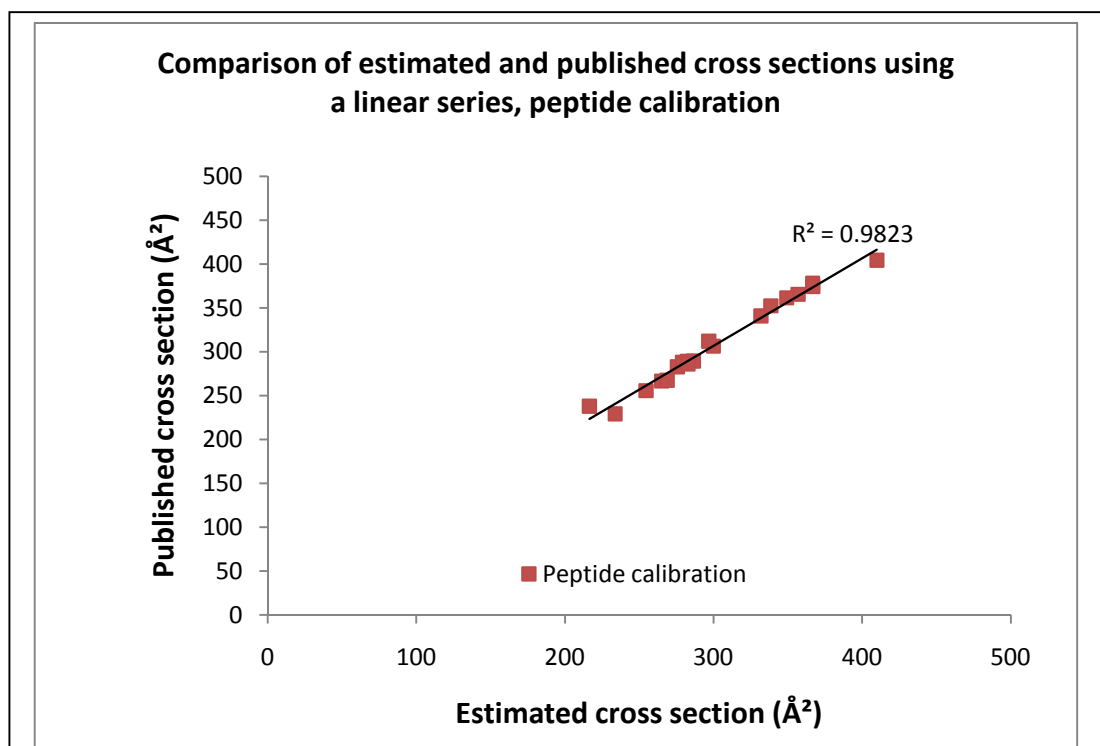


**Figure 3.6:** A comparison of published absolute and estimated cross sections for 19 tryptic peptides estimated using a peptide based calibration



To verify the accuracies of the two calibrations, a plot of published absolute cross sections and estimated cross sections calculated using each of the dextran and peptide based calibrations have been made (Figures 5-6). A perfect calibration will yield a linear trend line with a correlation co-efficient of 1.0. Although both gave good calibrations, the dextran based cross section calibration was observed to have a marginally better correlation, and was based on the compound type to be studied and has therefore been used for the cross section calculations presented here.

### **Cation Attachment**

Dextran and maltodextrin were both successfully cationised with all cations investigated (H, Li, Na, K, Rb, Cs). Singly, doubly and triply cationised species were observed covering a wide mass range (500 – 6000 Da). No significant differences were observed between the individually averaged ESI mass spectra of the dextran and maltodextrin samples demonstrating that, due to the isomeric nature of the systems, these samples cannot be differentiated using simple mass spectra alone. A small difference in relative abundances of some charge states was observed between the dextran and maltodextrin, but this may be due to differences in the molecular weight distribution of the samples. The polydispersity of the samples precluded measurement of the average molecular weight directly using MALDI mass spectrometry. This value could have been obtained via fractionation of the samples followed by analysis of the individual narrow molecular weight distributions (Montaudou and Lattimer, 2001).

### **TWIMS-MS Separation and Cross Section Estimation**

Ion mobility separations were achieved for all observed cationised dextran and maltodextrin oligomers. Extracted ATD data for mobility separated poly-Glc

oligomers has been used to calculate estimated cross sections for a range of cationised species.

Figures 3.7– 3.12 show plots of estimated cross sections of dextran and maltodextrin ionised with each cation type.  $m/z$  values for poly-Glc species have been converted to oligomer length to allow comparisons of species independent of cation mass.

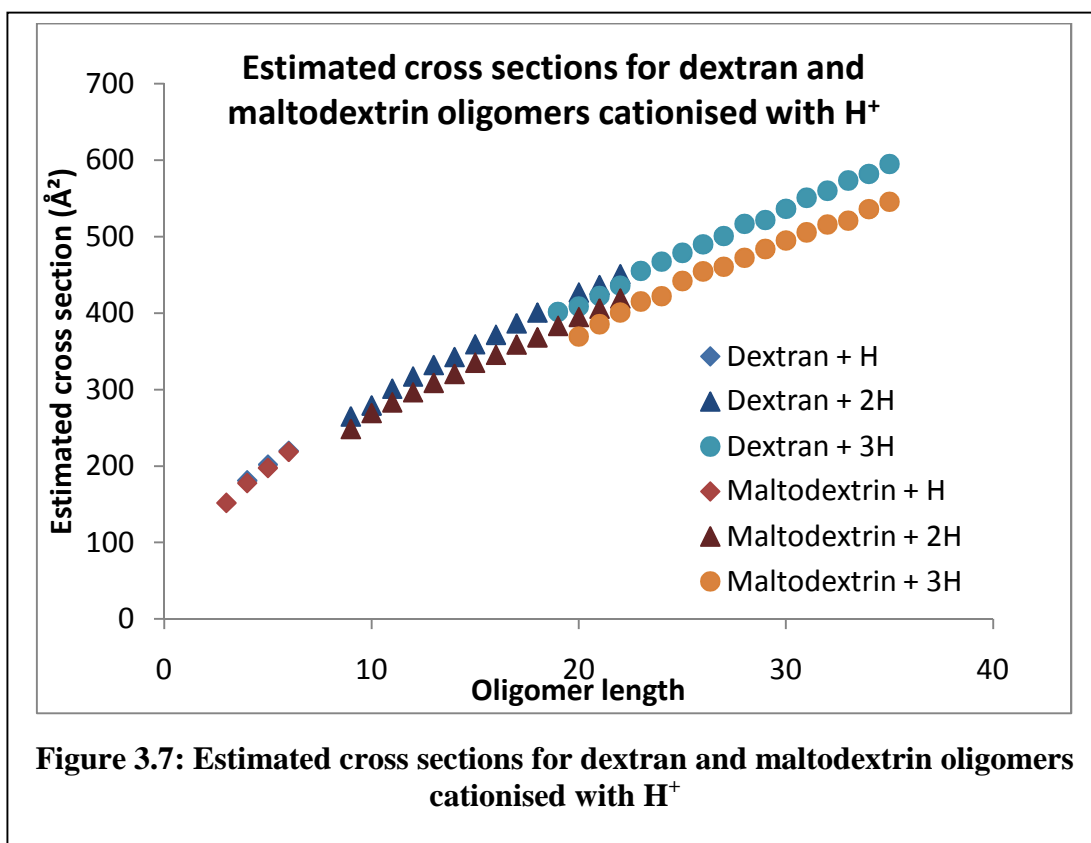


Figure 3.7: Estimated cross sections for dextran and maltodextrin oligomers cationised with H<sup>+</sup>

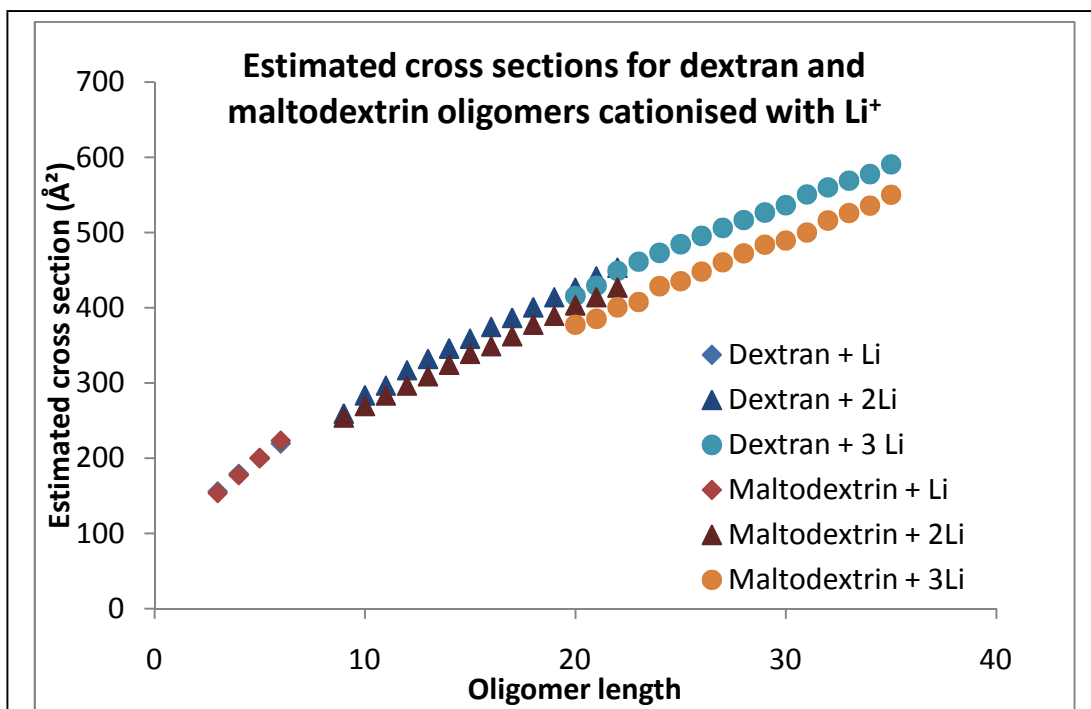


Figure 3.8: Estimated cross sections for dextran and maltodextrin oligomers cationised with  $\text{Li}^+$

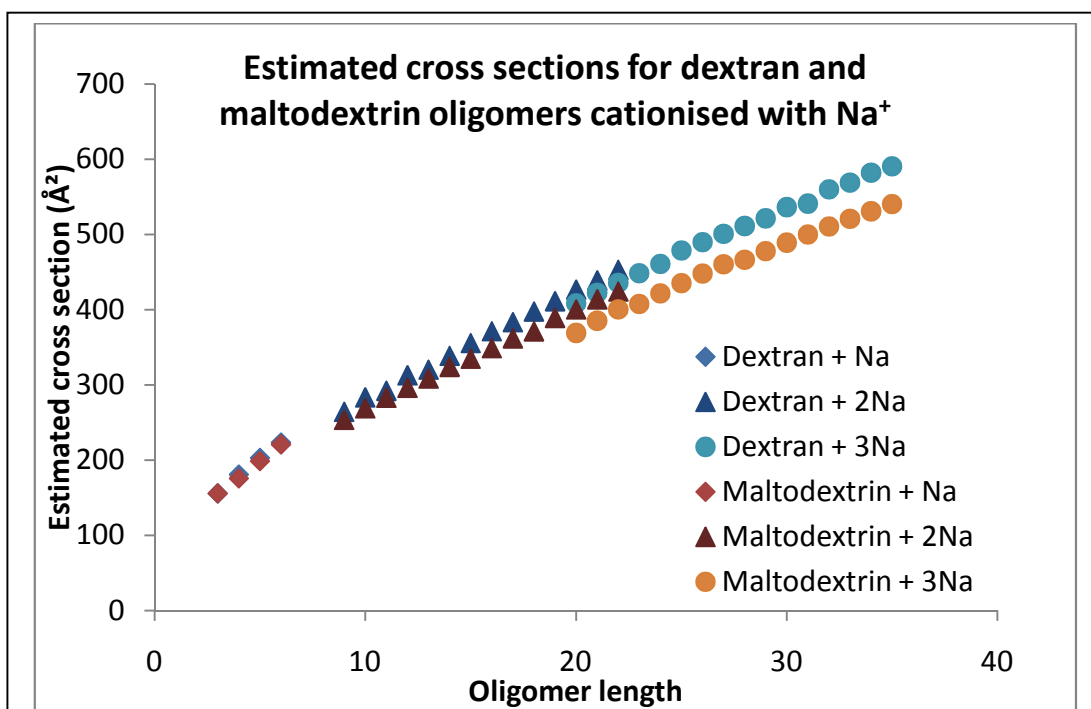
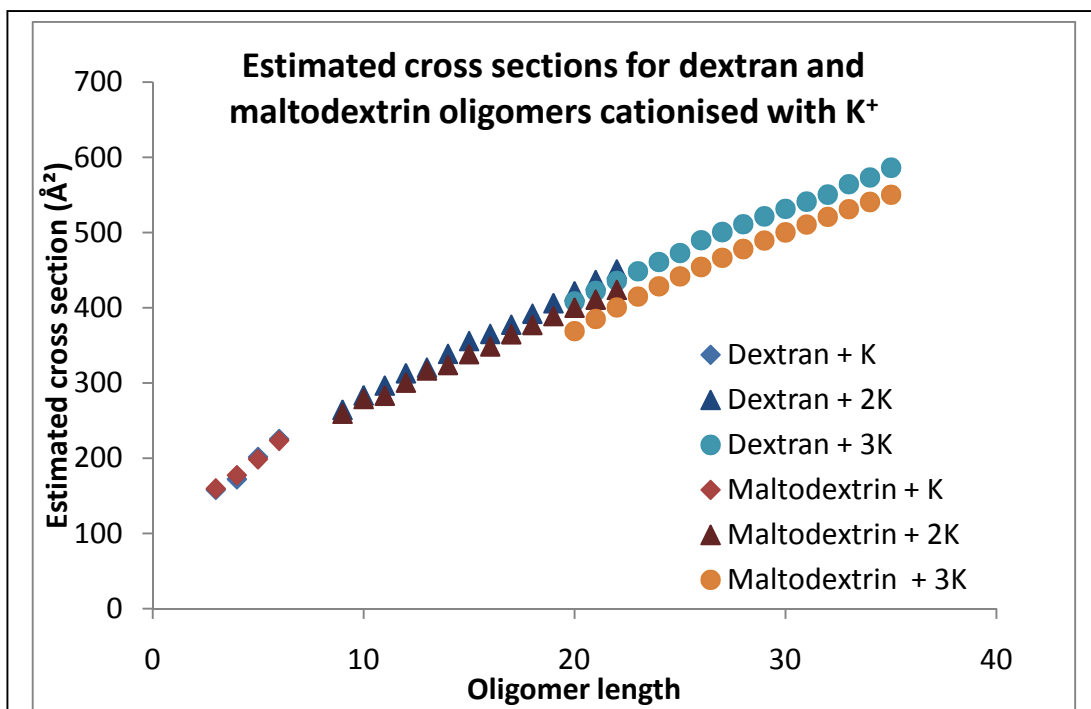
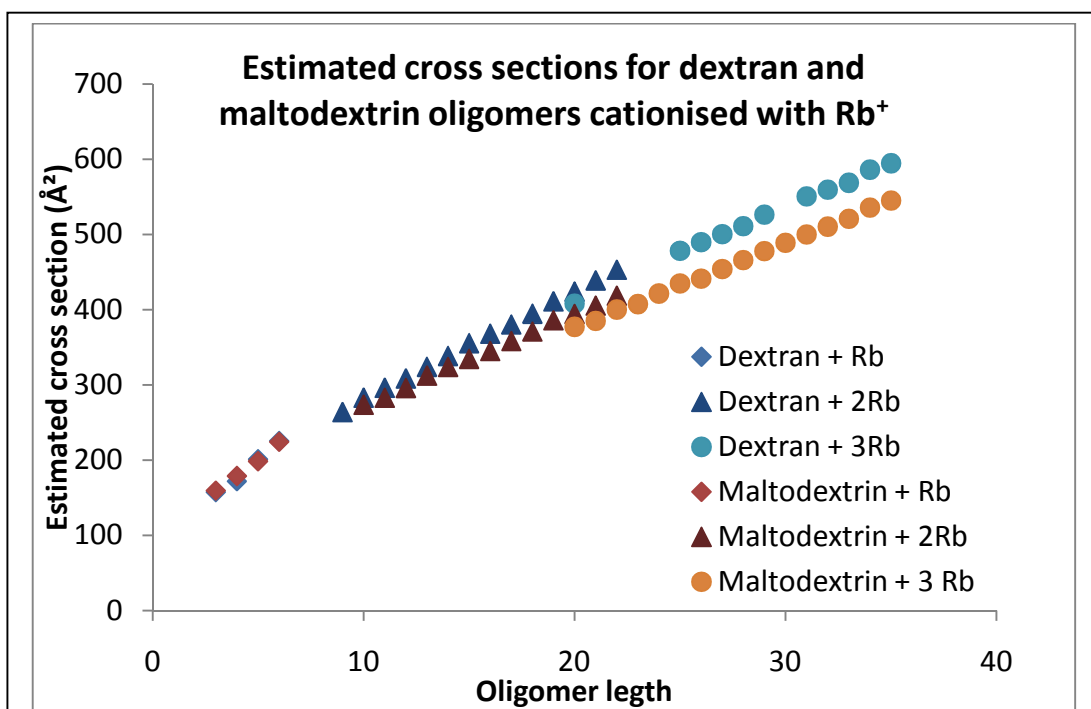


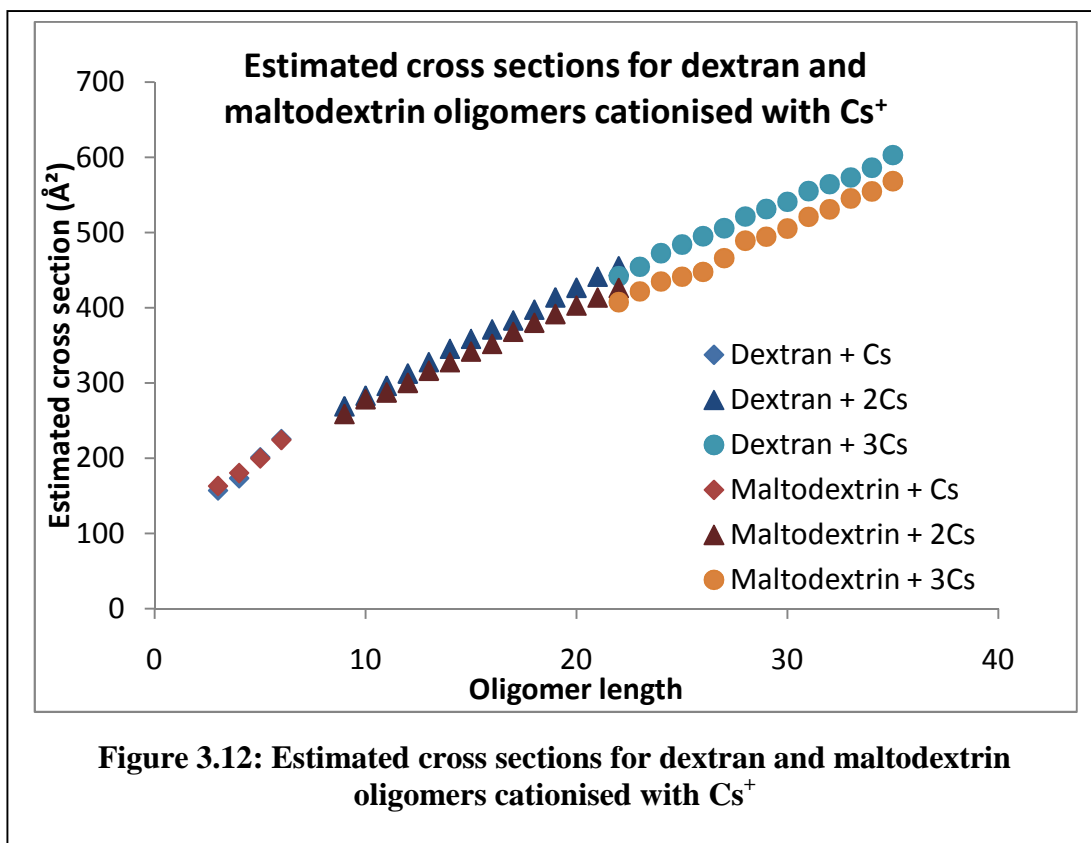
Figure 3.9: Estimated cross sections for dextran and maltodextrin oligomers cationised with  $\text{Na}^+$



**Figure 3.10: Estimated cross sections for dextran and maltodextrin oligomers cationised with  $K^+$**



**Figure 3.11: Estimated cross sections for dextran and maltodextrin oligomers cationised with  $Rb^+$**



From these measurements a number of interesting observations may be made.

For all singly cationised species, which cover a relatively narrow oligomer range of [3-6] there is no observable difference between dextran and maltodextrin within the calibrated cross section range. This indicates that cation size and presumably mode of interaction, are not dominant features over this narrow oligomeric range.

For doubly cationised species, which cover the rather larger oligomeric range of [9-22], maltodextrin estimated cross sections are lower than those calculated for dextran. This measured difference in cross section increases with increasing oligomer length.

For triply cationised species, which overlap the doubly charged region and cover the oligomer range [19-35], maltodextrin estimated cross sections are consistently lower than those calculated for dextran. The differences in cross section are larger than

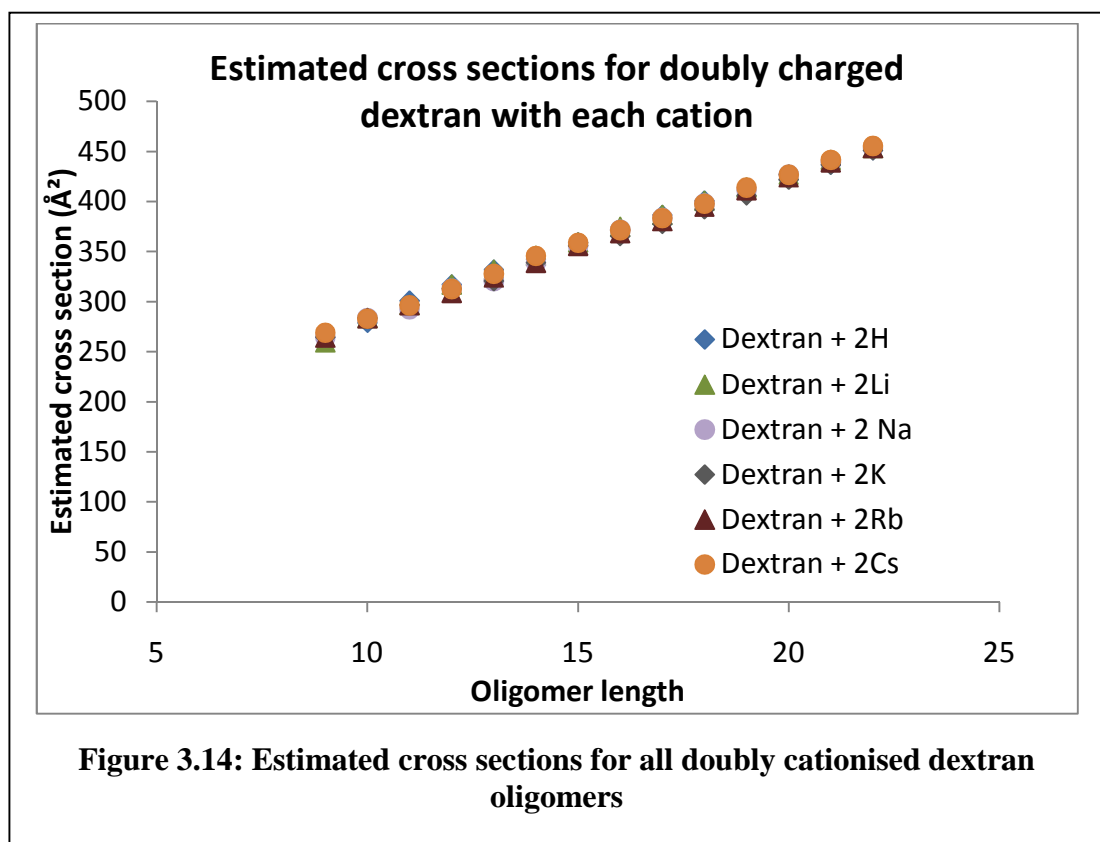
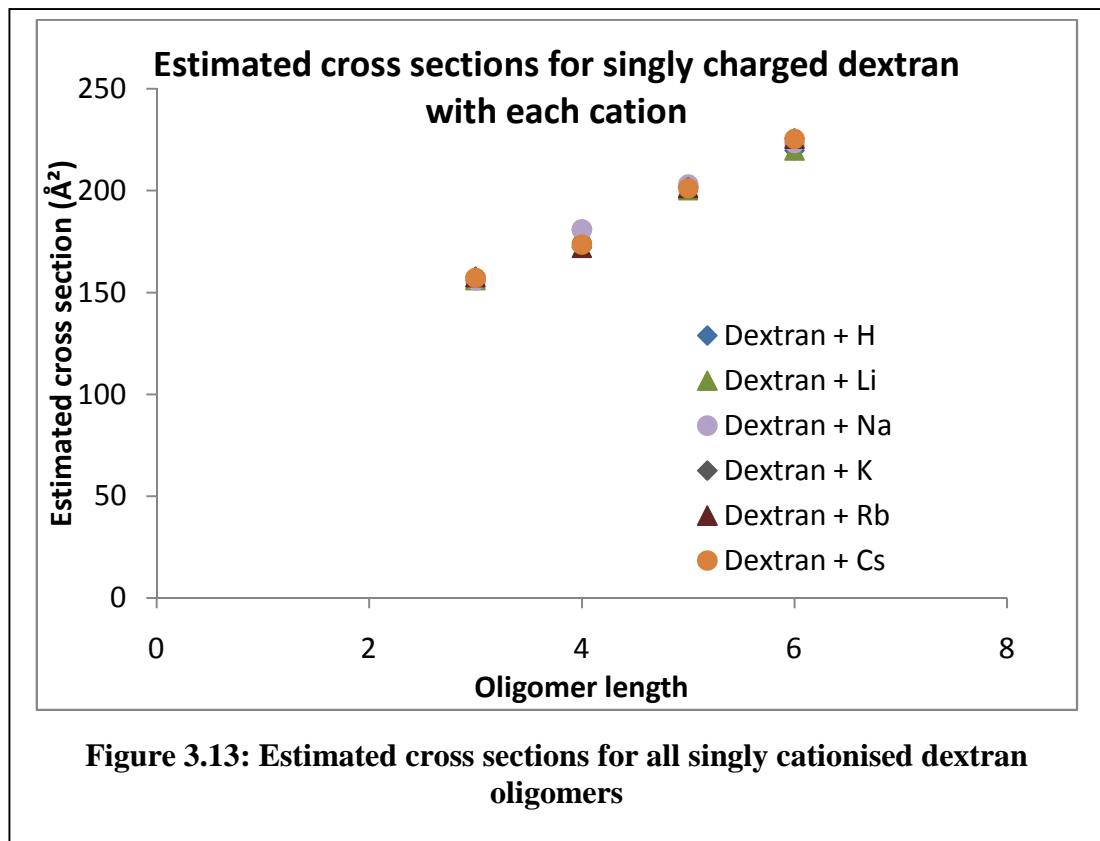
those observed in the doubly charged region, and increase with increasing oligomer length.

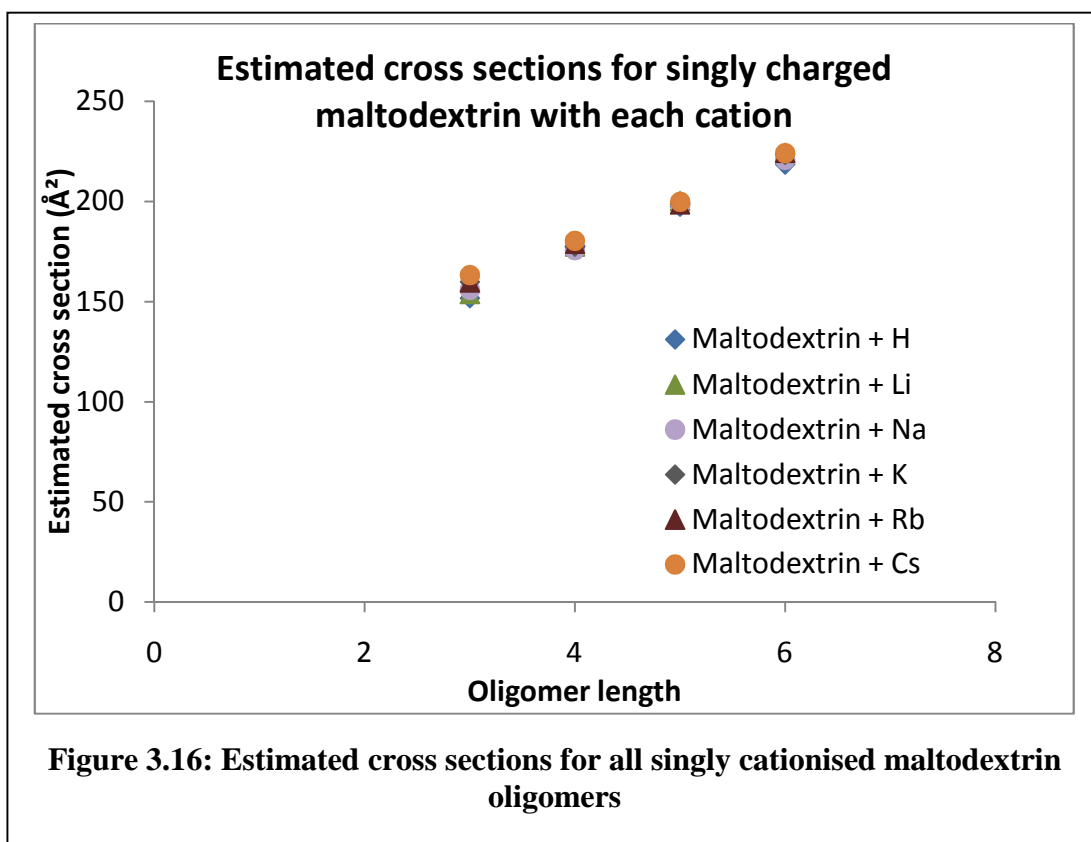
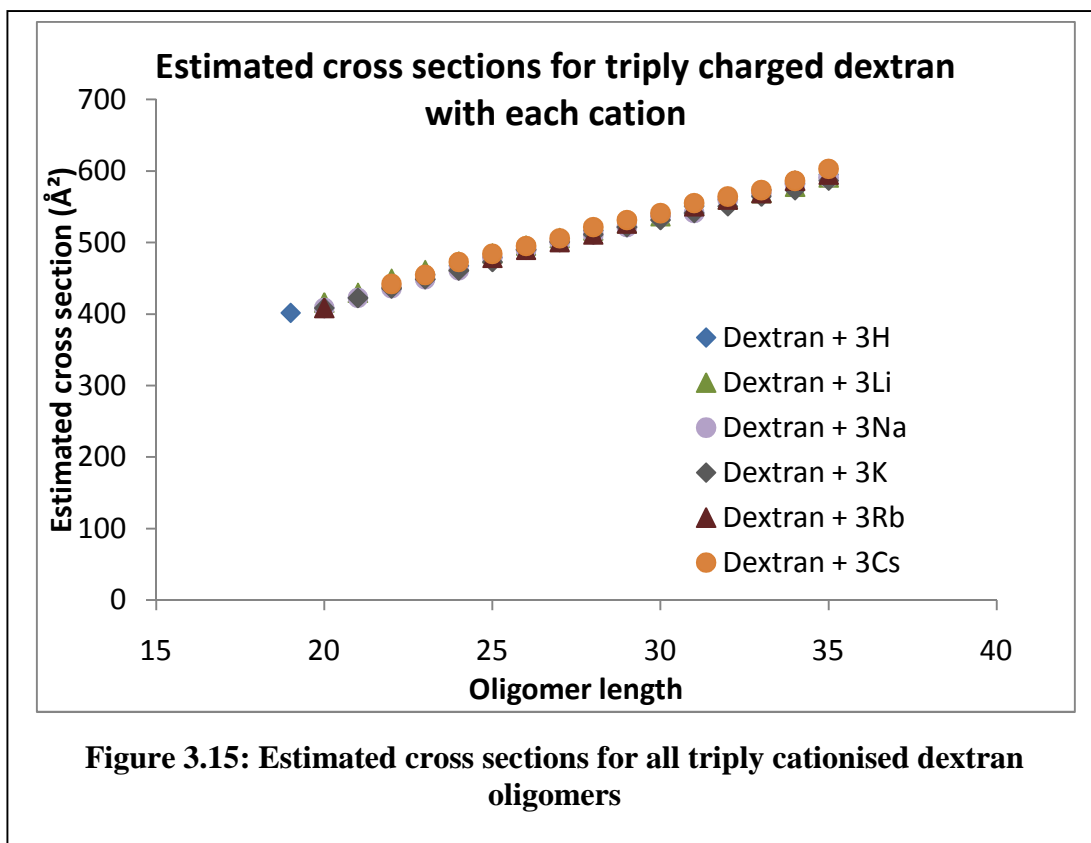
For species where both doubly and triply charged oligomers are observed, the triply charged species have a lower observed cross section than those observed for the equivalent doubly charged species.

These results indicate, as expected, that the ability of the carbohydrate chain to coordinate with more than one cation increases with oligomer length. The fact that the triply cationised species has a smaller cross-section than that of the doubly charged species can be explained by the need for more atoms to be coordinated.

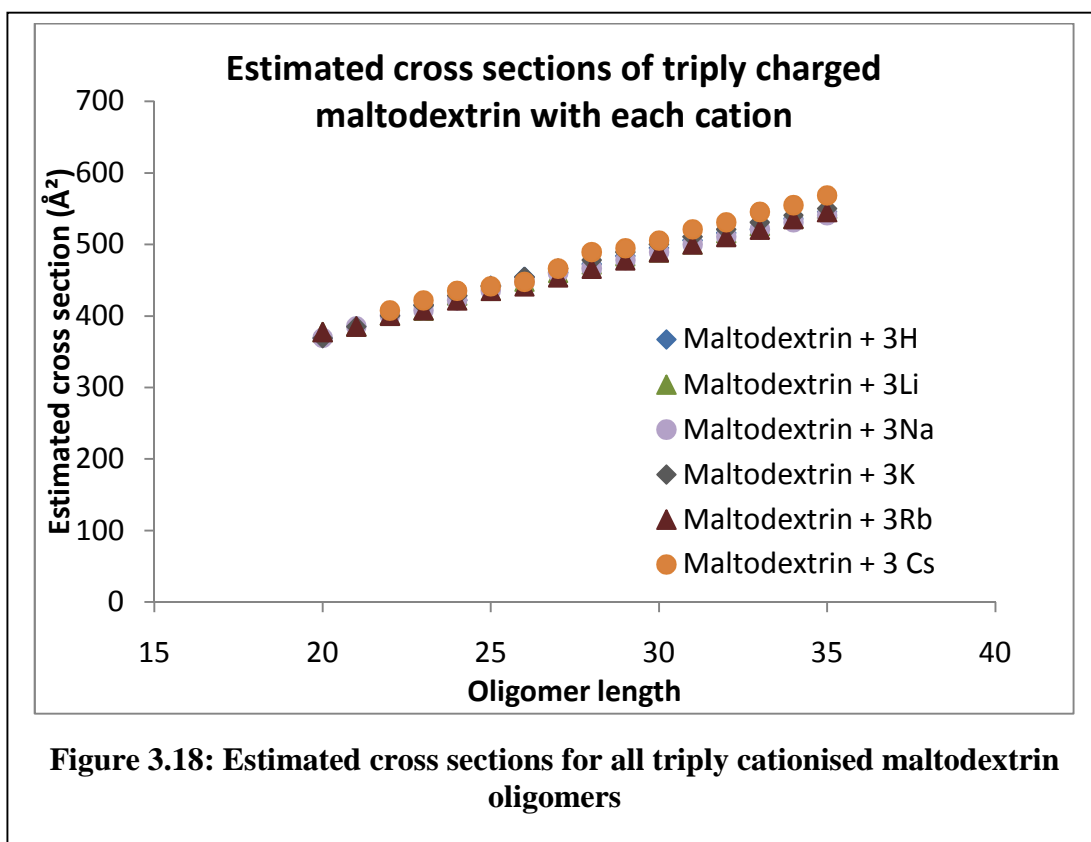
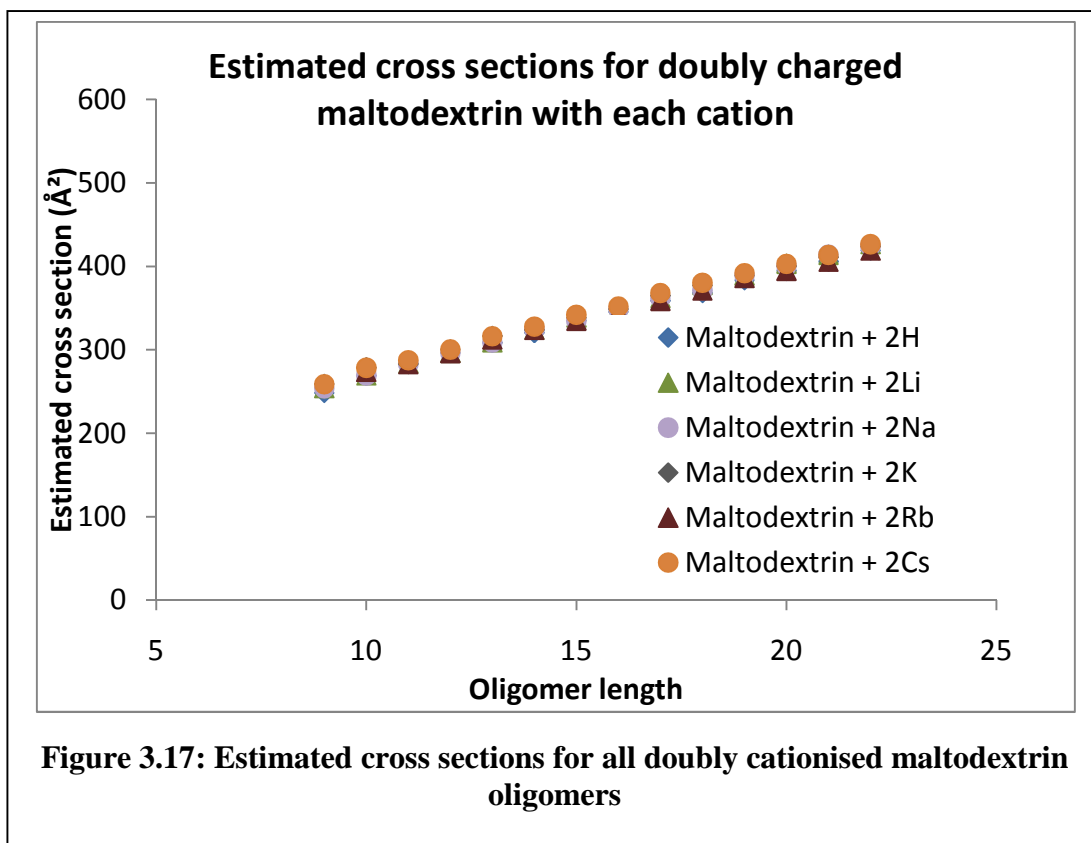
### **Variation of Cross Section with Attached Cation**

Figures 3.13 – 3.18 show estimated cross sections of dextran and maltodextrin oligomers at individual charge states with each cation. These results show clearly that the estimated cross sections observed for a selected oligomer and charge state do not vary with the nature of cation bound, over the calibrated range, within the expected variation of the experiment which has previously been estimated at (2-3%) (Scarff *et al.*, 2008). A small difference is observed at higher oligomer numbers as seen in Figures 3.15 and Figure 3.18 where the triply caesiated species have a larger estimated cross-section due, presumably, to the coordination requirements of the larger cation.









## Conclusions

The use of Nafion-117 membrane enables the selective cationisation of carbohydrates for study by mass spectrometry. Multiple cationisation enables a wide range of molecular weight species to be studied. In this experiment, singly, doubly and triply charged species, covering a mass range of 500 – 6000 Da have been observed.

The T-Wave ion mobility based Synapt instrument enables the rapid and sensitive shape selective separation of complex carbohydrate mixtures. When calibrated with molecules of known cross section, estimated cross sections can be calculated from the arrival time data recorded for each ion in the mass spectrum.

Long linear carbohydrates can provide multiple sites for cation attachment. The cation bound to these poly-Glc structures does not cause a significant change in rotationally averaged cross section.

Estimated cross sections for dextran and maltodextrin were observed to be in agreement with trends proposed from solution phase NMR structures (Brant *et al.*, 1995), with maltodextrin (where measurable differences were seen) having consistently smaller cross sections than the equivalent dextran oligomers. This supports the view that gaseous structures, studied using ion mobility mass spectrometry experiments of the type employed here, maintain important features of their solution behaviour.

TWIM-MS provides a rapid, sensitive and shape selective technique for the analysis of isomeric carbohydrates. This approach enables a number of important questions regarding the nature of interaction of the oligomeric chains with cations to be probed.

The fact that the nature of the coordinating cation has such a small effect on estimated cross section indicates that the dominant conformation is driven by the carbohydrate structure itself. The relative size at which multiple cation binding takes place is also related to the cation attachment process. The ability of the approach to measure relatively small differences in the gaseous conformation of isomeric carbohydrate oligomers gives confidence in the selectivity of the technique. The relatively large molecular weight range of oligomeric species that can be studied in one experiment (500-6000 Da) enables molecular weight dependant features to be readily studied. The speed, selectivity and information content of the mobility experiments that can be carried out on the commercial instrument mean that comprehensive, detailed studies of complex systems can be undertaken for the first time giving access to data that was not previously accessible in a reasonable timescale.

## References

**Bashir, S., Derrick, P. J., Critchley, P., Gates, P. and Staunton, J.** (2003). "Matrix-assisted laser desorption/ionization time-of-flight mass spectrometry of dextran and dextrin derivatives." *European Journal of Mass Spectrometry* **9**(1): 61-70.

**Bashir, S., Giannakopoulos, A. E., Derrick, P. J., Critchley, P., Bottrill, A. and Padley, H. J.** (2004). "Matrix-assisted laser desorption/ionisation time-of-flight mass spectrometry. A comparison of fragmentation patterns of linear dextran obtained by in-source decay, post-source decay and collision-induced dissociation and the stability of linear and cyclic glucans studied by in-source decay." *European Journal of Mass Spectrometry* **10**(1): 109-120.

**Bluhm, T. L. and Zugenmaier, P.** (1981). "Detailed structure of the Vh-amylose-iodine complex: a linear polyiodine chain." *Carbohydrate Research* **89**(1): 1-10.

**Börnsen, K. O., Mohr, M. D. and Widmer, H. M.** (1995). "Ion exchange and purification of carbohydrates on a Nafion® membrane as a new sample pretreatment for matrix-assisted laser desorption/ionization mass spectrometry." *Rapid Communications in Mass Spectrometry* **9**(11): 1031-1034.

**Brant, D. A., Liu, H.-S. and Zhu, Z. S.** (1995). "The dependence of glucan conformational dynamics on linkage position and stereochemistry." *Carbohydrate Research* **278**(1): 11-26.

**Choi, S.-S., Lee, H. M., Jang, S. and Shin, J.** (2009). "Comparison of ionization behaviors of ring and linear carbohydrates in MALDI-TOFMS." *International Journal of Mass Spectrometry* **279**(1): 53-58.

**Domon, B. and Costello, C. E.** (1988). "A Systematic nomenclature for carbohydrate fragmentations in FAB-MS spectra of glycoconjugates." *Glycoconjugate Journal* **5**(4): 397-409.

**Gidden, J., Bowers, M. T., Jackson, A. T. and Scrivens, J. H.** (2002). "Gas-phase conformations of cationized poly(styrene) oligomers." *Journal of the American Society for Mass Spectrometry* **13**(5): 499-505.

**Gidden, J., Wyttenbach, T., Jackson, A. T., Scrivens, J. H. and Bowers, M. T.** (2000). "Gas-phase conformations of synthetic polymers: Poly(ethylene glycol), poly(propylene glycol), and poly(tetramethylene glycol)." *Journal of the American Chemical Society* **122**(19): 4692-4699.

**Montaudou, G. and Lattimer, R. P.** (2001). *Mass spectrometry of polymers*, CRC Press.

**Scarff, C. A., Thalassinos, K., Hilton, G. R. and Scrivens, J. H.** (2008). "Travelling wave ion mobility mass spectrometry studies of protein structure: biological significance and comparison with X-ray crystallography and nuclear magnetic resonance spectroscopy measurements." *Rapid Communications in Mass Spectrometry* **22**: 3297-3304.

**Shvartsburg, A. A. and Smith, R. D.** (2008). "Fundamentals of Traveling Wave Ion Mobility Spectrometry." *Analytical Chemistry* **80**(24): 9689-9699.

**Thalassinos, K., Grabenauer, M., Slade, S. E., Hilton, G. R., Bowers, M. T. and Scrivens, J. H.** (2009). "Characterization of Phosphorylated Peptides Using Traveling Wave-Based and Drift Cell Ion Mobility Mass Spectrometry." *Analytical Chemistry* **81**(1): 248-254.

**Tvaroska, I. and Kozár, T.** (1981). "The conformational properties of the glycosidic linkage." *Carbohydrate Research* **90**(2): 173-185.

**Valentine, S. J., Counterman, A. E. and Clemmer, D. E.** (1999). "A database of 660 peptide ion cross sections: Use of intrinsic size parameters for bona fide predictions of cross sections." *Journal of the American Society for Mass Spectrometry* **10**(11): 1188-1211.

**Vetter, D. and Thorn, W.** (1992). " $C^{13}$  NMR spectroscopic detection of maltooligosaccharide complexes." *Starch-Starke* **44**(7): 271-274.

**Wildgoose, J. L., Giles, K., Pringle, S. D., Koeniger, S. J., Valentine, R. H., Bateman, R. H. and Clemmer, D. E.** (2006). *A comparison of travelling wave and drift tube ion mobility separations*. Proc. 54th ASMS Conf. Mass Spectrometry and Allied Topics, Seattle.

## **Chapter 4:**

# **Ion Mobility of Glycans**

## Introduction

### Characterisation of Glycosylation

Glycosylation is the co- and post-translational attachment of carbohydrate structures to a protein backbone. The carbohydrate moieties of these glycoconjugates have many important roles in biological systems. These roles include protein folding, cell-cell recognition and protection from proteolysis (Dwek, 1996). Glycosylation is one of the most prevalent forms of covalent protein modification, occurring for approximately 50% of all proteins in eukaryotic systems. Mammalian and plant glycoproteins can be either *N*-linked or *O*-linked. In *N*-linked glycosylation, oligosaccharides bind to the amide nitrogen of asparagine side chains. In *O*-linked glycosylation, they bind to the hydroxy oxygen of serine and threonine side chains. Addition of carbohydrate-containing GPI anchors to proteins to allow for membrane attachment can also be considered a special form of glycosylation.

Despite the importance of oligosaccharides in biological systems, structural determination of these molecules is an analytical challenge compared to other biomolecules. Not only do the constituent monosaccharides (and their stereochemistry) have to be identified, but how they link together to form the polymer needs to be determined. Given that monosaccharides have multiple linkage sites and each site has two possible anomeric linkage configurations, oligosaccharide structure can be very complex (Harvey, 2001). Mass spectrometry (MS) has proven to be a valuable tool in the study of oligosaccharides. With the help of chemical degradation, derivatisation and mass spectral fragmentation, oligosaccharide structure can be elucidated. There are also practical motivations for advancing glycomic research. For example, the pharmaceutical industry makes increasing use



of recombinant synthesis of proteins due to the reduced cost and increased quality over extraction and purification approaches (Ma *et al.*, 2003). Modern methods can incorporate post-translational modifications such as phosphorylation and glycosylation and there is a requirement for a rapid, sensitive, information-rich method to monitor glycosylation in these systems for process optimization and quality control purposes.

### **Ion mobility-mass spectrometry**

Conventional mass spectrometry only takes advantage of mass separation and gives no direct information about three-dimensional shape. Ion mobility-mass spectrometry (IMMS) uses not only traditional mass separation techniques, but also separates ions based on their mobility in an inert buffer gas. The method can, therefore, distinguish isomers with identical masses but different cross sections. In traditional IMMS, a weak uniform electric field is applied across a mobility cell (using direct current) to pull ions through a helium buffer gas. Compact isomers with higher mobilities exit the cell before more extended isomers that have lower mobilities. This direct-current ion mobility spectrometry (DCIMS) configuration allows for the measurement of a well-defined ion mobility and thus, using kinetic theory, determination of an ion's collision cross section. Comparing experimental cross sections to those of theoretical structures reveals information about the true gas-phase structures being observed experimentally. In the Bowers group, this method has been applied successfully to a number of biological systems, including DNA helices (Gidden *et al.*, 2004; Gidden *et al.*, 2005), G-quadruplexes (Baker *et al.*, 2005; Baker *et al.*, 2006; Gabelica *et al.*, 2007) and the Alzheimer's peptides A $\beta$ 40 and A $\beta$ 42 (Bernstein *et al.*, 2005; Baumketner *et al.*, 2006). Despite the fact that these biomolecules have undergone electrospray ionization (ESI) for transfer to

the gas phase, evidence suggests that to a significant extent, solution-phase conformations are retained. This characteristic has also been observed by other mass spectrometry groups. Pioneering work by Robinson (Last and Robinson, 1999) demonstrated “compelling evidence for preservation of tertiary structure under controlled conditions” and a review by Heck (Heck and van den Heuvel, 2004), describing the analysis of intact protein complexes by mass spectrometry, strongly supports this view.

The development of travelling wave ion mobility spectrometry (TWIMS) (Giles *et al.*, 2004) has significantly increased sensitivity and speed in comparison with the traditional DCIMS device, allowing for the analysis of samples at biologically-relevant concentrations. TWIMS has been integrated into a commercial quadrupole time-of-flight instrument, the Synapt HDMS System (Waters, UK). (Pringle *et al.*, 2007) The Synapt operates with excellent reproducibility and mass accuracy, and is capable of providing a wealth of information being able to achieve ion mobility spectrometry-tandem mass spectrometry (IMS-MS/MS) with the choice of performing collision-induced dissociation before or after the mobility cell. The nature of the TWIMS device means that, unlike in DCIMS, the ion drift time is not inversely proportional to ion mobility and thus absolute collision cross sections cannot be obtained directly from drift cell information. It has been shown, however, that estimates of collision cross sections can be obtained by reference to samples with known cross sections (Ruotolo *et al.*, 2005; Scarff *et al.*, 2008; Williams and Scrivens, 2008; Thalassinos *et al.*, 2009), provided that the data is obtained under the same experimental conditions; i.e. mobility gas, gas pressure, wave velocity, wave height, pusher frequency and injection energy.

## **Ion mobility based analysis of oligosaccharides**

Ion mobility methods have previously been used to study oligosaccharides. DCIMS investigations have been used to obtain structures of several small sodiated sugars (Lee *et al.*, 1997; Jin *et al.*, 2005) and to demonstrate the separation capability for a number of carbohydrate isomers (Liu and Clemmer, 1997; Lee *et al.*, 1998; Clowers *et al.*, 2005). Clemmer and co-workers have lately used traditional DCIM-MS to examine glycans released from ovalbumin (Plasencia *et al.*, 2008). Recent work from the group of Hill (Dwivedi *et al.*, 2007) expands on previous research by describing the successful resolution of carbohydrate isomers with different anomeric configurations together with the use of adducts and variation of mobility gas to improve separation. Differential mobility spectrometry has been employed to study aggregate formation in the analysis of oligosaccharides (Levin *et al.*, 2007). This work describes the results of a combined DCIMS and TWIMS investigation of a range of oligosaccharides. The ability of the TWIMS method, coupled with MS and MS/MS approaches, to characterize carbohydrates released from a number of glycoproteins (Table 4.1) is explored. The structures of the carbohydrate moieties associated with each of these proteins have been previously studied by methods such as NMR and traditional mass spectrometry (Yoshima *et al.*, 1981; Green *et al.*, 1988; de Waard *et al.*, 1991; Fu *et al.*, 1994; Da Silva *et al.*, 1995; Harvey *et al.*, 2000). With standard analysis methods, structural characterization can only occur after some sort of chromatographic separation technique, such as HPLC, has been applied.

## Objectives

The sensitivity of the TWIM-MS technique, together with the rapid experimental timescale, reproducibility and high information content make this an attractive approach for the characterization of complex mixtures in glycomic research.

The following experiments aimed to rapidly separate N-glycans released from glycoproteins based on their ion mobility in TWIM-MS. Glycans released from a number of glycoproteins have been analysed by TWIM-MS, and it has been observed that the carbohydrates are readily separated by this method.

A series of isomeric penta- and hexasaccharides have also been examined (Table 4.1) using both the DCIMS and TWIMS techniques to evaluate the isomer separation capabilities of the two methods. In the DCIMS experiments, collision cross sections for the sodiated oligosaccharides were obtained. By comparing these values with cross sections of model structures acquired by molecular mechanics calculations, it has been possible to determine potential gas-phase structures of these species. In addition, the DCIMS experimental cross sections are compared to the TWIMS results. Carbohydrates (glycans) released from the glycoproteins are readily separated by ion mobility in TWIM-MS. Common glycans (e.g. Man<sub>5-7</sub>GlcNAc<sub>2</sub>, where Man = mannose, GlcNAc = *N*-acetylglucosamine) were observed to have the same arrival time distribution independent of their source. This indicates that, despite the presence of other species in a complex mixture, arrival time measurements are reproducible. Tandem mass spectrometry experiments on components separated using ion mobility are also demonstrated and found to provide additional information regarding carbohydrate structure.



## Experimental

### Ion mobility spectrometry-mass spectrometry (IMS-MS)

#### DCIM-MS

All DCIM-MS based experiments were performed by collaborators in the Bowers group at UCSB.

IMS-MS experiments at UCSB were performed on a home-built spectrometer consisting of a nano-ESI source, an ion funnel, and a mobility drift cell followed by a quadrupole mass analyzer and detector (Wytttenbach *et al.*, 2001). Samples were introduced into the nano-ESI source by means of a metal coated borosilicate capillary (Proxeon, Odense, Denmark). The ions generated are transferred, via a metal capillary, to the ion funnel where they can be accumulated and pulsed into the drift cell. A weak uniform electric field is applied across the drift cell (using direct current) to pull ions through a helium buffer gas (at ~1-5 mbar). To measure arrival time distributions (ATDs), ions are pulsed from the funnel into the drift cell. Ions are separated by their mobility, with compact structures travelling faster than extended structures. Ions exit the drift cell and are mass analysed and detected as a function of arrival time,  $t_A$ . To measure mobility ( $K_0$ ),  $t_A$  for a particular ion is measured as a function of the drift voltage ( $V$ ) applied to the cell (of known pressure ( $p$ ) and length ( $\ell$ )). As shown in eq 1, a plot of  $t_A$  versus  $p/V$  yields a straight line with a slope inversely proportional to  $K_0$  and has a y-intercept equal to  $t_0$ , the amount of time the ions spend outside the cell.

$$t_A = \frac{\ell^2 T_0}{K_0 p_0 T} \frac{p}{V} + t_0$$

## 4. 1

In this equation, standard temperature ( $T_0 = 273.15$  K) and pressure ( $p_0 = 1.013$  bar) are used to obtain a mobility independent of cell temperature and pressure, i.e., the reduced mobility,  $K_0$ .

The mobilities obtained in this experiment can be used to calculate an ion's collision cross section using the following relationship obtained from kinetic theory (Mason and McDaniel, 1988).

$$\sigma = \frac{3ze}{16N} \left( \frac{2\pi}{\mu kT} \right)^{1/2} \frac{1}{K_0}$$

## 4. 2

Here,  $z$  is the number of charges on the ion,  $e$  is the electronic charge,  $N$  is the buffer gas number density,  $\mu$  is the reduced mass of the ion and buffer gas,  $k$  is the Boltzmann constant and  $T$  is temperature.

**TWIM-MS instrument**

All TWIM-MS experiments were performed in a hybrid quadrupole-ion mobility-orthogonal acceleration time-of-flight (oa-TOF) mass spectrometer (Synapt HDMS, Waters, Manchester, UK) at the University of Warwick. The instrument was equipped with a nano-ESI source and operated at a source temperature of 120 °C. The sample solutions were introduced into the source region of the instrument by means of metal coated borosilicate capillaries (Waters Corporation, Manchester, UK). The cone was optimized between 60 and 130 V for ESI-MS/MS experiments and the collision energy was optimized to fragment the ion of interest, typically 110 eV in positive and 70 eV for negative ESI mode. A detailed explanation of the

Synapt HDMS technology can be found in chapter 1.5.2.1. Briefly: the machine is comprised of three travelling wave enabled stacked ion guides: trap, ion mobility separator and transfer. The trap ion guide is used to accumulate ions and releases these as ion packets into the ion mobility separator for mobility separation. The transfer ion guide is used to convey the mobility-separated ions to the oa-TOF mass analyzer. Ions were mass selected using the quadrupole prior to MS/MS experiments. All MS/MS experiments were performed after ion mobility separation in the transfer cell. Optimised TWIM-MS operating conditions are listed in Table 4.2. The TOF analyzer recorded 200 orthogonal acceleration pushes (mass spectra) with the pusher period set to an appropriate value depending on m/z acquisition range. The total acquisition time for the data shown was combined and averaged over 2 minutes. The TOF analyser was tuned in V-optic mode for an operating resolution of 7,000 (FWHM). Mass spectra were acquired at an acquisition rate of one spectrum per second with an interscan delay of 100 ms. Data acquisition and processing were carried out using MassLynx™ (v4.1) software (Waters Corp., Milford, MA, USA).



Table 4.2. Optimised TWIMS Cell Parameters

Sample	ESI Mode	Cell Pressure	Gas	T-Wave Height	T-Wave Velocity
Released Glycans	<i>N</i> -Positive	0.5		11	400
Released Glycans	<i>N</i> -Negative	0.5		18	500
Isomeric Carbohydrates	Positive	0.75		14	300

## Materials

Bovine ribonuclease B, chicken ovalbumin, porcine thyroglobulin, bovine fetuin and human  $\alpha$ 1-acid glycoprotein were purchased from Sigma Chemical Co. Ltd. (Poole, Dorset, UK). Ribonuclease B (Fu *et al.*, 1994) and chicken ovalbumin (Da Silva *et al.*, 1995; Harvey *et al.*, 2000) contain only neutral sugars. Thyroglobulin (de Waard *et al.*, 1991), fetuin (Green *et al.*, 1988) and human  $\alpha$ 1-acid glycoprotein (Yoshima *et al.*, 1981) contained both sialylated and neutral sugars. Desialylated versions of thyroglobulin, fetuin and  $\alpha$ 1-acid glycoprotein were generated using 10% acetic acid for 30 min at 80 °C. The glycans from these proteins were released with hydrazine (Patel *et al.*, 1993) and dissolved in a mixture of H<sub>2</sub>O/methanol (1:1; v/v) to a concentration between 10-25 pmol  $\mu$ L<sup>-1</sup> for analysis using the Synapt instrument.

The six oligosaccharides B-pentasaccharide, iso-B-pentasaccharide, lacto-*N*-fucopentaose I and V, and lacto-*N*-difucohexaose I and II were purchased from Sigma-Aldrich Company Ltd. (Poole, UK) and were dissolved in a mixture of

H<sub>2</sub>O/methanol (1:1; v/v) to a concentration of 10 pmol  $\mu\text{L}^{-1}$  for analysis using both the DCIMS-MS and Synapt instruments.

### **Molecular modelling**

Molecular modelling studies were performed by collaborators in the Bowers group at UCSB.

Theoretical modelling of the six oligosaccharides investigated with DCIMS-MS was done with the AMBER 8 package of molecular dynamics software (Case *et al.*, 2004) using the general AMBER force field. Using structures of the oligosaccharides built in Hyperchem (2002), partial charges were calculated following the RESP procedure within AMBER with Gaussian 03 (Frisch *et al.*, 2004) and the 6-31G\* basis set. A set of initial structures was created for each oligosaccharide by building the molecule in xleap, then varying the position of the sodium counter ion. A simulated annealing protocol was used to generate 150-200 low-energy candidate structures for each initial structure of the oligosaccharides. In this protocol an initial structure was subjected to 30 ps of molecular dynamics at 600 K followed by 10 ps of dynamics during which the temperature was lowered to 0 K. The resulting structure was then energy minimized, saved, and used as the starting structure for the next cycle. The collision cross sections of these candidate structures were then calculated using the exact hard-sphere scattering and trajectory models developed by the Jarrold group (Mesleh *et al.*, 1996). For each oligosaccharide the average cross sections of the lowest energy families of structures, which for the systems considered in this work showed only minor structural deviations, were reported. Figures were prepared using the UCSF Chimera package. (Pettersen *et al.*, 2004)

## Results and Discussion

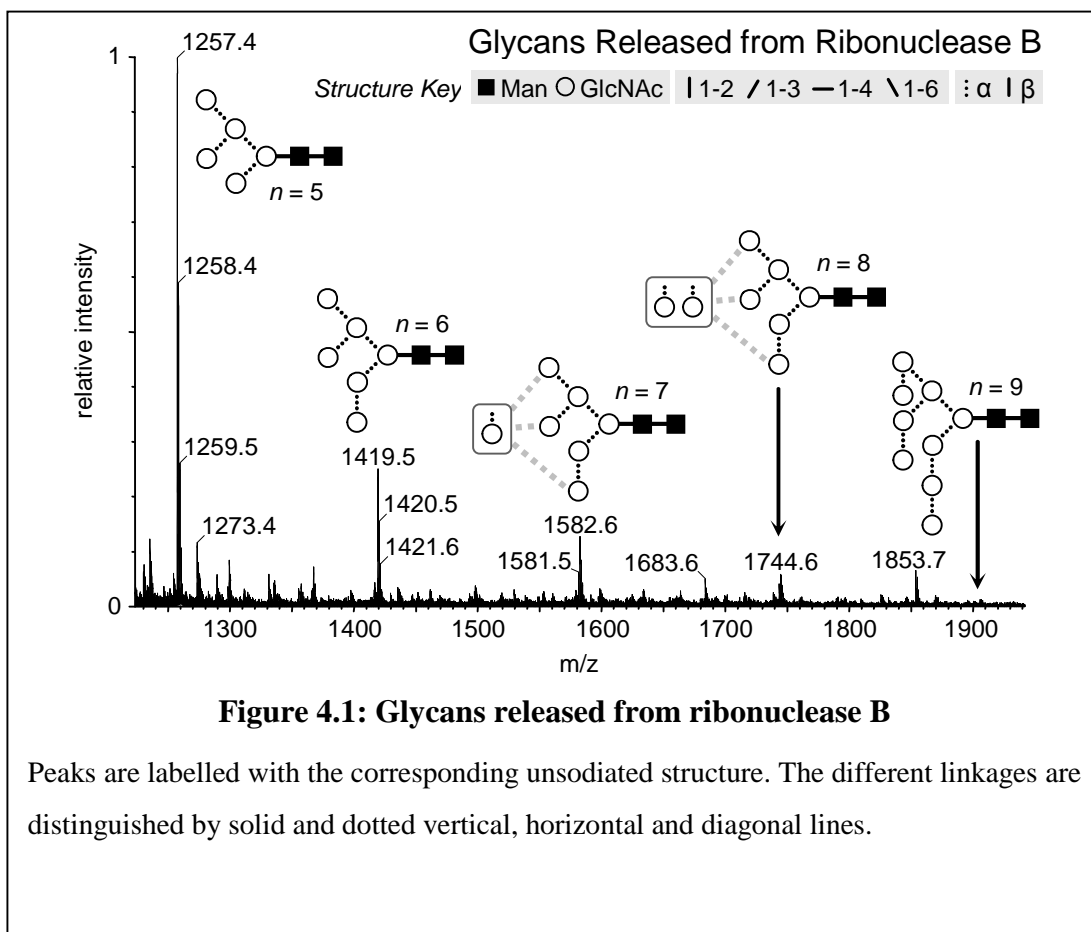
### The rapid separation of chemically released N-linked glycans

The TWIM-MS-based approach offers a number of advantages for the analysis of a complex mixture of released glycans. These include high sensitivity, rapid analysis, no requirement for further sample preparation and the extremely high information content of the experiment. In addition to mobility separation, mass spectral information (both MS and MS/MS) can be obtained. By using an established calibration approach, based on accepted rotationally averaged cross sectional values obtained from conventional DCIMS experiments, estimated cross sections can also be obtained. An attractive feature of IMMS is the millisecond timescale of ion separation in the gas phase. This dovetails well with the second timescale of liquid chromatography and the microsecond timescale of mass spectrometry data acquisition. The established technique for separating oligosaccharide mixtures is normal-phase high-performance liquid chromatography (HPLC) (Guile *et al.*, 1996). The IMMS approach can be used in a similar manner to HPLC for the rapid separation of these complex mixtures without prior HPLC separation. To this end, we have used the TWIM-MS and TWIM-MS/MS methods to investigate the N-linked glycans released from the set of well-studied glycoproteins listed in Table 4.1.

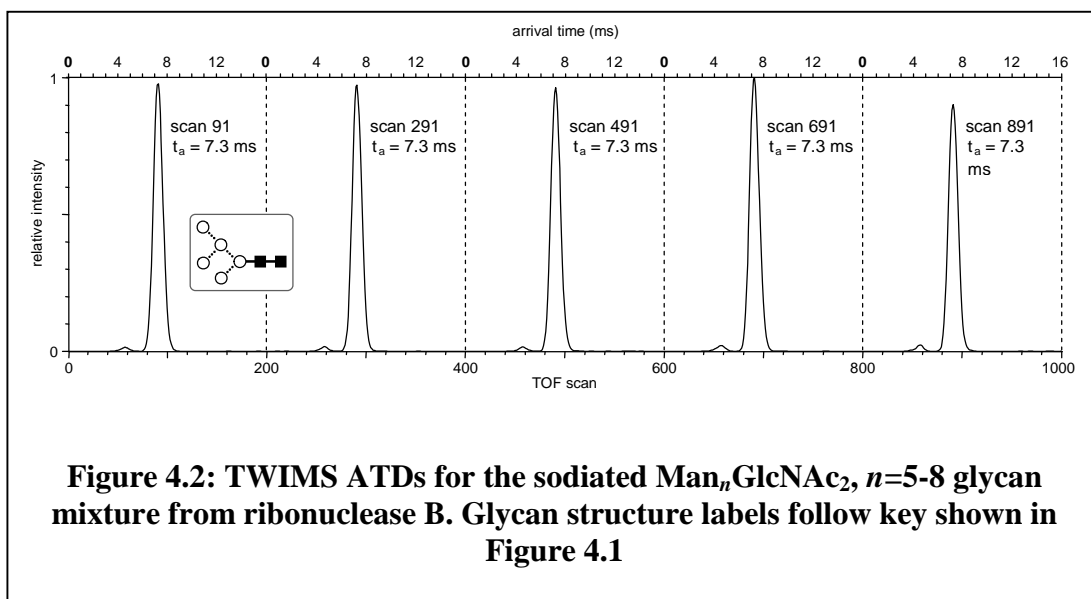
### Reproducibility of Ion Mobility Separations

The bovine ribonuclease B system will serve as a representative example of the type of results we are able to achieve with our techniques. This protein is known to have one glycosylation site that releases a mixture of oligosaccharides with the formulae  $\text{Man}_n\text{GlcNAc}_2$ ,  $n = 5-9$ . The glycan structures have been determined by NMR analysis (Fu *et al.*, 1994). The ESI mass spectrum of these oligosaccharides (Figure

4.1) is dominated by sodiated glycan species, which is consistent with previously published spectra (Harvey, 2000).

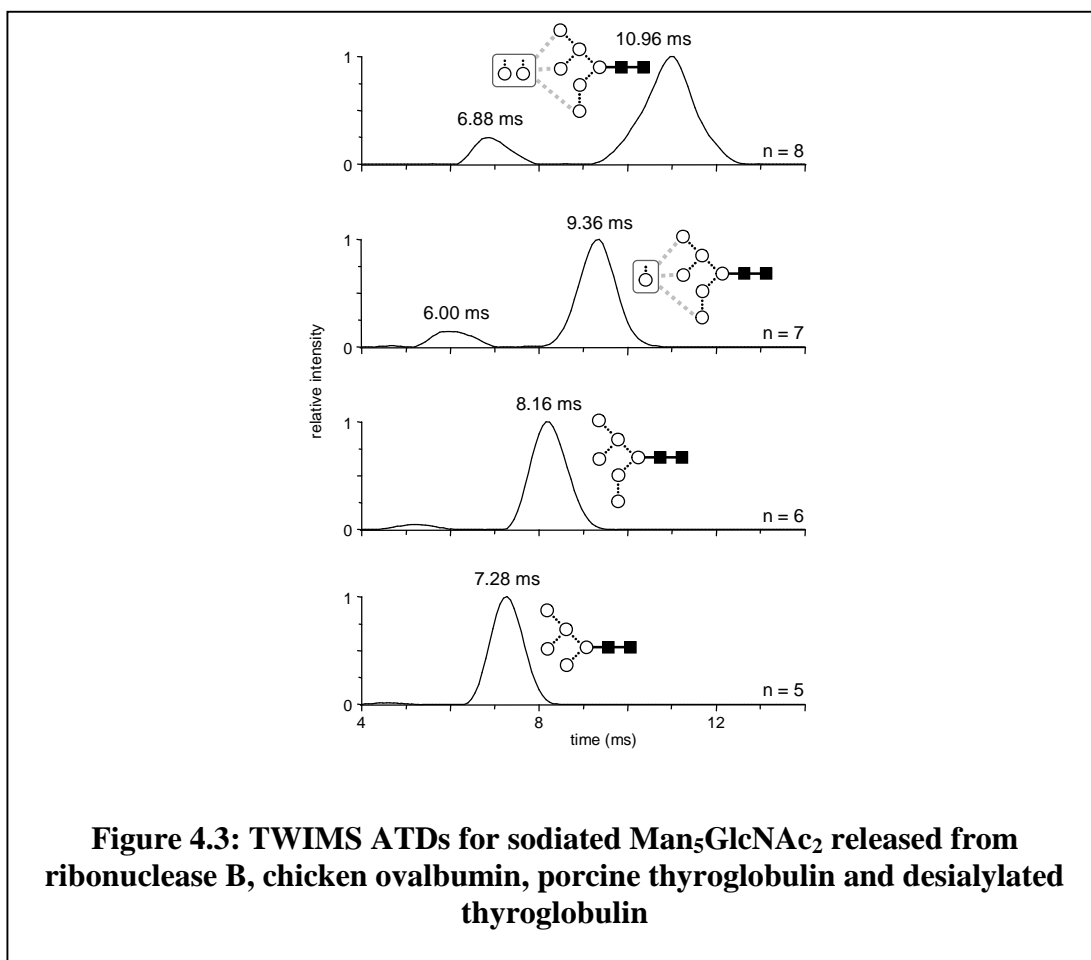


A typical set of ATDs for one of the sodiated glycans,  $\text{Man}_5\text{GlcNAc}_2$ , is shown in Figure 4.2. Each panel in the figure consists of 200 scans of 80  $\mu\text{s}$  duration, giving a total time for the experiment of 16 ms. In the first panel the ATD is centred on scan 91 giving an arrival time of 7.28 ms ( $91 \times 80 \mu\text{s}$ ). The other four panels, at intervals of 200 scans, also peak at the ninety-first scan in the panel, demonstrating the reproducibility of the method. Reproducibility of peak arrival time within one scan ( $\pm 80 \mu\text{s}$ ) is a typical result for the instrument. Subsequent ATDs shown in this paper will be presented with the x-axis converted from scan number to arrival time.



### Ion Mobility Separation of Glycans

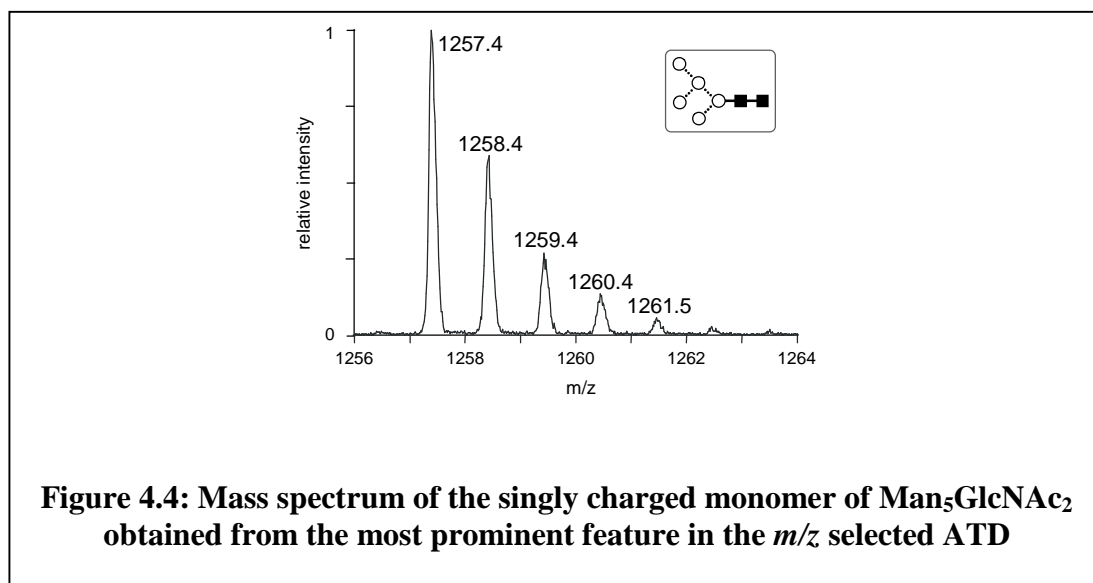
Figure 4.3 shows the ATDs measured for the four largest sodiated glycan peaks in the ribonuclease B mass spectrum ( $\text{Man}_n\text{GlcNAc}_2$ ,  $n = 5-8$ ). The distributions represent a typical glycan separation for this instrument which can be achieved in  $< 16$  ms. Each distribution is dominated by a single large peak that shifts to longer arrival times as  $n$  increases. This is an expected result, given that the increased size of an ion decreases its mobility as it passes through the mobility cell. For  $n = 5-7$ , the ATD peaks broaden slightly as  $n$  increases. Again, this is expected since the more time ions spend travelling through the mobility cell, the larger the spread in their cell transit times becomes. The ATD peak for  $n = 8$  is even broader than would be expected based on the trend for  $n = 5-7$ . This additional broadening could be due to the presence of  $\text{Man}_8\text{GlcNAc}_2$  isomers.



The NMR study by Fu *et al.* (Fu *et al.*, 1994) indicates that both  $\text{Man}_7\text{GlcNAc}_2$  and  $\text{Man}_8\text{GlcNAc}_2$  released from ribonuclease B have three linkage isomers (as depicted in Figure 4.1 and 4.3). It is not clear why the  $n = 7$  ATD peak is not broader like the  $n = 8$  peak, since  $\text{Man}_7\text{GlcNAc}_2$  also has three isomers. It may be that cross sections of the  $n = 8$  isomers happen to be different enough to give a broader ATD, while it is not the case for the  $n = 7$  isomers. The presence of conformers may also play a role, with differences in the  $n = 7$  and 8 species resulting in a wider range of conformer cross sections for the larger glycan.

### Charge state separation of multiply charged multimers

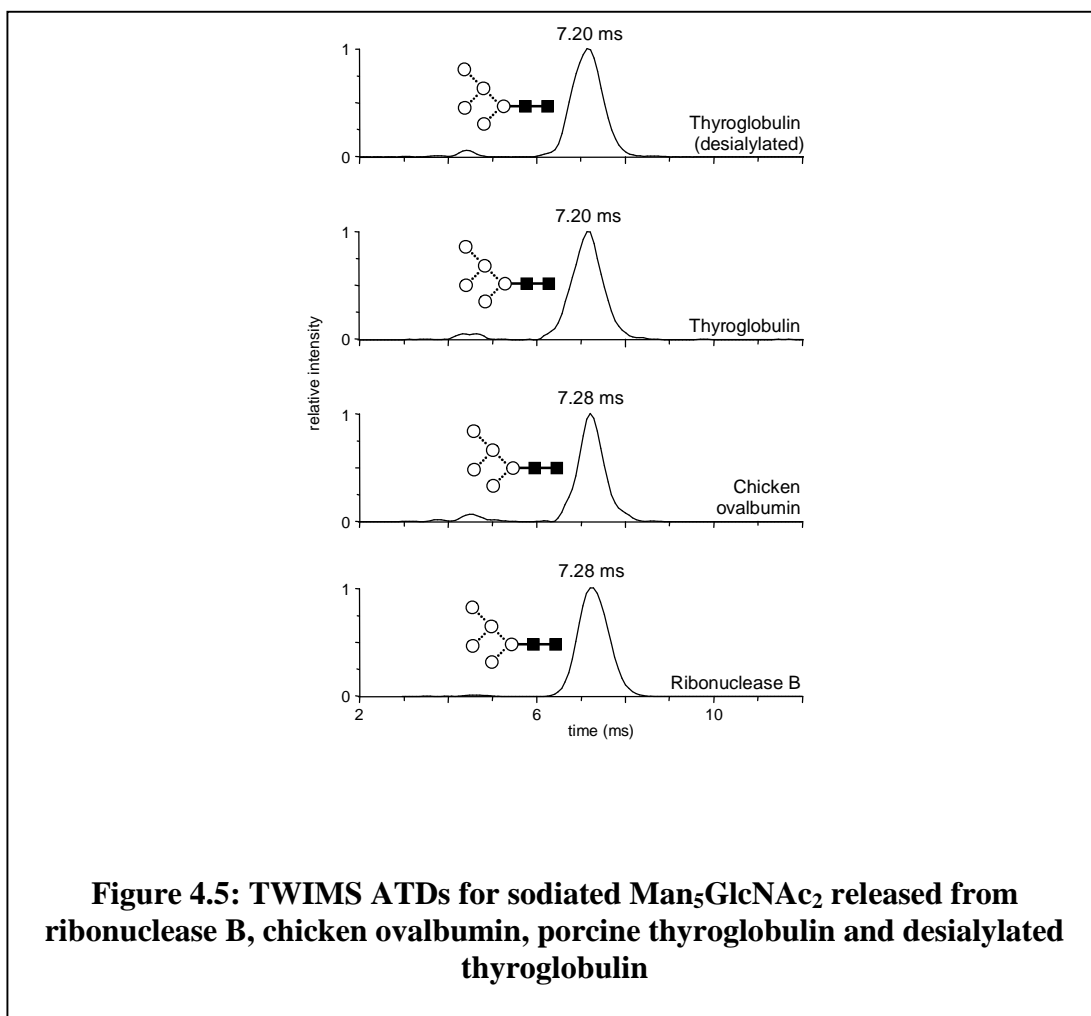
Each ATD in Figure 4.3 also has a small peak at shorter arrival times, for example, at 6.00 ms for  $n = 7$  and 6.88 ms for  $n = 8$ , which are due to glycan dimers of the form  $[2M + 2Na]^{2+}$ . This type of behaviour has been observed before for the Alzheimer's peptides  $A\beta_{40}$  and  $A\beta_{42}$ , where oligomers with the same  $m/z$  values as the monomer have shorter arrival times (Bernstein *et al.*, 2005; Baumketner *et al.*, 2006). Oligomer-size assignments can be verified by measuring high-resolution mass spectra for each peak in the ATD. For example, Figure 4.4 shows the mass spectrum obtained for the most prominent feature in the  $\text{Man}_5\text{GlcNAc}_2$  ATD shown in Figure 4.3. This ATD feature gives a  $^{13}\text{C}$ -isotope pattern with 1 Da spacings, unambiguously indicating a singly-charged species, the monomer. Similarly, doubly-charged dimers would give 0.5 Da spacings, triply-charged trimers, 0.33 Da spacings, etc. The ability to obtain MS and MS/MS spectra for each ATD observed in the experiment is an important aspect of this instrument that allows significantly more confident assignment of the source of features in ATDs.



## **Reproducibility of separation of common glycans from different sources**

To address whether the glycan source has an impact on the reproducibility of the separation, glycan  $\text{Man}_5\text{GlcNAc}_2$  released from four different sources: ribonuclease B, chicken ovalbumin, porcine thyroglobulin and desialylated thyroglobulin was studied with TWIM-MS. Figure 4.5 shows ATDs for  $m/z$  1257, the  $[\text{M} + \text{Na}]^+$  ion, obtained from each source. The arrival times were 7.20 to 7.28 ms and reproducible to within one scan ( $\pm 80 \mu\text{s}$ ) for all experiments. The 1 % difference between the top two scans and the bottom two scans is within experimental error. This demonstrates the independence of arrival time to other components within the complex glycan mixtures.





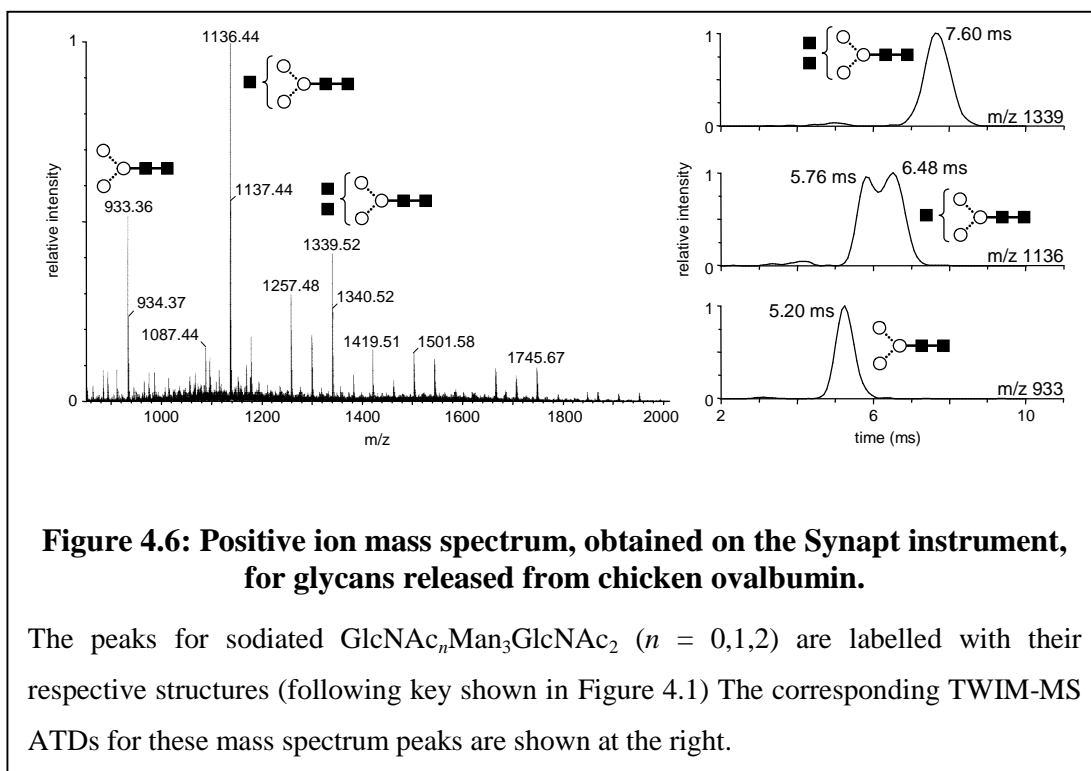
All of the ATDs presented in this paper, from complex released glycan mixtures to isolated glycan standards, were reproducible to within one scan ( $\pm 80 \mu\text{s}$ ) over multiple experiments. This excellent reproducibility, combined with MS and MS/MS data provides high confidence in the ability to identify structures from ATDs.

### Separation of Isomeric Glycan Structures

Figure 4.6 shows the positive ion ESI mass spectrum obtained for glycans released from chicken ovalbumin, which is dominated by sodiated glycan species,  $\text{GlcNAc}_n\text{Man}_3\text{GlcNAc}_2$ , ( $n = 0, 1, 2$ ), is similar to one obtained previously using matrix-assisted laser desorption ionization (MALDI) (Harvey *et al.*, 2000). The ion

mobility separation and mobility-resolved MS/MS capabilities of the Synapt instrument give it great potential as a tool in investigating the structures and conformations of these glycans. If linkage isomers with different mobilities exist for a particular glycan we should be able to detect them by measuring an ATD. Likewise, information on conformers could be obtained if their mobilities are sufficiently different. Further information can be provided by measuring mass spectra for particular ATD features.

A review of oligosaccharide conformation studies by Wormald and co-workers (Wormald *et al.*, 2002) indicates that different conformations can arise through rotation about Man-Man linkages. The three dominant glycan peaks seen in our ovalbumin mass spectrum each have one Man $\alpha$ 1-3Man link and one Man $\alpha$ 1-6Man link. The reviewed experimental and modelling studies indicate that the 1-3 link is flexible and that any different stable conformations present rapidly interconvert. The data available on the 1-6 link is less consistent. Analysis of existing crystal structures indicates that this link tends to take on three major and one minor conformation. NMR and modelling of a trisaccharide containing a Man $\alpha$ 1-6Man link indicate two stable conformations, while modelling of Man<sub>9</sub>GlcNAc<sub>2</sub> indicates the two Man $\alpha$ 1-6Man links present each prefer a different single conformation.

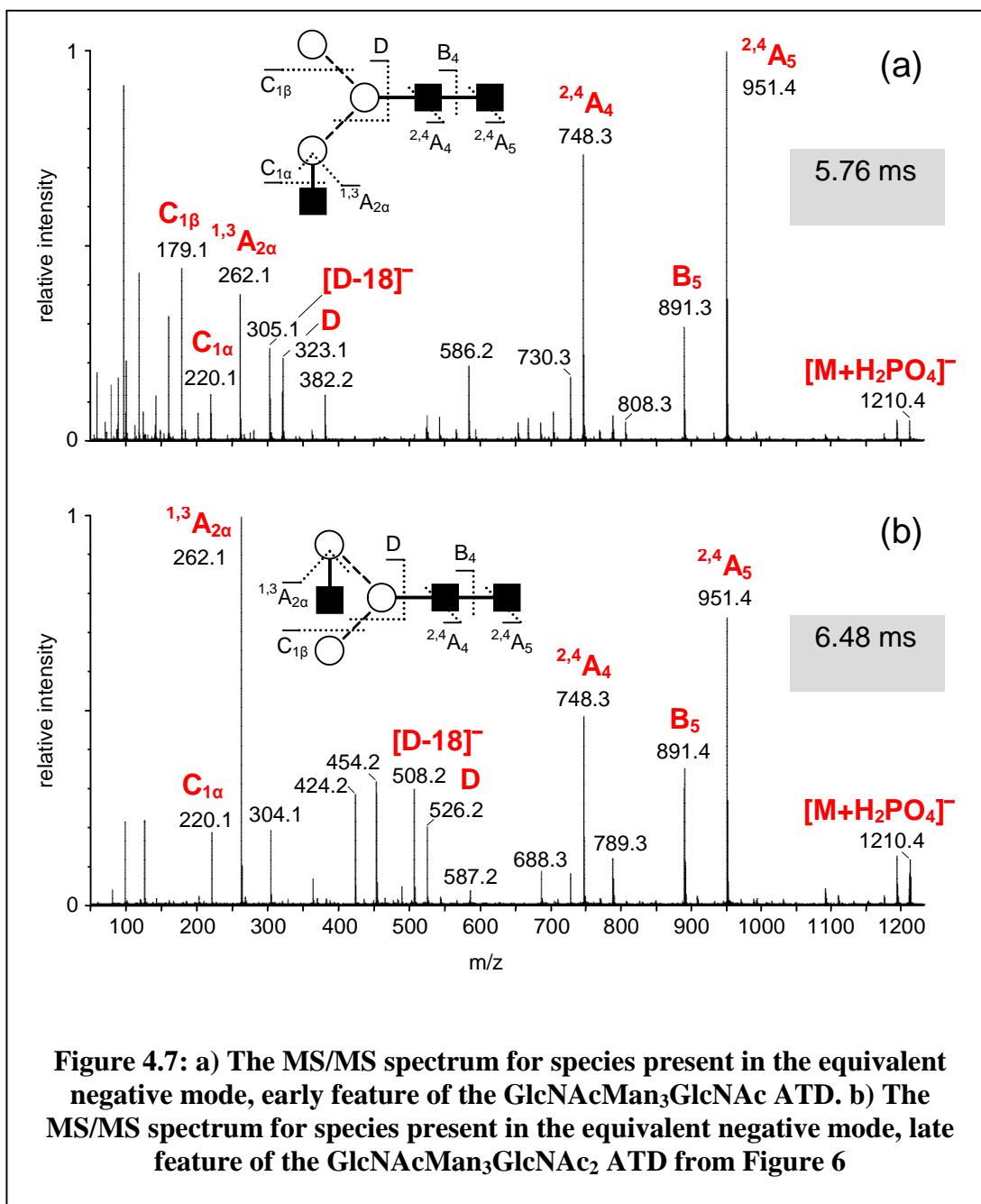


The core glycan  $\text{Man}_3\text{GlcNAc}_2$  should have only one linkage isomer as shown in Figure 4.6 (Egge *et al.*, 1983; Yamashita *et al.*, 1983). It is possible that this glycan has up to three significant conformers due to rotation around the  $\text{Man}\alpha 1\text{-6Man}$  link (since the  $\text{Man}\alpha 1\text{-3Man}$  link is not expected to take on distinct conformations). The differences in cross section of the potential conformers might not be significant since only one sugar group is being moved by rotation about the 1-6 link. The ATD measured for the  $m/z$  933 mass spectrum peak (Figure 4.6) supports this contention since it has only a single, narrow feature. This result agrees well with the results of a DCIMS study of glycans released from ovalbumin by Plasencia *et al.* (Plasencia *et al.*, 2008). They find a single peak in their drift time distribution for permethylated, doubly-sodiated  $\text{Man}_3\text{GlcNAc}_2$ .

For  $\text{GlcNAc}_1\text{Man}_3\text{GlcNAc}_2$ , there is the possibility of multiple linkage isomers depending on where the third GlcNAc group is added. Again there is potential for conformers due to rotation about the  $\text{Man}\alpha 1\text{-6Man}$  link. These conformers may have

significantly different cross sections if the third GlcNAc group binds to the 1-6 branching Man group, since the 1-6 rotation would be moving this capping GlcNAc group. The ATD for the  $m/z$  1136 peak is shown in Figure 4.6 and has two dominant features.

To help identify these two species, mobility-resolved MS/MS spectra (using the transfer region of the Synapt instrument) have been obtained for the two ATD features. Positive ion (sodium attachment) spectra for the two ATD features (data not shown) did exhibit some differences. In particular, differences in the relative intensities of peaks at  $m/z$  399.2 corresponding to a sodiated ManGlcNAc group and  $m/z$  933.4 corresponding to the loss of a single GlcNAc group would suggest different linkage isomers. The positive ion data alone was not enough to identify the species associated with the two ATD features. Mobility-resolved MS/MS spectra were also obtained for phosphate attachment and were more helpful. These negative ion spectra shown in Figure 4.7 are notated using the carbohydrate nomenclature introduced by Domon and Costello. (Domon and Costello, 1988) Fragment ions that contain a non-reducing terminus are labelled with uppercase letters from the beginning of the alphabet (A, B, C), and those that contain the reducing end of the oligosaccharide are labelled with letters from the end of the alphabet (X, Y, Z); subscripts indicate the cleaved ions. The A and X ions are produced by cleavage across the glycosidic ring, and are labelled by assigning each ring bond a number and counting clockwise. Ions produced from cleavage of successive residues are labelled:  $A_m$ ,  $B_m$  and  $C_m$ , with  $m = 1$  for the non-reducing end and  $X_n$ ,  $Y_n$ , and  $Z_n$ , with  $n = 1$  for the reducing-end residue.



The negative ion MS/MS data also indicate that the two features in the ATD represent two different linkage isomers of GlcNAc<sub>1</sub>Man<sub>3</sub>GlcNAc<sub>2</sub>. These results allow the structures to be unambiguously assigned. The mass spectrum obtained for the 5.76 ms feature in the ATD is shown in Figure 4.7a. It has peaks at  $m/z$  323 and 305, which can be assigned as the D and D-18 fragments, respectively, from the isomer with the capping GlcNAc group bound to the Man group of the 1-3

branch. The  $^{1-3}A_{2\alpha}$  fragment at  $m/z$  262 in the spectrum indicates that this capping GlcNAc group is bound by a  $\beta$ 1-2 linkage. (Harvey, 2005) The mass spectrum for the 6.48 ms ATD feature (Figure 4.7b) has peaks at  $m/z$  526 and 508. These D and D-18 fragment masses correspond to the isomer with the capping GlcNAc group bound to the man group of the 1-6 branch, again by a  $\beta$ 1-2 linkage as indicated by the  $^{1,3}A_{2\alpha}$  fragment at  $m/z$  262.

Since the two features in the  $\text{GlcNAc}_1\text{Man}_3\text{GlcNAc}_2$  ATD can be assigned to linkage isomers, there is no evidence for the presence of different conformers. Multiple conformers may exist in our experiment but if they are present they either interconvert rapidly on our experimental time scale or have very similar cross sections. A high-resolution DCIMS instrument may be able to distinguish conformers. Plasencia *et al.* (Plasencia *et al.*, 2008) found four features in the drift time distribution for permethylated, double sodiated  $\text{Man}_3\text{GlcNAc}_3$  with associated cross sections ranging from approximately 292 – 328  $\text{\AA}^2$ .

For  $\text{GlcNAc}_2\text{Man}_3\text{GlcNAc}_2$ , there is again the possibility of linkage isomers as well as conformers. As shown in Figure 4.6, the mass spectrum peak at  $m/z$  1339 gives an ATD single feature centred around 7.60 ms. While this ATD feature is broader than that obtained for  $\text{Man}_3\text{GlcNAc}_2$ , an increase in the spread of arrival times is expected due to the later average arrival time of  $\text{GlcNAc}_2\text{Man}_3\text{GlcNAc}_2$  and does not necessarily indicate the presence of multiple isomers or conformations. Plasencia *et al.* (Plasencia *et al.*, 2008) also found only one feature in their drift time distribution for the permethylated, doubly-sodiated version of this glycan. MALDI MS experiments (Harvey *et al.*, 2000) have suggested that there are two linkage isomers possible for this species with a GlcNAc residue bisecting the trimannose subunit and

another bound to either the Man $\alpha$ 1-3Man or Man $\alpha$ 1-6Man branch, while an NMR study (Da Silva *et al.*, 1995) finds only the first isomer. The MS/MS data acquired for this species (not shown) reveals no evidence for the bisecting GlcNAc residue (Harvey, 2005). One linkage isomer with a GlcNAc residue bound to the 1-3 branch and another to the 1-6 branch would be in better agreement with our observation of a single-peak ATD and the corresponding MS/MS results.

The set of experiments described in this section is an example of the high information content of the TMIM-MS/MS experiment. Mobility separation, mass spectra and product ion mass spectra can all be acquired in a single experiment.

### **Comparison of the TWIMS and DCIMS methods**

The measurement of absolute cross sections is currently impossible using the TWIMS approach due to the very complex path the ions take as they traverse the mobility cell. TWIMS results can however be successfully calibrated against cross sections of compounds measured in a DCIMS device. The resulting estimated cross sections have been shown to be in good agreement with those measured using the established drift cell approach (Ruotolo *et al.*, 2005; Scarff *et al.*, 2008; Williams and Scrivens, 2008). Here we compare values measured using DCIMS to those estimated using TWIMS for a series of oligosaccharides: BP-S and iso-BP-S; LNFP I and LNFP V; and finally LNDFH I and LNDFH II (Table 4.1).

All of these systems have been examined using the DCIMS instrument at UC Santa Barbara (Wytenbach *et al.*, 2001). In each instance a strong sodiated parent ion was present in the mass spectrum, and for each of these cases a single symmetric ATD was observed (data not shown). Experimental cross sections determined in each case are listed in Table 4.3. Molecular modelling calculations revealed a single family of

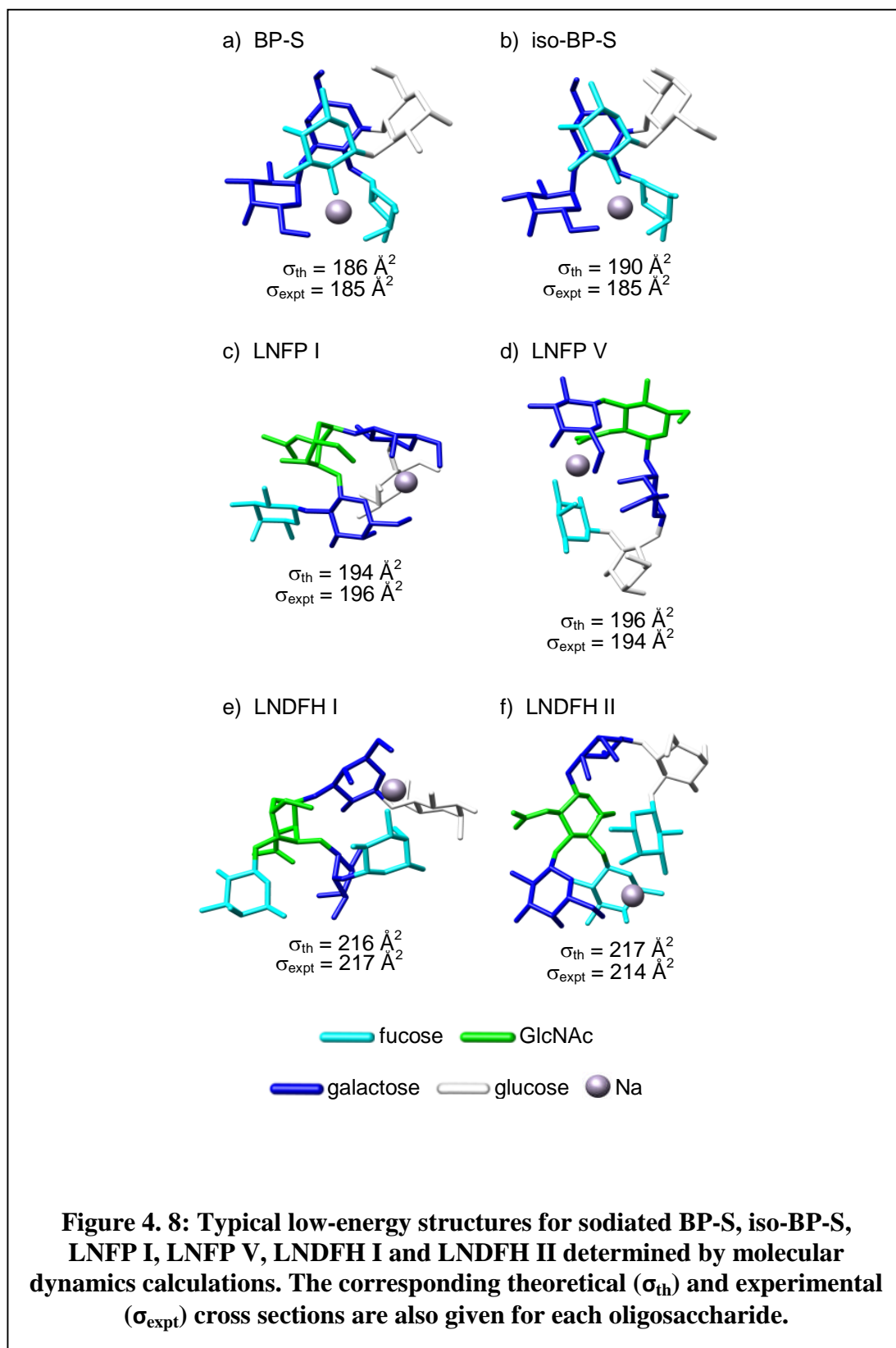
low-energy structures for each oligosaccharide. Representative structures, with the experimentally obtained cross sections, are shown in Figure 4.8 along with the corresponding average theoretical cross sections for each family of structures. The theoretical cross sections are also listed in Table 4.3. Several aspects of these results deserve comment. First, there is excellent agreement between experiment and theory in all cases. The  $\text{Na}^+$  ions were randomly placed on the molecules during simulated annealing runs and the same families of low-energy structures always emerged. Second, the BP-S and iso-BP-S structures observed are very similar, consistent with the identical experimental cross sections. The other two sets of sodiated isomers have quite different structures yet they also have nearly identical cross sections. This example provides a caution that the observation of very similar cross sections does not necessarily imply the presence of similar conformations.

Table 4.3. Experimental and Theoretical Results for Penta- and

Oligosaccharide	DCIMS	Theory	TWIMS	
	Cross	Cross	Arrival	Est. Cross
[BP-S + Na] <sup>+</sup>	185	186	3.20	185
[iso-BP-S + Na] <sup>+</sup>	185	190	3.20	185
[LNFP I + Na] <sup>+</sup>	196	194	3.65	196
[LNFP V + Na] <sup>+</sup>	194	196	3.51	193
[LNDFH I + Na] <sup>+</sup>	217	216	4.50	217
[LNDFH II + Na] <sup>+</sup>	214	217	4.28	211
[LNFP I + H] <sup>+</sup>	185, 201	–	3.15, 3.87	184, 201
[LNFP V + H] <sup>+</sup>	195	–	3.47	191

*a* Estimated from calibration



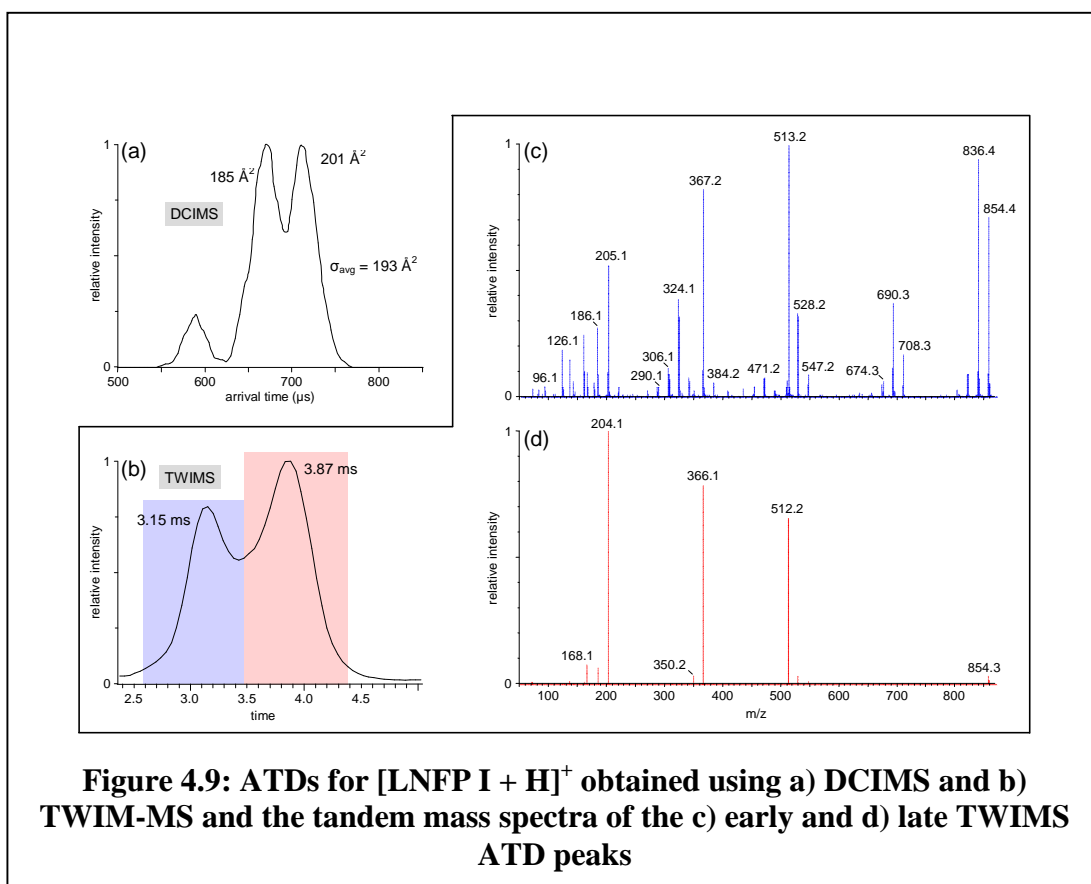


This same set of six oligosaccharides was examined using the TWIM-MS device and arrival time distributions obtained (data not shown). The corresponding average

arrival times are given in Table 4.3. Essentially identical arrival times were obtained for sodiated BP-S and iso-BP-S. Sodiated LNFP I and LNFP V also have very similar arrival times, and to a lesser extent, so do LNDFH I and II. It has been shown that the TWIM-MS device can be calibrated using cross sections measured with a DCIMS instrument. It is important that calibration is carried out under identical TWIMS experimental conditions and using DCIMS calibration values that bracket the mobilities of interest (Shvartsburg and Smith, 2008). The calibration method has been described in Chapter and elsewhere (Thalassinos *et al.*, 2009). It entails comparing corrected effective TWIMS drift times to DCIMS cross sections. The estimated TWIMS cross sections are given in Table 4.3 along with the absolute cross sections measured using DCIMS, the cross sections derived from the molecular modelling structures and the arrival times from TWIMS. The  $[\text{BP-S} + \text{Na}]^+$  ion was used as the reference for calibration. Good agreement is obtained between the absolute DCIMS values and the estimated values from the TWIM-MS device.

The LNFP I and LNFP V systems have significant protonated parent peaks, in addition to the sodiated peaks seen for the other species. It should be noted the protonated peak in the mass spectrum of the DCIMS instrument was quite weak while the same peak was quite strong on the TWIM-MS instrument. The differences in spray methods and sampling, together with intrinsic sensitivity differences could account for this observation. While the ATDs for all the sodiated oligosaccharides and protonated LNFP V have just a single peak, the protonated LNFP I ATD has an additional feature as shown by both the DCIMS and TWIMS approaches (a and b). The corresponding DCIMS cross sections for protonated LNFP I and V are given in Table 4.3 along with the TWIMS arrival times and estimated cross sections, which agree well with the DCIMS values. The additional ATD feature for protonated

LNFP I was initially thought to represent another conformer. Using the capability of the Synapt to obtain MS/MS data on mobility separated compounds, MS/MS spectra were obtained in the transfer region for both ATD features. The results are given in Figure 9 c and d, which show product ion spectra of  $m/z$  854 for both species. The mass spectrum for the later ATD feature (Figure 4.9d) is consistent with the simple fragmentation pattern expected for oligosaccharides in positive ion mode and is similar to a positive-ion ESI mass spectrum obtained by Levin *et al.* (Levin *et al.*, 2007). The mass spectrum for the earlier ATD feature (C) has a much more complicated fragmentation pattern and is unlikely to be a result of a second conformation of LNFP I but rather an isomer or some other impurity. Unlike our bimodal ATD, the LNFP I differential mobility spectrum measured by Levin and co-workers has only one peak.



## Conclusions

The ion mobility separation characteristics of the TWIMS device have been shown to be similar to the DCIMS device, although the theoretical relationship between measured arrival times and mobility has not yet established for the travelling wave technique. Previous work has indicated that mobility calibration of the TWIMS is possible using species of known collision cross section (Ruotolo *et al.*, 2005; Scarff *et al.*, 2008; Williams and Scrivens, 2008). This method has been successfully applied during this study. While the resolving power of the TWIMS is not as high as some DCIMS systems the separation capability is valuable for reducing mass spectral complexity, as shown for the complex released glycans. A particular advantage of the Synapt instrument over most DCIMS configurations is that the radial ion confinement in the mobility cell increases the overall instrument sensitivity, allowing investigations on analytically significant (fmol) levels of sample. This work illustrates that the TWIMS device provides rapid, sensitive and information-rich experimental data for the analysis of complex mixtures of glycans. The arrival times obtained are reproducible and independent of the source of the glycan. Some isomeric glycans can be separated and characterized using MS/MS experiments in favourable circumstances. The TWIMS device shows significant promise for screening complex glycan samples and for many other analytical applications in the characterization of biological systems.

## References

(2002). *Hyperchem 7.0* Hypercube, Inc. Gainesville, FL

**Baker, E. S., Bernstein, S. L. and Bowers, M. T.** (2005). "Structural characterization of G-quadruplexes in deoxyguanosine clusters using ion mobility mass spectrometry." *Journal of the American Society for Mass Spectrometry* **16**(7): 989-997.

**Baker, E. S., Bernstein, S. L., Gabelica, V., De Pauw, E. and Bowers, M. T.** (2006). "G-quadruplexes in telomeric repeats are conserved in a solvent-free environment." *International Journal of Mass Spectrometry* **253**(3): 225-237.

**Baumketner, A., Bernstein, S. L., Wyttenbach, T., Bitan, G., Teplow, D. B., Bowers, M. T. and Shea, J.-E.** (2006). "Amyloid  $\beta$ -protein monomer structure: A computational and experimental study." *Protein Science* **15**(3): 420-428.

**Bernstein, S. L., Wyttenbach, T., Baumketner, A., Shea, J.-E., Bitan, G., Teplow, D. B. and Bowers, M. T.** (2005). "Amyloid  $\beta$ -protein: Monomer structure and early aggregation states of A $\beta$ 42 and its Pro<sup>19</sup> alloform." *Journal of the American Chemical Society* **127**(7): 2075-2084.

**Case, D. A., Darden, T. A., III, T. E. C., Simmerling, C. L., Wang, J., Duke, R. E., Luo, R., Merz, K. M., Wang, B., Pearlman, D. A., Crowley, M., Brozell, S., Tsui, V., Gohlke, H., Mongan, J., Hornak, V., Cui, G., Beroza, P., Schafmeister,**

**C., Caldwell, J. W., Ross, W. S. and Kollman, P. A.** (2004). *AMBER 8* University of California San Francisco

**Clowers, B. H., Dwivedi, P., Steiner, W. E., Hill, H. H. and Bendiak, B.** (2005). "Separation of sodiated isobaric disaccharides and trisaccharides using electrospray ionization-atmospheric pressure ion mobility-time of flight mass spectrometry." *Journal of the American Society for Mass Spectrometry* **16**(5): 660-669.

**Da Silva, M. L. C., Stubbs, H. J., Tamura, T. and Rice, K. G.** (1995). "(1)Hr Characterization of a Hen Ovalbumin Tyrosinamide N-Linked Oligosaccharide Library." *Archives of Biochemistry and Biophysics* **318**(2): 465-475.

**de Waard, P., Koorevaar, A., Kamerling, J. P. and Vliegthart, J. F. G.** (1991). "Structure Determination by H-1-Nmr Spectroscopy of (Sulfated) Sialylated N-Linked Carbohydrate Chains Released from Porcine Thyroglobulin by Peptide-N4-(N-Acetyl-Beta-Glucosaminyl)Asparagine Amidase-F." *Journal of Biological Chemistry* **266**(7): 4237-4243.

**Domon, B. and Costello, C. E.** (1988). "A Systematic Nomenclature for Carbohydrate Fragmentations in FAB-MS/MS Spectra of Glycoconjugates." *Glycoconjugate* **5**: 397-409.

**Dwek, R. A.** (1996). "Glycobiology: Toward understanding the function of sugars." *Chemical Reviews* **96**(2): 683-720.

**Dwivedi, P., Bendiak, B., Clowers, B. H. and Hill, H. H.** (2007). "Rapid resolution of carbohydrate isomers by electrospray ionization ambient pressure ion mobility spectrometry-time-of-flight mass spectrometry (ESI-APIMS-TOFMS)." *Journal of the American Society for Mass Spectrometry* **18**(7): 1163-1175.

**Egge, H., Peter-Katalinic, J., Paz-Parente, J., Strecker, G., Montreuil, J. and Fournet, B.** (1983). "Carbohydrate structures of hen ovomucoid: A mass spectrometric analysis." *FEBS Letters* **156**(2): 357-362.

**Frisch, M. J., Trucks, G. W., Schlegel, H. B., Scuseria, G. E., Robb, M. A., Cheeseman, J. R., Montgomery, J., J. A., Vreven, T., Kudin, K. N., Burant, J. C., Millam, J. M., Iyengar, S. S., Tomasi, J., Barone, V., Mennucci, B., Cossi, M., Scalmani, G., Rega, N., Petersson, G. A., Nakatsuji, H., Hada, M., Ehara, M., Toyota, K., Fukuda, R., Hasegawa, J., Ishida, M., Nakajima, T., Honda, Y., Kitao, O., Nakai, H., Klene, M., Li, X., Knox, J. E., Hratchian, H. P., Cross, J. B., Bakken, V., Adamo, C., Jaramillo, J., Gomperts, R., Stratmann, R. E., Yazyev, O., Austin, A. J., Cammi, R., Pomelli, C., Ochterski, J. W., Ayala, P. Y., Morokuma, K., Voth, G. A., Salvador, P., Dannenberg, J. J., Zakrzewski, V. G., Dapprich, S., Daniels, A. D., Strain, M. C., Farkas, O., Malick, D. K., Rabuck, A. D., Raghavachari, K., Foresman, J. B., Ortiz, J. V., Cui, Q., Baboul, A. G., Clifford, S., Cioslowski, J., Stefanov, B. B., Liu, G., Liashenko, A., Piskorz, P., Komaromi, I., Martin, R. L., Fox, D. J., Keith, T., Al-Laham, M. A., Peng, C. Y., Nanayakkara, A., Challacombe, M., Gill, P. M. W., Johnson, B., Chen, W., Wong, M. W., Gonzalez, C. and Pople, J. A.** (2004). *Gaussian 03, Revision C.02*  
Gaussian, Inc. Wallingford CT

**Fu, D. T., Chen, L. and O'Neill, R. A.** (1994). "A Detailed Structural Characterization of Ribonuclease-B Oligosaccharides by H-1-Nmr Spectroscopy and Mass-Spectrometry." *Carbohydrate Research* **261**(2): 173-186.

**Gabelica, V., Shammel Baker, E., Teulade-Fichou, M.-P., De Pauw, E. and Bowers, M. T.** (2007). "Stabilization and Structure of Telomeric and c-myc Region

Intramolecular G-Quadruplexes: The Role of Central Cations and Small Planar Ligands." *Journal of the American Chemical Society* **129**(4): 895-904.

**Gidden, J., Baker, E. S., Ferzoco, A. and Bowers, M. T.** (2005). "Structural motifs of DNA complexes in the gas phase." *International Journal of Mass Spectrometry* **240**(3): 183-193.

**Gidden, J., Ferzoco, A., Baker, E. S. and Bowers, M. T.** (2004). "Duplex formation and the onset of helicity in poly d(CG)<sub>n</sub> oligonucleotides in a solvent-free environment." *Journal of the American Chemical Society* **126**(46): 15132-15140.

**Giles, K., Pringle, S. D., Worthington, K. R., Little, D., Wildgoose, J. L. and Bateman, R. H.** (2004). "Applications of a travelling wave-based radio-frequency-only stacked ring ion guide." *Rapid Communications in Mass Spectrometry* **18**: 2401-2414.

**Green, E. D., Adelt, G., Baenziger, J. U., Wilson, S. and Vanhalbeek, H.** (1988). "The Asparagine-Linked Oligosaccharides on Bovine Fetuin - Structural-Analysis of N-Glycanase-Released Oligosaccharides by 500-Megahertz H-1-Nmr Spectroscopy." *Journal of Biological Chemistry* **263**(34): 18253-18268.

**Guile, G. R., Rudd, P. M., Wing, D. R., Prime, S. B. and Dwek, R. A.** (1996). "A rapid high-resolution high-performance liquid chromatographic method for separating glycan mixtures and analyzing oligosaccharide profiles." *Analytical Biochemistry* **240**(2): 210-226.

**Harvey, D. J.** (2000). "Collision-induced fragmentation of underivatized N-linked carbohydrates ionized by electrospray." *Journal of Mass Spectrometry* **35**(10): 1178-1190.



**Harvey, D. J.** (2001). "Identification of protein-bound carbohydrates by mass spectrometry." *Proteomics* **1**(2): 311-328.

**Harvey, D. J.** (2005). "Fragmentation of Negative Ions from Carbohydrates: Part 2. Fragmentation of High-Mannose N-Linked Glycans." *Journal of the American Society for Mass Spectrometry* **16**(5): 631-646.

**Harvey, D. J.** (2005). "Fragmentation of Negative Ions from Carbohydrates: Part 3. Fragmentation of Hybrid and Complex N-Linked Glycans." *Journal of the American Society for Mass Spectrometry* **16**(5): 647-659.

**Harvey, D. J., Wing, D. R., Kuster, B. and Wilson, I. B. H.** (2000). "Composition of N-linked carbohydrates from ovalbumin and Co-purified glycoproteins." *Journal of the American Society for Mass Spectrometry* **11**(6): 564-571.

**Heck, A. J. R. and van den Heuvel, R. H. H.** (2004). "Investigation of intact protein complexes by mass spectrometry." *Mass Spectrometry Reviews* **23**(5): 368-389.

**Jin, L., Barran, P. E., Deakin, J. A., Lyon, M. and Uhrin, D.** (2005). "Conformation of glycosaminoglycans by ion mobility mass spectrometry and molecular modelling." *Physical Chemistry Chemical Physics* **7**(19): 3464-3471.

**Last, A. M. and Robinson, C. V.** (1999). "Protein folding and interactions revealed by mass spectrometry." *Current Opinion in Chemical Biology* **3**(5): 564-570.

**Lee, D. S., Wu, C. and Hill, H. H.** (1998). "Detection of carbohydrates by electrospray ionization ion mobility spectrometry following microbore high-performance liquid chromatography." *Journal of Chromatography A* **822**(1): 1-9.

**Lee, S., Wyttenbach, T. and Bowers, M. T.** (1997). "Gas phase structures of sodiated oligosaccharides by ion mobility/ion chromatography methods." *International Journal of Mass Spectrometry and Ion Processes* **167**: 605-614.

**Levin, D. S., Miller, R. A., Nazarov, E. G. and Vouros, P.** (2007). "Using a Nano-electrospray-Differential Mobility Spectrometer-Mass Spectrometer System for the Analysis of Oligosaccharides

with Solvent Selected Control Over ESI Aggregate Ion Formation." *J Am Soc Mass Spectrom* **18**(3): 502-511.

**Liu, Y. S. and Clemmer, D. E.** (1997). "Characterizing oligosaccharides using injected-ion mobility mass spectrometry." *Analytical Chemistry* **69**(13): 2504-2509.

**Ma, J. K.-C., Drake, P. M. W. and Christou, P.** (2003). "Genetic modification: The production of recombinant pharmaceutical proteins in plants." *Nature Reviews Genetics* **4**: 794-805

**Mason, E. A. and McDaniel, E. W.** (1988). *Transport properties of ions in gases*. New York, Wiley.

**Mesleh, M. F., Hunter, J. M., Shvartsburg, A. A., Schatz, G. C. and Jarrold, M. F.** (1996). "Structural information from ion mobility measurements: Effects of the long-range potential." *Journal of Physical Chemistry* **100**(40): 16082-16086.

**Patel, T., Bruce, J., Merry, A., Bigge, C., Wormald, M., Jaques, A. and Parekh, R.** (1993). "Use of Hydrazine to Release in Intact and Unreduced Form Both N-Linked and O-Linked Oligosaccharides from Glycoproteins." *Biochemistry* **32**(2): 679-693.

**Pettersen, E. F., Goddard, T. D., Huang, C. C., Couch, G. S., Greenblatt, D. M., Meng, E. C. and Ferrin, T. E.** (2004). "UCSF chimera - A visualization system for exploratory research and analysis." *Journal of Computational Chemistry* **25**(13): 1605-1612.

**Plasencia, M. D., Isailovic, D., Merenbloom, S. I., Mechref, Y. and Clemmer, D. E.** (2008). "Resolving and Assigning N-Linked Glycan Structural Isomers from Ovalbumin by IMS-MS." *Journal of the American Society for Mass Spectrometry* **19**(11): 1706-1715.

**Pringle, S. D., Giles, K., Wildgoose, J. L., Williams, J. P., Slade, S. E., Thalassinos, K., Bateman, R. H., Bowers, M. T. and Scrivens, J. H.** (2007). "An investigation of the mobility separation of some peptide and protein ions using a new hybrid quadrupole/travelling wave IMS/oa-ToF instrument." *International Journal of Mass Spectrometry* **261**(1): 1-12.

**Ruotolo, B. T., Giles, K., Campuzano, I., Sandercock, A. M., Bateman, R. H. and Robinson, C. V.** (2005). "Evidence for macromolecular protein rings in the absence of bulk water." *Science* **310**(5754): 1658-1661.

**Scarff, C. A., Thalassinos, K., Hilton, G. R. and Scrivens, J. H.** (2008). "Travelling wave ion mobility mass spectrometry studies of protein structure: biological significance and comparison with X-ray crystallography and nuclear magnetic resonance spectroscopy measurements." *Rapid Communications in Mass Spectrometry* **22**: 3297-3304.

**Shvartsburg, A. A. and Smith, R. D.** (2008). "Fundamentals of Traveling Wave Ion Mobility Spectrometry." *Analytical Chemistry* **80**(24): 9689-9699.

**Thalassinos, K., Grabenauer, M., Slade, S. E., Hilton, G. R., Bowers, M. T. and Scrivens, J. H.** (2009). "Characterization of Phosphorylated Peptides Using Traveling Wave-Based and Drift Cell Ion Mobility Mass Spectrometry." *Analytical Chemistry* **81**(1): 248-254.

**Williams, J. P. and Scrivens, J. H.** (2008). "Coupling desorption electrospray ionisation and neutral desorption/extractive electrospray ionisation with a travelling-wave based ion mobility mass spectrometer for the analysis of drugs." *Rapid Communications in Mass Spectrometry* **22**(2): 187-196.

**Wormald, M. R., Petrescu, A. J., Pao, Y. L., Glithero, A., Elliott, T. and Dwek, R. A.** (2002). "Conformational studies of oligosaccharides and glycopeptides: Complementarity of NMR, X-ray crystallography, and molecular modelling." *Chemical Reviews* **102**(2): 371-386.

**Wytttenbach, T., Kemper, P. R. and Bowers, M. T.** (2001). "Design of a new electrospray ion mobility mass spectrometer." *International Journal of Mass Spectrometry* **212**(1-3): 13-23.

**Yamashita, K., Kamerling, J. P. and Kobata, A.** (1983). "Structural studies of the sugar chains of hen ovomucoid. Evidence indicating that they are formed mainly by the alternate biosynthetic pathway of asparagine-linked sugar chains." *J. Biol. Chem.* **258**(5): 3099-3106.

**Yoshima, H., Matsumoto, A., Mizuochi, T., Kawasaki, T. and Kobata, A.** (1981). "Comparative-Study of the Carbohydrate Moieties of Rat and Human-Plasma Alpha-1-Acid Glycoproteins." *Journal of Biological Chemistry* **256**(16): 8476-8484.

# **Chapter 5:**

# **Conclusions**

## **Summary of Project and Future Directions**

The work undertaken in this thesis described a number of examples of the use of recently developed mass spectrometry experimental approaches to characterise biologically important mixtures. Ambient ionisation techniques and ion-mobility mass spectrometry have been demonstrated to improve the rate of analysis of a range of sample types including pharmaceuticals and complex mixtures of carbohydrates while maintaining the high sensitivity, selectivity and information content provided by traditional mass spectrometry-based approaches.

### **Ambient Ionisation**

The field of ambient ionisation has continued to grow since DESI was first reported in 2004. A number of research groups are continuing work on existing ionisation sources, and their potential applications.

Recently introduced ambient ionisation mass spectrometry approaches have been utilised in the rapid, sensitive, information rich characterisation of pharmaceutical formulations. Little, or no, sample treatment was required and the experiments were shown to provide detailed information on active ingredients in the presence of a number of other components. A range of pharmaceutical formulations were analysed containing active ingredients in the molecular weight range of 150 – 750 Da. A number of ambient ionisation approaches including DART, DESI and DAPCI were compared and advantages and disadvantages of each approach outlined and discussed.

The potential future use of these ambient ionisation approaches is wide ranging. Ambient ionisation sources are being produced as commercial products by some instrument manufacturers, including the DART source (JEOL, Peabody, MA, USA)

and a commercial DESI source (Prosilia Inc., Indianapolis, IN, USA). Some applications for which they may be amenable for routine use are the detection of explosives and drugs (with significant potential when coupled with lightweight portable mass spectrometers), and imaging of tissues and surfaces for spatially resolved mass spectral information.

### **Ion Mobility-Mass Spectrometry of Carbohydrates**

The exciting technology of travelling wave-based ion mobility has recently been commercially interfaced with mass spectrometry. This has been utilised in a series of fundamental experiments that probe the interaction of varied cations with isomeric oligomers of carbohydrates. The approach enables conformational changes to be rapidly measured over a wide (500-6000 Da) mass range. Changes in conformations were observed for multiply cationised species which agree with previously measured solution phase measurements. Potential future work in this area includes the investigation of additional polymers, alternative cations, the behaviour of carbohydrate polymers in negative ionisation mode, and extended mass range experiments to further characterise carbohydrate behaviour in TWIM-MS.

The TWIM-MS approach has also been used successfully to characterise a number of N-linked glycans released from glycoproteins. The experiments enable some isomeric structures to be differentiated. Estimated cross sectional measurements have been calculated and found to be in good agreement with those obtained from conventional drift cell approaches. The TWIM-MS and –MS/MS based analysis of glycans may provide the opportunity to develop methods for the rapid, high information content, batch-to batch characterisation of glycosylated

biopharmaceutical products, and detection of a range of diseases and disorders that present diagnostic markers in the form of changes in glycosylation profile.



# Appendix

# The use of recently described ionisation techniques for the rapid analysis of some common drugs and samples of biological origin

Jonathan P. Williams\*, Vibhuti J. Patel, Richard Holland and James H. Scrivens

Department of Biological Sciences, University of Warwick, Gibbet Hill Rd, Coventry CV4 7AL, UK

Received 5 February 2006; Revised 8 March 2006; Accepted 13 March 2006

**Three ionisation techniques that require no sample preparation or extraction prior to mass analysis have been used for the rapid analysis of pharmaceutical tablets and ointments. These methods were (i) the novel direct analysis in real time (DART), (ii) desorption electrospray ionisation (DESI), and (iii) desorption atmospheric pressure chemical ionisation (DAPCI). The performance of the three techniques was investigated for a number of common drugs. Significant differences between these approaches were observed. For compounds of moderate to low polarity DAPCI produced more effective ionisation. Accurate DESI and DAPCI tandem mass spectra were obtained and these greatly enhance the selectivity and information content of the experiment. The detection from human skin of the active ingredients from ointments is reported together with the detection of ibuprofen metabolites in human urine. Copyright © 2006 John Wiley & Sons, Ltd.**

Desorption electrospray ionisation (DESI) is a newly developed ionisation technique for the analysis and detection of samples present on a variety of surfaces.<sup>1</sup> Rapid high-throughput analysis can be undertaken for a variety of sample types. The technique can be used to detect analytes on surface areas of sub-mm<sup>2</sup> dimensions. Applications utilising the DESI technique include the detection of rhodamine dyes and pharmaceutical samples separated on thin-layer chromatography (TLC) plates,<sup>2</sup> the rapid detection of pharmaceutical samples using ion mobility/time-of-flight mass spectrometry (ToFMS),<sup>3</sup> high-throughput analysis of pharmaceutical samples,<sup>4</sup> the detection of explosives,<sup>5,6</sup> the rapid accurate mass tandem mass spectrometry (MS/MS) of pharmaceutical samples,<sup>7</sup> intact biological tissue imaging,<sup>8</sup> direct analysis of alkaloids from plant tissue,<sup>9</sup> and the analysis of controlled substances.<sup>10,11</sup> Several possible mechanisms of ionisation have been postulated, including chemical sputtering involving gas-phase ions generated by electrospray ionisation (ESI) or corona discharge and subsequent charge transfer between these primary ions and sample molecules on the surface. The occurrence of gas-phase ion-molecule reactions has also been suggested together with a droplet splashing or pick-up mechanism. This involves the impacting of multiply charged solvent droplets dissolving sample molecules from the surface leading to the formation of secondary charged droplets carrying sample molecules and resulting in ion formation mechanisms similar to that of ESI.<sup>1,4–6</sup>

Desorption atmospheric pressure chemical ionisation (DAPCI) was first reported for the trace level detection of

TNT, PETN and RDX explosives,<sup>5</sup> and has not received as much attention to date as DESI. Ionisation of the explosives was provided by the initial formation of toluene or methanol reagent ions produced by a corona discharge. These reagent ions formed are thought to ionise the analyte molecules by either electron or proton transfer in a chemical ionisation step.<sup>5</sup> For those compounds that do not provide sufficient ion intensity by DESI, DAPCI offers an alternative option. DAPCI has been shown to provide increased sensitivity for compounds of moderate polarity.<sup>7</sup> DAPCI generated higher signal intensities for the active ingredient hydrocortisone, a weakly polar corticosteroid, than DESI using the same solvent system normally used for conventional ESI experiments.<sup>7</sup> The DAPCI technique previously reported<sup>7</sup> used nitrogen sheath gas and a mixture of methanol/water (1:1) from which ions were produced by a corona discharge. Reagent ions formed in the corona discharge region react with desorbed analyte molecules forming, depending on the ionisation mode, for the most part, protonated or deprotonated molecules.<sup>7</sup> A variant to the DAPCI technique for the rapid analysis of volatile and semi-volatile compounds, referred to as atmospheric pressure solids analysis probe (ASAP), was recently used in the analysis of a number of steroids and biological tissues.<sup>12</sup> Vapourisation of the sample is accomplished by placing it within the hot flowing nitrogen gas at atmospheric pressure.

Another rapid and newly developed ionisation method, direct analysis in real time (DART), was recently reported.<sup>13</sup> Pharmaceutical samples, explosives and metabolites in urine were analysed on a single ToF instrument. Sample analysis

\*Correspondence to: J. P. Williams, Department of Biological Sciences, University of Warwick, Gibbet Hill Road, Coventry CV4 7AL, UK.  
E-mail: j.p.williams@warwick.ac.uk

by the DART technique is carried out at ambient temperature and ionisation is brought about by exposing the sample to a stream of excited gas, typically helium. An electrical discharge produces ions, electrons and excited state metastable neutral species. Several ionisation mechanisms have been postulated, including Penning ionisation, in which ionisation of the sample occurs by energy transfer from an excited atom or molecule of energy greater than the ionisation energy of the sample.<sup>13</sup> It was reported that when helium is used as the gas, the mechanism involves the formation of ionised water clusters followed by proton transfer reactions.<sup>13</sup>

In this present study we have made use of these three newly developed ionisation techniques. The main focus of this study was to evaluate the potential of the ionisation techniques for the rapid analysis of active ingredients formulated into a variety of pharmaceutical tablets, gels and ointments. The rapid analysis of pharmaceutical drug formulations, the detection from human skin of the active ingredients from ointments or gels, and the detection of ibuprofen metabolites in human urine have been carried out. The increased selectivity and specificity of the DESI and DAPCI techniques used with a hybrid quadrupole ToF instrument were compared with that obtained by the use of DART with a single ToF instrument. Accurate mass MS and accurate mass MS/MS measurements, to within 2 mTh, has allowed elemental compositions for the product ions to be determined, thereby facilitating the identification of fragmentation pathways. We believe this to be the first report exploiting all three newly developed ionisation techniques combined with accurate mass DAPCI-MS/MS.

## EXPERIMENTAL

The tablets and ointment formulations investigated are listed in Table 1, together with the molecular formulae and molecular weights of the active ingredients. Ibuprofen tablets and gel (Tesco, UK), Anadin Extra (Wyeth, UK) and Solpadeine Max (Tesco, UK) were purchased without prescription from a pharmacy. Proctosedyl ointment (Aventis)

and metoclopramide (APS) were obtained by prescription. Solvents were obtained from Sigma-Aldrich (Poole, UK).

## Mass spectrometry

DART experiments were carried out on an AccuToF LC ToF mass spectrometer (Jeol, Peabody, MA, USA) and DESI/DAPCI experiments were carried out on a Q-ToF I (Waters, Manchester, UK). Experimental conditions for each are given below.

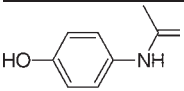
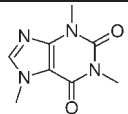
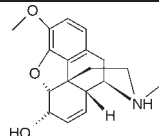
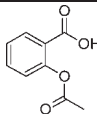
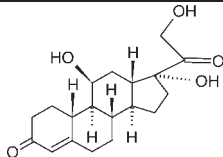
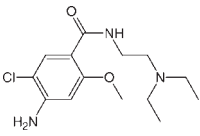
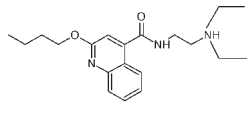
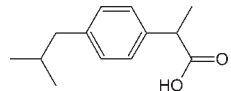
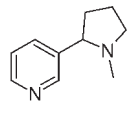
### DART

A detailed description of the DART source can be found elsewhere.<sup>13</sup> The AccuToF instrument was operated with helium flowing into the DART source and a voltage of 2 kV applied to the discharge needle in positive mode of ionisation. Orifice 1 of the interface was set to 27 eV. This voltage can be increased or decreased depending on the amount of fragmentation desired. The gas temperature was maintained at 80°C and the operating resolution of the instrument was approximately 6000 (FWHM). Mass spectra were acquired over the mass range of  $m/z$  50–500 at an acquisition rate of 0.5 spectrum/s. For DART sample analysis the helium gas was directed towards the sample or allowed to interact with vapour-phase samples. Tablets were broken, to expose an uncoated sample surface, before being held with tweezers in the path of the flowing helium at atmospheric pressure. Samples in solution were analysed by placing filter paper (1 cm × 8 cm) in the solution prior to being held similarly. For ointments, approximately 100 mg was applied to the surface of a piece of matt-finished cardboard (1 cm × 2 cm) and held in the same position.

### DESI

The Q-ToF I instrument was operated in positive and negative mode with a capillary voltage of 3.5 kV and –3.2 kV. The ion source block and nitrogen desolvation gas temperatures were set to 100°C and 400°C and the desolvation gas was set to a flow rate of 300 L/h. The cone voltage was set at 20 V for MS and MS/MS experiments and the collision energy used for MS/MS experiments was ramped between

**Table 1.** Structures, molecular formulae and molecular weights of the compounds investigated

				
$C_8H_9NO_2$ paracetamol MW:151	$C_8H_{10}N_4O_2$ caffeine MW:194	$C_{18}H_{22}NO_3$ codeine MW:299	$C_9H_8O_4$ aspirin MW:180	$C_{21}H_{30}O_5$ hydrocortisone MW:362
				
$C_{14}H_{22}ClN_3O_2$ metoclopramide MW:299	$C_{20}H_{29}N_3O_2$ cinchocaine hydrochloride MW:343	$C_{13}H_{18}O_2$ ibuprofen MW:206	$C_{10}H_{14}N_2$ nicotine MW:162	

10 and 25 eV during the acquisition. The ToF mass analyser was operated at a resolution of approximately 6000 (FWHM), with spectra acquired over the mass range of  $m/z$  50–500 at an acquisition rate of 1 spectrum/s. For all MS/MS experiments argon was used as the collision gas. For DESI sample analysis, each tablet was broken, to expose an uncoated sample surface, before being held with tweezers, at an angle of approximately 45° to the solvent spray and a distance of 5 mm from the source sampling cone. Approximately 100 mg of the ointment was applied to the surface of a piece of matt-finished cardboard (1 cm × 2 cm) and held in the same position as the solid tablets. The surface of the tablet or card was then sprayed with a solution of acetonitrile/H<sub>2</sub>O (1:1) in negative mode and a solution of acetonitrile/H<sub>2</sub>O + 0.2% formic acid in positive mode at a flow rate of 10 μL/min, using a model 22 syringe pump from Harvard Apparatus (South Natick, MA, USA). No extensive modification of solvents, buffers and pH was carried out.

### DAPCI

DAPCI experiments were performed on the Q-ToF I in both positive and negative modes of ionisation. The corona discharge pin voltage was set to 3.5 kV and –3.0 kV in positive and negative modes, respectively. The cone voltage was optimised between 10 and 25 V for each sample. The collision energy used for MS/MS experiments was ramped between 10 and 25 eV during the acquisition. The flow rate of the nitrogen desolvation gas was set to 150 L/h. The source and probe temperatures were set to 100°C and 400°C, respectively. A solvent mixture of methanol and water (1:1) flowing at 10 μL/min was infused into the heated nebuliser probe where it was converted into an aerosol which was rapidly heated in a stream of nitrogen gas, forming a vapour at the probe tip. The probe tip directly faced the tablet or ointment (which had been deposited onto the card) positioned between the corona discharge pin and the sampling cone. Reagent ions formed in the corona discharge region reacted with desorbed analyte molecules from the tablet or card forming, depending on the ionisation mode, for the most part, protonated or deprotonated molecules. The same experiments were also performed without any solvent flowing into the heated probe. This solventless DAPCI experiment is similar to the ASAP experiment previously described.<sup>12</sup>

### Accurate mass measurement protocol for the Q-ToF I

Instrumental mass drift was corrected for by using a single internal reference lock mass in MS and MS/MS mode on the Q-ToF. Since the target compounds in this study are known, the precursor ion selected for MS/MS experiments provided the internal reference lock mass in MS/MS mode. Data acquisition and processing were carried out using the digital dead-time correction algorithm embedded in the operating software, MassLynx (V3.5), supplied by Waters UK. The high ion counts generated using the DAPCI and DESI techniques caused time-to-digital (TDC) dead-time saturation.<sup>7</sup> The TDC correction software was utilised and displayed a peak centroid with the correct mass and signal intensity.

## RESULTS AND DISCUSSION

An investigation has been carried out of a number of prescription and non-prescription pharmaceutical formulations. Active ingredients from a gel applied to human skin and drug metabolites in human urine were also investigated. DART, DESI and DAPCI (solvent/solventless) techniques were employed. The DESI and DAPCI techniques can be used as a rapid screen for the analysis of solids and liquids and can be set up quickly on most instruments by the use of a home-built source,<sup>1,10</sup> or where the samples are handled manually.<sup>7,11</sup> The relative signal intensities of the active ingredients are different when samples are held manually. This is due to the non-reproducibility of positioning of the sample in the solvent spray. The use of these techniques for the rapid analysis of samples provides similar information to that provided by the DART source. The active ingredients formulated in the solid tablets were detected by the DART technique and the analysis time in MS mode of operation was, for the majority of samples, as rapid as in the DESI and DAPCI techniques, requiring, in most cases, less than 5 s.

The analysis of solid tablets and the identification of ranitidine metabolites in human urine using the DART source have previously been reported.<sup>13</sup> Since DAPCI has received little attention, a representative sample of results will focus on this together with others obtained using DESI. A comparison of the three techniques is made for the detection of a range of drugs. Tandem mass spectrometry (MS/MS) was performed on either the protonated or deprotonated molecule. The ion selected for collision-induced dissociation (CID) using the DAPCI and DESI techniques is annotated with a filled black circle and included in each figure for clarity. Some of the fragmentation pathways are complex and a detailed description of these has not been included. The proposed fragmentation schemes for some of the molecules are not assumed to be sequential. MS/MS of the protonated molecule  $[M+H]^+$  of nicotine, for example, forms a product ion at  $m/z$  106. This ion could possibly be formed by more than one route;  $m/z$  163 → 106 (loss of C<sub>3</sub>H<sub>7</sub>N) or  $m/z$  163 → 132 → 106 (sequential loss of CH<sub>3</sub>NH<sub>2</sub> and C<sub>2</sub>H<sub>2</sub>).

### Analysis of solid tablets in positive ion DAPCI, DESI and DART mode

A solid Anadin Extra tablet, which contained 45 mg of caffeine, 200 mg of paracetamol and 300 mg of aspirin, was analysed by DAPCI, DESI and DART. The mass spectra obtained for Anadin Extra using the DAPCI, DESI and the DART sources are shown in Figs. 1(A)–1(C). The protonated molecules for each of the active ingredients, paracetamol at  $m/z$  152, aspirin at  $m/z$  181 and caffeine at  $m/z$  195, were observed in the DAPCI and DESI mass spectra but the protonated aspirin molecule was absent in the DART spectrum. The base peak in all the spectra is  $m/z$  195, protonated caffeine. Accurate mass measurement confirms that the ion at  $m/z$  163 is formed by loss of H<sub>2</sub>O from protonated aspirin. This ion was observed in all three spectra. The ion at  $m/z$  198 in the DAPCI and DESI spectra is ammoniated aspirin,  $[M+NH_4]^+$ ,  $m/z$  203 in the DESI spectrum is sodiated aspirin,  $[M+Na]^+$ . Figure 1(D) shows

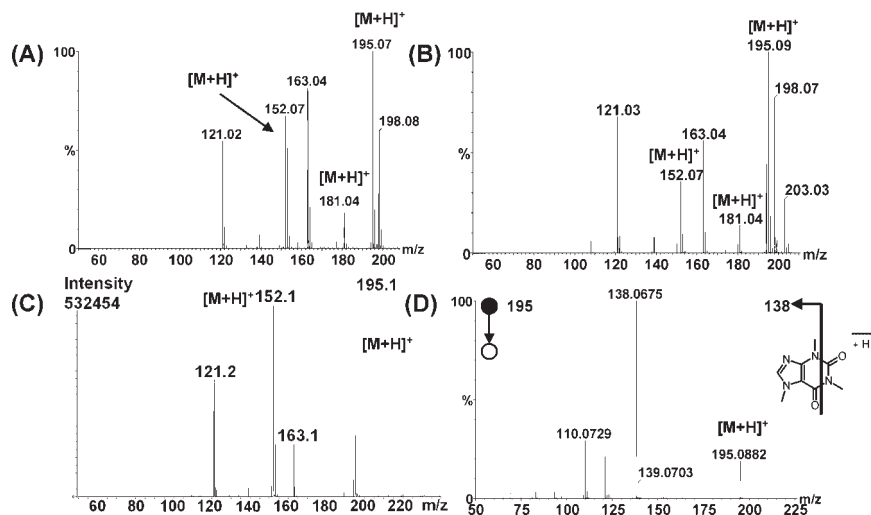


**Figure 1.** (A) Positive ion DAPCI-MS spectrum of an Anadin Extra tablet. (B) Positive ion DESI-MS spectrum of an Anadin Extra tablet. (C) Positive ion DART MS spectrum of an Anadin Extra tablet. (D) Positive ion DAPCI accurate mass MS/MS spectrum obtained from the protonated molecule of caffeine,  $[M+H]^+$  of  $m/z$  195.

the accurate mass MS/MS spectrum obtained for protonated caffeine. The elemental composition assignments for the product ions obtained for caffeine are given in Table 2. The base peak in the MS/MS spectrum is  $m/z$  138. The MS/MS spectrum obtained during this study is very similar to that obtained previously.<sup>14</sup> Elemental composition assignment shows that the protonated molecule primarily fragments by the loss of methyl isocyanate (57 Da) forming an even-electron ion at  $m/z$  138 with the formula of  $C_6H_8N_3O$ . Two other product ions were generated with sufficient ion counts for the generation of elemental formulae:  $m/z$  121 is an odd-electron radical cation with probable formula of  $C_5H_3N_3O$  and the ion at  $m/z$  110 has the elemental formula of  $C_5H_8N_3$  formed through loss of CO from  $m/z$  138.

A Solpadeine Max tablet containing 500 mg of paracetamol and 12.8 mg of codeine phosphate was analysed. The mass spectra obtained using the DAPCI, DESI and DART sources are shown in Figs. 2(A)–2(C). The  $m/z$  152 base peak in the DAPCI and DART spectra is from protonated paracetamol. The base peak in the DESI spectrum is the dimer  $[2M+H]^+$  at  $m/z$  303 from paracetamol. The formation of dimers has been observed in all three techniques and is related to the local concentration of the active ingredient under study. The ratio of monomer to dimer species can vary with the exposed part of the tablet under investigation. The protonated molecule from codeine was more abundant than the protonated dimer of paracetamol using DART. The reverse was observed for

DAPCI and DESI. Other minor ions observed in the spectra are probably due to additives in the tablet formulation. The MS/MS spectrum of protonated codeine is shown in Fig. 2(D). The product ion spectrum generated from protonated codeine can be seen to be very complex but it is also specific and reproducible. The elemental composition assignments for some of the product ions obtained for codeine are given in Table 3.

### Analysis of the active ingredients of a gel formulation by desorption from human skin by DESI

A thin layer of Ibuprofen gel containing 5% w/w of the active ingredient was applied to the surface of a human finger. The gel was gently massaged until absorbed by the skin. Using the DESI technique, with a source and desolvation temperature of 100°C, one could readily detect the drug at the point of application. Figure 3(A) shows the negative DESI mass spectrum, generated in 2 s, obtained 20 min after applying the gel. The base peak in the spectrum is deprotonated ibuprofen. Figure 3(B) shows the accurate mass MS/MS spectrum obtained for the deprotonated ibuprofen molecule 20 min after applying the gel. The deprotonated ibuprofen,  $[M-H]^-$  at  $m/z$  205.1229, was used as the internal lock mass. Accurate mass measurement of the product ion at  $m/z$  161.1321 confirms that  $CO_2$  is lost from the deprotonated molecule. This ion has an empirical formula of  $C_{12}H_{17}$ , a mass difference of  $-0.9$  mTh from the theoretical monoisotopic mass. [Caution: there is a risk of electric shock from the capillary. Although the capillary carries only limited current, it is advisable to keep the finger well away from the capillary tip in the experiment].

### Comparison of DART/DESI/DAPCI for the detection of two active ingredients in Proctosedyl ointment

It has been previously demonstrated that the detection of the two active ingredients formulated into proctosedyl ointment, cinchocaine hydrochloride (5 mg/g) and hydrocortisone

**Table 2.** DAPCI-MS/MS accurate mass of  $m/z$  195  $[M+H]^+$  of caffeine

Measured mass	Formulae	Error (mTh)
138.0675	$C_8H_{10}O_2$	-0.6
	$C_6H_8N_3O$	0.8
121.0293	$C_7H_5O_2$	0.4
	$C_5H_3N_3O$	1.7
110.0729	$C_6H_{10}O$	-0.3
	$C_5H_8N_3$	1.1

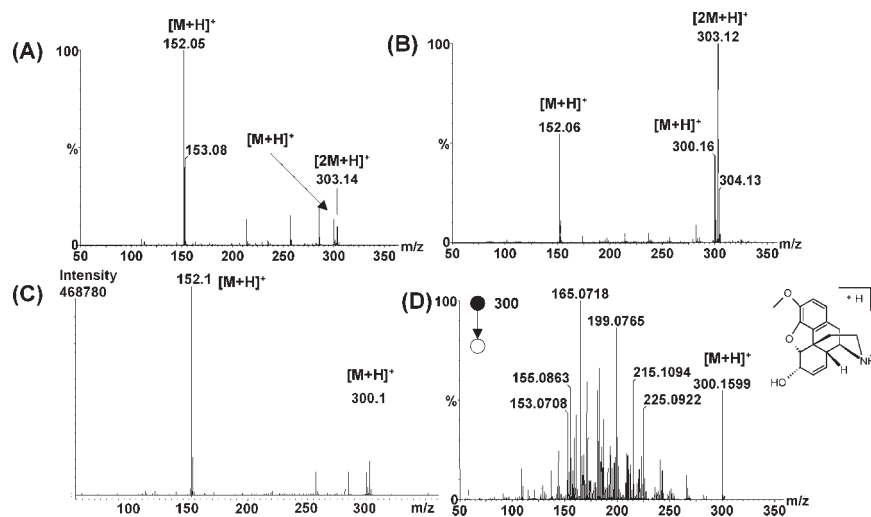


**Figure 2.** (A) Positive ion DAPCI-MS spectrum of a Solpadeine Max tablet. (B) Positive ion DESI-MS spectrum of a Solpadeine Max tablet. (C) Positive ion DART MS spectrum of a Solpadeine Max tablet. (D) Positive ion DAPCI accurate mass MS/MS spectrum obtained from the protonated molecule of codeine,  $[M+H]^+$  of  $m/z$  300.

(5 mg/g), was better with DAPCI than with DESI experiments. In positive ion mode, hydrocortisone, a weakly polar corticosteroid, was more effectively ionised by DAPCI.<sup>7</sup> During this investigation, the ointment was applied to the card in the usual way and investigated in both negative and positive ion DAPCI modes of operation. The mass spectrum obtained for the ointment in negative ion mode is shown in Fig. 4(A). High ion counts were generated, highlighting the sensitive response of the ointment to the DAPCI process in negative mode. The base peak in the spectrum is the deprotonated molecule of cinchocaine at  $m/z$  342. Other ions observed in the spectrum arise from additives in the ointment formulation. No ion was observed for deprotonated hydrocortisone. The mass spectrum obtained for the ointment in positive ion mode is shown in Fig. 4(B). High ion counts were generated, highlighting the sensitive response of the ointment to the DAPCI process in positive ion mode. The base peak in the spectrum is protonated cinchocaine at  $m/z$  344. The ion at  $m/z$  363 corresponds to protonated hydrocortisone.

The product ion spectra of the deprotonated and protonated molecules of cinchocaine can be compared in Figs. 4(C) and 4(D). Figure 4(C) shows the negative ion accurate mass MS/MS spectrum obtained for deprotonated cinchocaine. The elemental composition assignments for the product ions are given in Table 4. The base peak in the MS/MS spectrum is formed by the loss of  $C_7H_{14}N_2O$  from the deprotonated molecule to the ion at  $m/z$  200. This ion further

fragments to  $m/z$  144 by loss of 56 Da. Accurate mass measurement confirms this to be a loss of  $C_4H_8$ . A proposed fragmentation scheme is shown in Fig. 4(E).

Figure 4(D) shows the positive ion accurate mass MS/MS spectrum obtained for protonated cinchocaine. The probable elemental composition assignments for the product ions are given in Table 5. The base peak in the MS/MS spectrum is formed by the loss of  $C_4H_{11}N$  from the protonated molecule to the ion at  $m/z$  271. This ion further fragments to  $m/z$  215 by loss of 56 Da. Accurate mass measurement confirms this to be a loss of  $C_4H_8$ . A proposed fragmentation scheme is shown in Fig. 4(F).

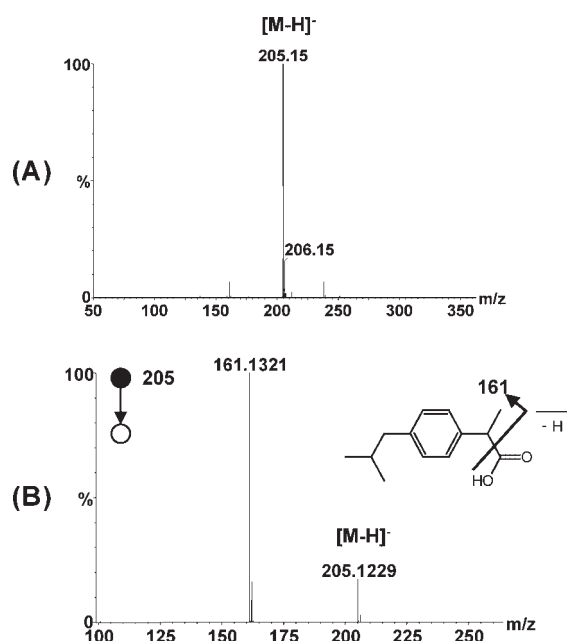


**Figure 3.** (A) Negative ion DESI-MS spectrum of Ibuprofen gel desorbed off skin. (B) Negative ion DAPCI accurate mass MS/MS spectrum obtained from the deprotonated molecule of ibuprofen,  $[M-H]^-$  of  $m/z$  205.

**Table 3.** DAPCI-MS/MS accurate mass of  $m/z$  300  $[M+H]^+$  of codeine

Measured mass	Formulae	Error (mTh)
266.1196	$C_{17}H_{16}NO_2$	1.5
225.0922	$C_{15}H_{13}O_2$	0.6
215.1094	$C_{14}H_{15}O_2$	2.2
199.0765	$C_{13}H_{11}O_2$	0.6
183.0800	$C_{13}H_{11}O$	-0.9

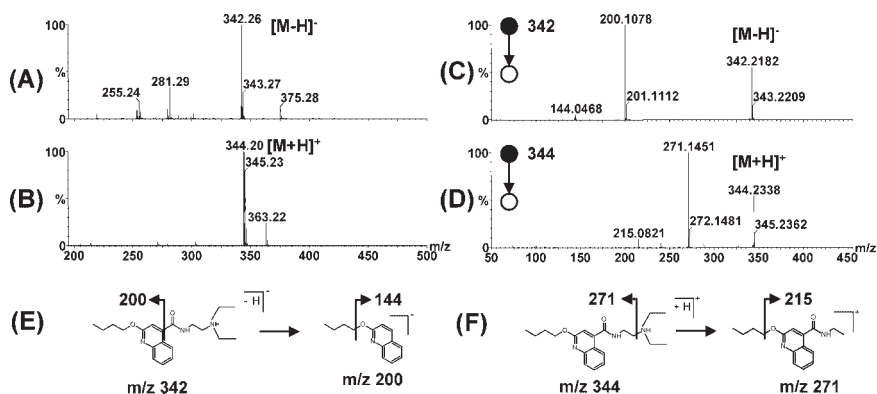


**Figure 4.** (A) Negative ion DAPCI-MS spectrum of Proctosedyl ointment. (B) Positive ion DAPCI-MS spectrum of Proctosedyl ointment. (C) Negative ion DAPCI accurate mass MS/MS spectrum of  $m/z$  342, the deprotonated molecule  $[M-H]^-$  of cinchocaine hydrochloride. (D) Positive ion DAPCI accurate mass MS/MS spectrum of  $m/z$  344, the protonated molecule  $[M+H]^+$  of cinchocaine hydrochloride. (E) Proposed negative ion fragmentation pathway of  $[M-H]^-$  of cinchocaine hydrochloride. (F) Proposed positive ion fragmentation pathway of  $[M+H]^+$  of cinchocaine hydrochloride.

The detection of active ingredients in ointments and creams using this approach is non-labour-intensive since the analysis requires no prior analyte extraction. A comparison of the DESI and DAPCI (solvent and solventless) techniques was made for this ointment since it contained both polar and weakly polar ingredients. Figure 5 shows the comparison. The mass spectrum of each is shown over the  $m/z$  region of 300–400. The top spectrum was obtained using DESI, the middle spectrum obtained using DAPCI without the use of solvent, and the bottom spectrum was obtained using DAPCI with solvent flowing into the heated probe. Protonated molecules were detected for both cinchocaine ( $m/z$  344) and hydrocortisone ( $m/z$  363) by all three techniques. The top two spectra have been magnified ( $\times 16$ ) over the  $m/z$  region for hydrocortisone. The  $[M+H]^+$  ion from cinchocaine is the base peak in all three spectra showing that this compound ionises more efficiently than hydrocortisone. The hydrocortisone has a relative abundance of approximately 3%, 4% and 35% compared with cinchocaine in DESI, DAPCI without solvent and DAPCI with solvent modes, respectively. This demonstrates the more effective detection of all the active ingredients in this formulation when using DAPCI with solvent.

Figure 6(A) shows the positive ion mass spectra, over the region  $m/z$  340–365, for the same ointment when using DART and DAPCI with solvent. DART shows results similar to the

**Table 4.** DAPCI-MS/MS accurate mass of  $m/z$  342  $[M-H]^-$  of cinchocaine

Measured mass	Formulae	Error (mTh)
200.1078	$C_{13}H_{14}NO$	0.3
144.0468	$C_9H_6NO$	1.9

**Table 5.** DAPCI-MS/MS accurate mass of  $m/z$  344  $[M+H]^+$  of cinchocaine

Measured mass	Formulae	Error (mTh)
271.1451	$C_{16}H_{19}N_2O_2$	0.4
215.0821	$C_{12}H_{11}N_2O_2$	0.0

DESI and DAPCI without solvent experiments. The active ingredient cinchocaine produces the base peak and the peak due to the hydrocortisone has a relative abundance of approximately 10% compared with cinchocaine.

### Comparison of positive and negative DAPCI-MS/MS

Metoclopramide is a medicine that increases the movements or contractions of the stomach and intestines and it is used to treat the symptoms of a stomach problem called diabetic gastroparesis. A metoclopramide tablet which contained 10 mg of the active ingredient was investigated by DAPCI in positive and negative ion modes. The negative ion mass spectrum of metoclopramide is shown in Fig. 7(A). The deprotonated molecule for the active ingredient was

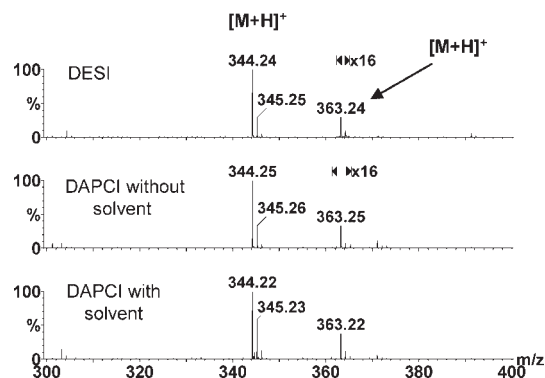


**Figure 5.** Top: positive ion DESI-MS spectrum of Proctosedyl ointment. The  $m/z$  range over  $m/z$  363 (protonated molecule,  $[M+H]^+$  of hydrocortisone) has been expanded showing a low abundance ion at  $m/z$  363 which has been magnified ( $\times 16$ ). Middle: positive ion DAPCI-MS spectrum of Proctosedyl ointment obtained without solvent. The  $m/z$  range over  $m/z$  363 has been expanded showing a low abundance ion at  $m/z$  363 which has been magnified ( $\times 16$ ). Bottom: positive ion DAPCI-MS spectrum of Proctosedyl ointment obtained with solvent.

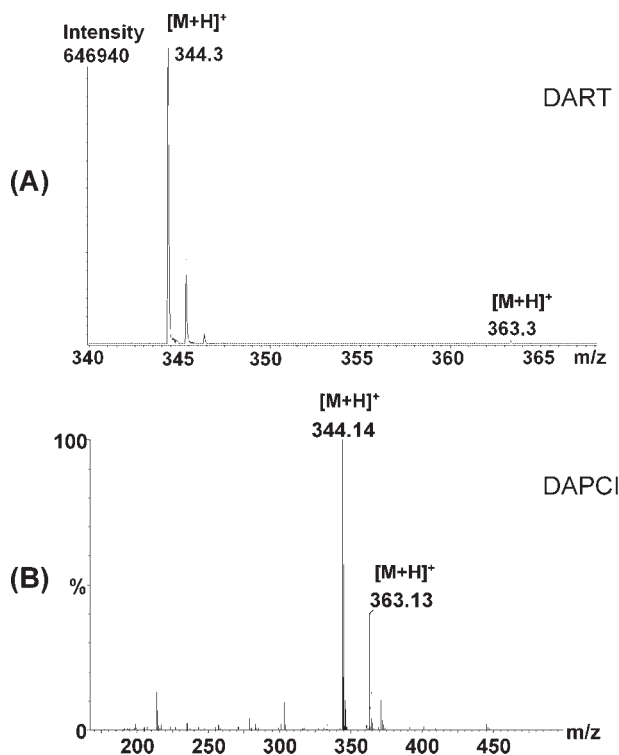


**Figure 6.** (A) Positive ion DART-MS spectrum of Proctosedyl ointment. (B) Positive ion DAPCI-MS spectrum of Proctosedyl ointment obtained with solvent.

observed in the spectrum at  $m/z$  298 and 300. These two peaks have relative signal intensities of 3:1, consistent with the presence of one chlorine atom in the molecule. The positive ion mass spectrum is shown in Fig. 7(B). The protonated

molecule for the active ingredient was observed as the base peak in the spectrum at  $m/z$  300. The positive ion mass spectrum obtained using DART for metoclopramide is shown in Fig. 7(E). Once again, the protonated molecule for the active ingredient at  $m/z$  300 was the base peak.

A comparison of the product ion mass spectra of protonated and deprotonated metoclopramide is shown in Figs. 7(C) and 7(D). Figure 7(C) shows the accurate mass MS/MS spectrum obtained for deprotonated metoclopramide. The elemental composition assignments for the product ions are given in Table 6. The deprotonated molecule appears to fragment by the unusual loss of a methyl radical forming an odd-electron radical anion of  $m/z$  283. This ion further fragments to  $m/z$  211 by loss of 72 Da, the diethylamine moiety. Accurate mass measurement confirms this to be a loss of  $C_4H_{10}N$ . A proposed fragmentation scheme is shown in Fig. 7(F).

Figure 7(D) shows the accurate mass MS/MS spectrum obtained for protonated metoclopramide. The spectrum shows ions at  $m/z$  227 and 184, in agreement with results obtained previously.<sup>15</sup> The elemental composition assignments for the product ions are given in Table 7. The base peak in the MS/MS spectrum at  $m/z$  227 shows that the protonated molecule primarily fragments by the loss of  $C_4H_{11}N$ , diethylamine. This ion further fragments to  $m/z$  184 by loss of 43 Da. Accurate mass measurement confirms this to be a loss of  $C_2H_5N$ . A proposed fragmentation scheme is shown in Fig. 7(G).

### Analysis of a naturally occurring plant alkaloid

DAPCI, DESI and DART analysis of tobacco was performed by removing the tobacco from a cigarette and holding the

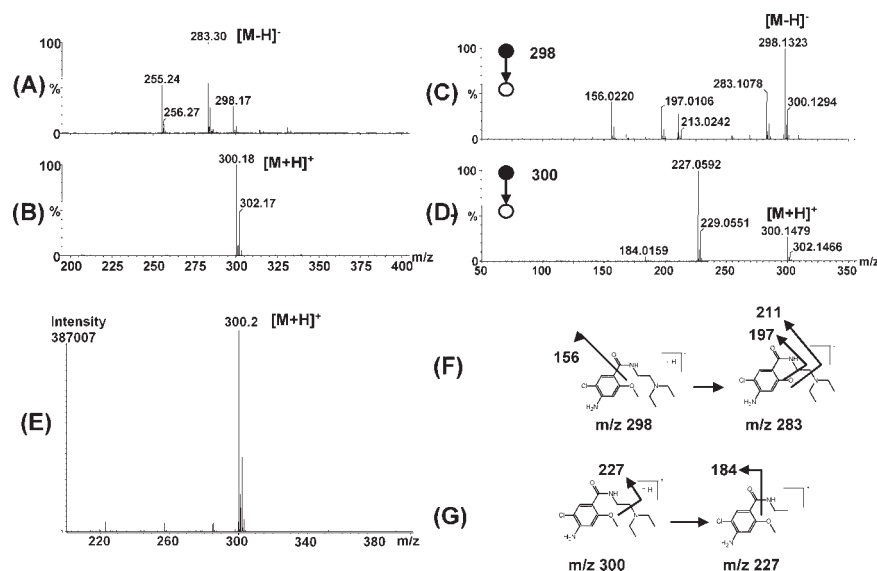


**Figure 7.** (A) Negative ion DAPCI-MS spectrum of metoclopramide. (B) Positive ion DAPCI-MS spectrum of metoclopramide. (C) Negative ion DAPCI accurate mass MS/MS spectrum of  $m/z$  298, the deprotonated molecule  $[M-H]^-$  of metoclopramide. (D) Positive ion DAPCI accurate mass MS/MS spectrum of  $m/z$  300, the protonated molecule  $[M+H]^+$  of metoclopramide. (E) Positive ion DART-MS spectrum of metoclopramide. (F) Proposed negative ion fragmentation pathway of  $[M-H]^-$  of metoclopramide. (G) Proposed positive ion fragmentation pathway of  $[M+H]^+$  of metoclopramide.



**Table 6.** DAPCI-MS/MS accurate mass of  $m/z$  298  $[M-H]^-$  of metoclopramide

Measured mass	Formulae	Error (mTh)
283.1078	$C_{13}H_{18}ClN_3O_2$	-0.9
211.0258	$C_9H_8ClN_2O_2$	-1.6
197.0106	$C_8H_6ClN_2O_2$	-1.2
156.0220	$C_7H_7ClNO$	0.3

**Table 7.** DAPCI-MS/MS accurate mass of  $m/z$  300  $[M+H]^+$  of metoclopramide

Measured mass	Formulae	Error (mTh)
227.0592	$C_{10}H_{12}ClN_2O_2$	0.4
184.0159	$C_8H_7ClNO_2$	-0.7

contents with tweezers by the method described in the Experimental section. Nicotine is an alkaloid and is known to be found naturally in the tobacco plant. The DAPCI, DESI and DART mass spectra obtained in positive ion mode are shown in Figs. 8(A)–8(C). A low cone voltage produced a single ion at  $m/z$  163, corresponding to protonated nicotine, using DAPCI and DESI. Figure 8(C) shows the spectrum obtained using the DART source at a high cone voltage. A high cone voltage produced in-source fragmentation and the DART spectrum is very similar to the DAPCI-MS/MS spectrum of  $m/z$  163 shown in Fig. 8(D). The elemental composition assignments for the product ions obtained for nicotine are given in Table 8. These show that the protonated molecule fragments by the loss of 31 Da to form an ion at  $m/z$  132. Accurate mass measurement confirms this loss to be  $CH_3NH_2$  from the methyl-substituted pyrrolidine ring. The base peak in the MS/MS spectrum is  $m/z$  130 formed by loss

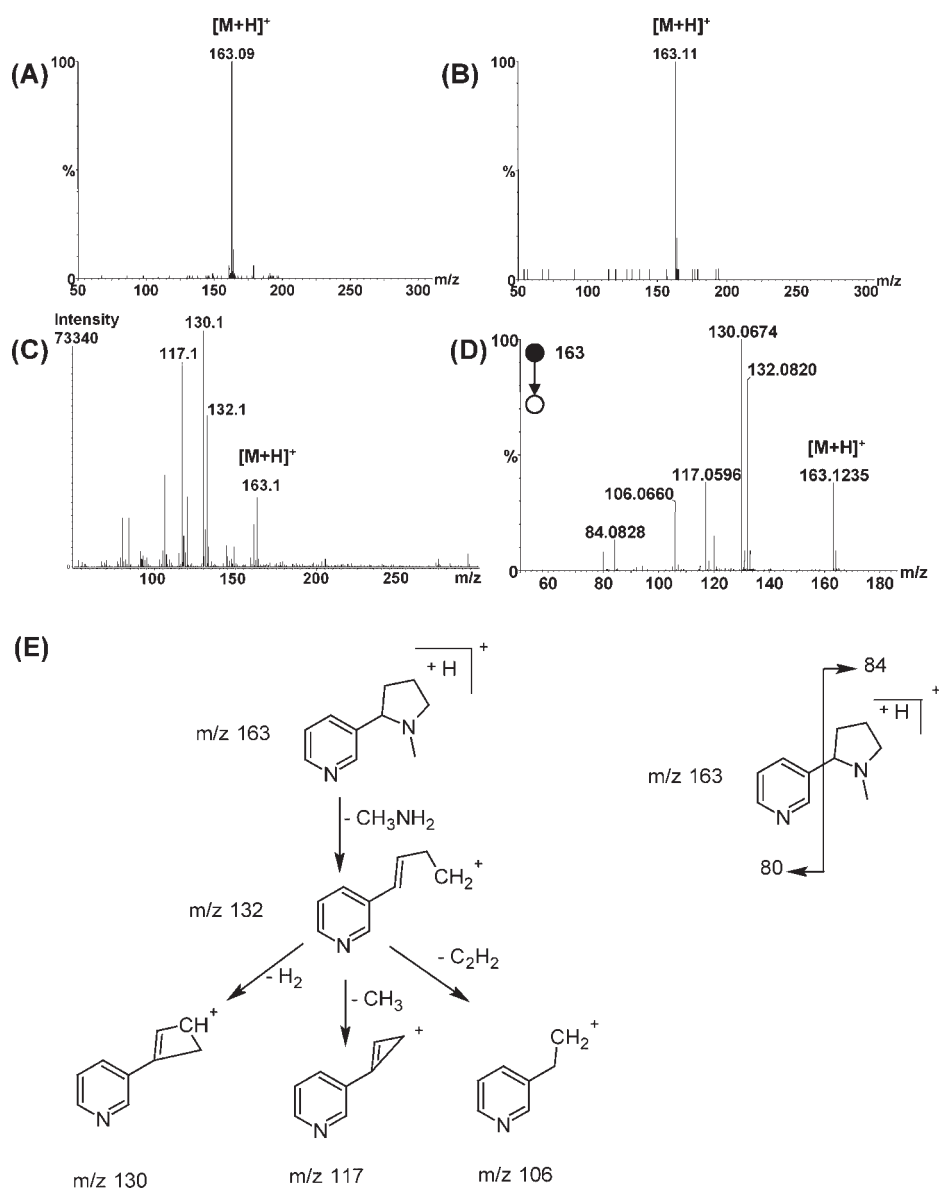


**Figure 8.** (A) Positive ion DAPCI-MS spectrum of tobacco. (B) Positive ion DESI-MS spectrum of tobacco. (C) Positive ion DART-MS spectrum of tobacco. (D) Positive ion DAPCI accurate mass MS/MS spectrum of  $m/z$  163, the protonated molecule  $[M+H]^+$  of the active ingredient nicotine found in tobacco. (E) Proposed positive ion fragmentation pathway of  $[M+H]^+$  of nicotine.

**Table 8.** DAPCI-MS/MS accurate mass of  $m/z$  163  $[M+H]^+$  of nicotine

Measured mass	Formulae	Error (mTh)
132.0820	C <sub>9</sub> H <sub>10</sub> N	0.7
130.0674	C <sub>9</sub> H <sub>8</sub> N	1.7
117.0596	C <sub>8</sub> H <sub>7</sub> N	1.8
106.0660	C <sub>7</sub> H <sub>8</sub> N	0.4
84.0828	C <sub>5</sub> H <sub>10</sub> N	1.5
80.0524	C <sub>5</sub> H <sub>6</sub> N	2.4

of H<sub>2</sub> from  $m/z$  132. Other ions at  $m/z$  117 and 106 are possibly formed by the loss of a methyl radical and a C<sub>2</sub>H<sub>2</sub> molecule, respectively, from  $m/z$  132. The methyl radical loss has been observed previously.<sup>16</sup> Other easily recognised product ions include the ion of  $m/z$  84 due to the methyl-substituted pyrrolidine ring moiety obtained from cleavage of the bond between the two rings and the ion of  $m/z$  80 due to the pyridine ring moiety of the molecule, obtained in the same way. A proposed fragmentation scheme is shown in Fig. 8(E), and is similar to the scheme previously proposed.<sup>16</sup> Accurate mass MS/MS confirms that the previous proposals are correct.

### Identification of ibuprofen metabolites from human urine

The development of a rapid screen for the detection of drug or drug metabolites in urine is simplified by the use of these newly developed ionisation techniques. The study of drug metabolites in urine can be challenging due to the low levels of metabolites and high levels of endogenous materials such as salts. Ibuprofen is a non-steroidal anti-inflammatory drug and the known bio-transformations of ibuprofen include hydroxylation, carboxylation and glucuronidation.<sup>17</sup> A control sample of human urine was obtained 60 min after administration of two ibuprofen tablets which each con-

tained 200 mg of the active ingredient. We used DAPCI, with a mixture of methanol/water flowing into the heated probe, for the detection of ibuprofen metabolites in human urine.

A urine sample was absorbed onto filter paper (1 cm × 8 cm) by placing the paper into the urine sample. Metabolites in the urine were then identified by holding the filter paper with tweezers as described in the Experimental section. Figure 9(A) shows the negative ion mass spectrum obtained without any pre-treatment of the urine sample. The spectrum contains ions attributable to the presence of endogenous components, of which many can be ascribed to components in the urine and some to background species. Ions detected other than the known bio-transformations of ibuprofen have been tentatively assigned to deprotonated pyruvic acid at  $m/z$  87, lactic acid at  $m/z$  89, methylmalonic acid at  $m/z$  117, xanthine at  $m/z$  151, and hippuric acid at  $m/z$  178.

Figure 9(B) shows the accurate mass spectrum obtained using the deprotonated molecule  $[M-H]^-$  at  $m/z$  205.1229 from the parent drug ibuprofen, as the internal lock mass. Ions corresponding to the deprotonated molecules of two low-level metabolites were detected, the hydroxyl-ibuprofen at  $m/z$  221 and carboxy-ibuprofen at  $m/z$  235. No glucuronide metabolites were detected. The specificity of the technique coupled with accurate mass measurement has allowed the determination of an elemental composition for  $m/z$  221. The probable elemental composition for the accurate mass of 221.1163 is C<sub>13</sub>H<sub>17</sub>O<sub>3</sub>, consistent with the formula for a hydroxylated ibuprofen metabolite. The mass error calculated is -1.5 mTh from the theoretical monoisotopic mass for hydroxyl-ibuprofen metabolite. The elemental composition for the accurate mass of 235.0983 is C<sub>13</sub>H<sub>15</sub>O<sub>4</sub>, consistent with the formula for a carboxylated ibuprofen metabolite. The mass error calculated is 1.2 mTh from the theoretical monoisotopic mass for the carboxy-ibuprofen metabolite. Figure 9(C) shows the MS/MS spectrum obtained for the

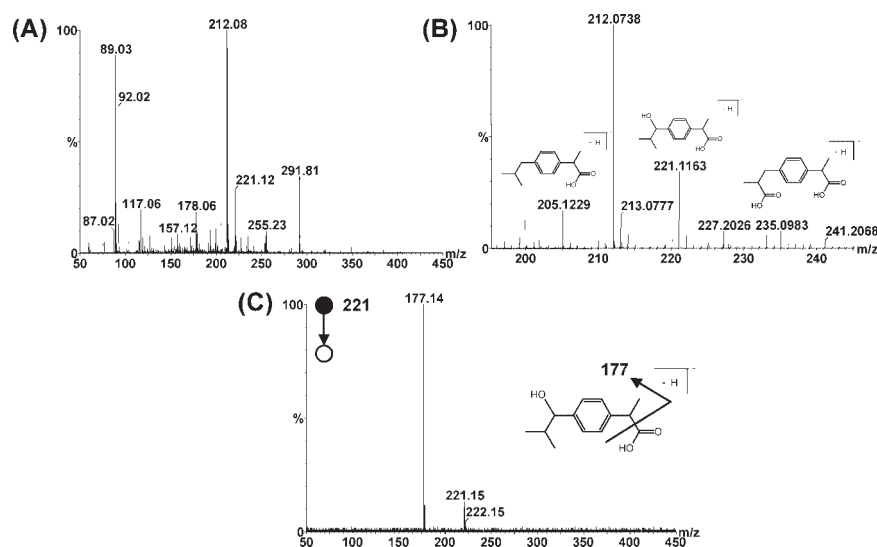


**Figure 9.** (A) Negative ion DAPCI-MS spectrum of urine sample, 75 min after oral dose of 400 mg of ibuprofen tablets. (B) Negative ion DAPCI accurate mass spectrum of a urine sample, 75 min after an oral dose of 400 mg of ibuprofen tablets. The mass spectrum has been expanded over the  $m/z$  range 195–245. (C) Negative ion DAPCI-MS/MS spectrum of  $m/z$  221 showing loss of CO<sub>2</sub>.

deprotonated hydroxy-ibuprofen metabolite at  $m/z$  221. This primarily fragments with the formation of a single product ion at  $m/z$  177 through the loss of  $\text{CO}_2$ .

## CONCLUSIONS

The use of DART, DESI and DAPCI (solvent and solventless) techniques has been demonstrated for a wide range of molecules of pharmaceutical interest. In all cases the sample to be studied has been desorbed from a solid substrate. The well-demonstrated ability of the DART technique to rapidly characterise gaseous samples was not utilised. Significant differences between these approaches were observed. For compounds of moderate to low polarity, DAPCI (solvent and solventless) produced more effective ionisation. DAPCI with solvent was observed to be more effective in the ionisation of these compounds than DART, DESI or solventless DAPCI. The previously described approach of ASAP<sup>12</sup> was found to be very similar to solventless DAPCI.

DESI and DAPCI techniques have provided a highly robust means of interrogating the active ingredients of a variety of pharmaceutical formulations. Sampling the formulation is rapid and ionisation occurs almost instantly. The orientation of the surface in front of the stream of excited gas seems to be more critical with the DART source. The current design of the DART source, although very effective for the analysis of gaseous samples, is less effective for the analysis of adsorbed molecules. This is due to the inability to visualise the gas stream and the relatively wide sampling geometry.

The surface to be analysed via DESI can be held in the solvent stream at an angle of  $45^\circ$  and at a distance of 5–20 mm prior to the sampling cone orifice or it can be held at an angle directly in front of the probe tip some distance from the sampling cone on the QToF 1 instrument. Since the spray emanating from the probe tip can be seen in DESI mode, the tip can be positioned exactly to spray the surface to be interrogated, which can be of the order of  $\text{cm}^2$  to  $\text{sub-mm}^2$ .

The use of a Q-ToF instrument, with elevated resolution and full-scan sensitivity, has improved the selectivity and specificity of the DAPCI technique originally shown by Cooks and co-workers<sup>5</sup> by allowing the generation of accurate mass MS/MS information to within 2 mTh using a single point internal lock mass to correct mass scale drift. The high information content has allowed probable elemental compositions and fragmentation pathways to be determined.

The development of these new ionisation techniques offers very significant advantages for a number of important

scientific areas. The ability to rapidly analyse complex mixtures with little, or no, sample preparation is very important. The techniques DART, DESI and DAPCI (solvent and solventless) have complex, potentially inter-related mechanisms but have been shown to provide complementary information on a range of compounds of pharmaceutical interest. The direct analysis of urine and molecules adsorbed on skin is of particular interest. This work has focused on samples desorbed from solid substrates although the study of gaseous samples is also possible, particularly with the DART technique. The techniques produce little fragmentation and so the addition of accurate mass MS and MS/MS greatly increases the selectivity of the approach.

## Acknowledgements

The authors would like to thank JEOL for the kind access to the AccuToF incorporating the DART source, the Proteomics Facility at the University of Warwick, and Professor Keith Jennings for helpful discussions concerning the manuscript.

## REFERENCES

1. Takats Z, Wiseman JM, Gologan B, Cooks RG. *Science* 2004; **306**: 471.
2. Van Berkel GJ, Ford MJ, Deibel MA. *Anal. Chem.* 2005; **77**: 1207.
3. Weston DJ, Bateman R, Wilson ID, Wood TR, Creaser CS. *Anal. Chem.* 2005; **77**: 7572.
4. Chen H, Talaty NN, Takats Z, Cooks RG. *Anal. Chem.* 2005; **77**: 6915.
5. Takats Z, Cotte-Rodriguez I, Talaty N, Chen H, Cooks RG. *Chem. Commun.* 2005; 1950.
6. Cotte-Rodriguez I, Takats Z, Talaty N, Chen H, Cooks RG. *Anal. Chem.* 2005; **77**: 6755.
7. Williams JP, Scrivens JH. *Rapid Commun. Mass Spectrom.* 2005; **19**: 3643.
8. Wiseman JM, Puolitaival SM, Takats Z, Cooks RG, Caprioli RM. *Angew. Chem. Int. Ed. Engl.* 2005; **44**: 7094.
9. Talaty N, Takats Z, Cooks RG. *Analyst* 2005; **130**: 1624.
10. Leuthold LA, Mandscheff JF, Fathi M, Giroud C, Augsburg M, Varesio E, Hopfgartner G. *Rapid Commun. Mass Spectrom.* 2006; **20**: 103.
11. Rodriguez-Cruz SE. *Rapid Commun. Mass Spectrom.* 2006; **20**: 53.
12. McEwen CN, McKay RG, Larsen BS. *Anal. Chem.* 2005; **77**: 7826.
13. Cody RB, Laramée JA, Durst HD. *Anal. Chem.* 2005; **77**: 2297.
14. Tuomi T, Johnsson T, Reijula K. *Clin. Chem.* 1999; **45**: 2164.
15. Abdel-Hamid ME, Sharma D. *J. Liquid Chromatogr. Rel. Tech.* 2004; **27**: 641.
16. Byrd GD, Davis RA, Ogden MW. *J. Chromatogr. Sci.* 2005; **43**: 133.
17. Kearney G, Khan T, Castro-Perez J, Pugh J. *Proc. 49th ASMS Conf. Mass Spectrometry and Allied Topics*, Chicago, Illinois, 2001.